

NGU Report 2002.020

Postglacial mass movements in western
Norway with special emphasis on the
2000-2200 BP and 2800-3200 BP periods -
final report

Report no.: 2002.020		ISSN 0800-3416	Grading: Open
Title: Postglacial mass movements in western Norway with special emphasis on the 2000-2200 BP and 2800-3200 BP periods - final report			
Authors: Reidulv Bøe, Aivo Lepland, Lars Harald Blikra, Oddvar Longva and Eivind Sønstegeard		Client: Norsk Hydro ASA, NGU	
County: Sogn og Fjordane, Møre og Romsdal		Commune:	
Map-sheet name (M=1:250.000) Florø, Årdal, Ulsteinvik, Ålesund, Kristiansund		Map-sheet no. and -name (M=1:50.000)	
Deposit name and grid-reference:		Number of pages: 115 Price (NOK): 470,- Map enclosures: 0	
Fieldwork carried out: June-July 2001	Date of report: 1st September 2002	Project no.: 293100	Person responsible:
<p>Summary: The Ormen Lange Gas Field was discovered in the Norwegian Sea outside Møre og Romsdal in 1997. The development of this field, which is located in the area of the Storegga Slide, requires safety assessment. NGU and Norsk Hydro ASA, in cooperation with the University of Bergen and Sogn og Fjordane College, have carried out a project with the aim to collect and compile data on slides, avalanches and gravitational faults that may have resulted from large earthquakes or tsunamis in northwest Western Norway. A major task in the present project has been to investigate the spatial extent and interpret the origin of a postulated mass-movement event ca. 2000 year ago and to evaluate its causes; climatic variations, a tsunami (possibly caused by an earthquake affecting the offshore area), an earthquake only affecting parts of western Norway, or a combination of an earthquake and a tsunami. Several other mass movements, including Storegga Slide tsunami deposits and pre-Storegga Slide slide and debrisflow deposits have been studied, both in fjord and lake sediments.</p> <p>Five of the 16 investigated fjords (Dalsfjorden, Førdefjorden, Syvdsfjorden, Voldafjorden, Ørstafjorden) provide evidence for a 2000-2200 years BP (calendar years before present, i.e. 1950) event. Previous investigations show no indication of a large shelf-edge slide in the Storegga area, that may have created a tsunami at that time, nor are any mass-movement deposits found on land or in the investigated lakes. This suggests that the 2000-2200 BP debrisflows and turbidites were most likely related to one or more earthquakes on land or close to the coast, and not an offshore megaslide-generated tsunami. Storegga Slide (8200 BP) tsunami deposits are observed in cores over most of the investigated area, both in the deep fjords and in lakes. Striking similarity between major slide and debrisflow deposits at the 2000-2200 BP and ca. 11 000-11 700 BP stratigraphic levels suggest a common triggering mechanism, probably earthquakes with epicenters in the Sunnfjord-Sunnmøre region. A period of debrisflows, turbidites and snow avalanches around 2800-3200 BP was most probably related to climatic irregularities, as also observed from previous studies elsewhere. Most of these deposits are only observed in cores and not in seismic data. Clusters of rock avalanches from the second half of the Holocene, in Romsdalen and Tafjorden, may be related to neotectonic activity of the newly discovered Berill fault, possibly around 3000 BP. Several other periods of mass-movement activity (turbidity currents, floods, snow avalanches) have been recorded, e.g. 1700-1800 BP and 5300-5600 BP. These are only observed in a few basins, and are thus interpreted to be related to local climatic variations. Clusters of rock avalanche deposits in the coastal area probably reflect old events, possibly just after the deglaciation. Many small debrisflows and turbidites in the early Holocene were probably related to rapid land uplift and high rates of erosion, at that time.</p>			
Keywords: Marine Geology	Tsunami	Earthquake	
Core	Debrisflow	Dating	
Geological hazard	Turbidite	Slide	

CONTENTS

1.	INTRODUCTION.....	7
2.	METHODS.....	12
2.1	Phase A1.....	12
2.2	Phase A2.....	12
2.3	Phase B1.....	12
2.4	Phase B2.....	13
2.5	Phase C.....	14
2.6	Phase D.....	15
2.7	Phase E.....	15
3.	CLIMATE, MASS-MOVEMENT ACTIVITY AND HUMAN INFLUENCE OVER THE PAST 11 500 YEARS (10 000 ¹⁴ C YEARS).....	15
3.1	Palaeoclimatic data.....	15
3.2	Climatic influence on mass movements and flood activity.....	16
3.3	Timing of high mass-movement activity.....	17
4.	ROCK AVALANCHES, GRAVITATIONAL FRACTURES AND NEOTECTONIC FAULTS ON LAND.....	18
4.1	Romsdalen and Innfjorden.....	19
4.2	Tafjord-Geirangerfjord-Sunnylvsfjord.....	24
4.3	Øtrefjellet, Oterøya and Sjørdalen.....	27
4.4	Sogn og Fjordane and Hordaland.....	29
4.4.1	Aurlandsfjorden.....	31
4.4.2	Fjærlandsfjorden.....	34
5.	FJORD INVESTIGATIONS.....	34
5.1	Sogn.....	34
5.1.1	Aurlandsfjorden.....	34
5.1.2	Barsnesfjorden.....	37
5.1.3	Fjærlandsfjorden.....	39
5.2	Sunnfjord.....	42
5.2.1	Dalsfjorden.....	42
5.2.2	Førdefjorden.....	45
5.3	Sunnmøre.....	45
5.3.1	Vanylvsfjorden.....	45
5.3.2	Syvdsfjorden.....	48
5.3.3	Voldafjorden.....	51
5.3.4	Ørstafjorden.....	52
5.3.5	Sulafjorden.....	55
5.3.6	Breisunddypet.....	59
5.3.7	Tafjorden.....	62
5.4	Romsdal.....	63
5.4.1	Mifjorden.....	63
5.4.2	Julsundet.....	64
5.5	Nordmøre.....	68
5.5.1	Tingvollfjorden.....	68
5.5.2	Halsafjorden.....	68
6.	LAKE INVESTIGATIONS IN SUNNMØRE AND NORDFJORD.....	72
6.1	Storsætervatnet.....	73
6.2	Medvatnet.....	76
6.3	Nedstevatnet.....	80
6.4	Rotevatnet.....	83

6.5	Hovdevatnet	86
7.	TSUNAMI SEDIMENTARY FACIES	86
8.	TEMPORAL AND SPATIAL DISTRIBUTION OF EVENTS AND THEIR CAUSES	87
8.1	Younger than 500 BP	88
8.2	Younger than 1500 BP	90
8.3	1700-1800 BP.....	90
8.4	2000-2200 BP.....	90
8.5	2800-3200 BP.....	92
8.6	5300-5600 BP.....	94
8.7	6000-6200 BP.....	94
8.8	6700 BP.....	95
8.9	7300 BP.....	95
8.10	8200 BP.....	95
8.11	9300 BP.....	96
8.12	10 000-11 700 BP.....	96
9.	CORRELATION OF SEISMIC DATA AND FJORD CORE DATA.....	97
10.	MASS-MOVEMENT TRIGGERING MECHANISMS	99
11.	CONCLUSIONS.....	104
12.	REFERENCES.....	106

FIGURES

- Figure 1. Map showing the location of the investigated areas and fjord cores.
- Figure 2. Seismic data coverage.
- Figure 3. Colour coding and interpreted ^{14}C -ages of reflectors in Voldafjorden according to Longva et al.(2001a).
- Figure 4. Map showing the location of investigated lakes in Nordfjord and Sunnmøre.
- Figure 5. Map showing the location of investigated areas on land.
- Figure 6. Rock avalanches and gravitational fractures in Møre og Romsdal.
- Figure 7. Historical rock avalanches with related tsunamis in Sogn og Fjordane and Møre og Romsdal.
- Figure 8. 3D image of of Romsdalen, showing rock avalanches. Based on topographic data.
- Figure 9. Topographic map of Romdalen showing fractures on Børa and distribution of rock-avalanche deposits.
- Figure 10. Unstable mountain plateau with fractures on Børa, Romsdalen.
- Figure 11. The postglacial Berill fault, Innfjorden.
- Figure 12. Topographic map with slide scars, Tafjorden.
- Figure 13. Shaded relief map based on swath bathymetry, Tafjorden.
- Figure 14. Seismic profile displaying rock avalanche deposits, Tafjorden.
- Figure 15. Langhammaren, Tafjord, with the 1934 slide scar and swath bathymetry showing rock avalanche deposits in the fjord.
- Figure 16. Fault and slide at Opstadhornet, Otrøya.
- Figure 17. Satellite image with gravitational slope failures between Odda and Aurland.
- Figure 18. 3D model with gravitational fractures and slide scars, Flåmsdalen and Aurlandsfjorden.
- Figure 19. Fractures, rock avalanches and creep deposits, Flåmsdalen and Aurland.
- Figure 20. Bathymetry and rock avalanche deposits, Aurlandsfjorden.
- Figure 21. Cores from Aurlandsfjorden, Barsnesfjorden and Fjærlandsfjorden
- Figure 22. Seismic profile at the location of cores P0103007 and P0103008, Barsnesfjorden.
- Figure 23. Seismic profile at the location of core P0103004, Fjærlandsfjorden.
- Figure 24. Seismic profile at the location of core P0103005, Fjærlandsfjorden.
- Figure 25. Shaded relief map based on swath bathymetry, and core locations, Dalsfjorden.
- Figure 26. Cores from Dalsfjorden and Førdefjorden.
- Figure 27. Seismic profile at the location of cores P0103012 and P0103013, Dalsfjorden.
- Figure 28. Cores from Vanylvsfjorden, Syvdsfjorden and Voldafjorden.
- Figure 29. Seismic profile at the location of core P0103015, Vanylvsfjorden.
- Figure 30. Shaded relief map based on swath bathymetry, and core locations, Syvdsfjorden.
- Figure 31. Seismic profile at the location of cores P0103018, -019 and -020, Syvdsfjorden.
- Figure 32. Shaded relief map based on swath bathymetry, and core locations, Ørstafjorden.
- Figure 33. Seismic profile at the location of core Ørsta-GC1, Ørstafjorden.
- Figure 34. Cores from Ørstafjorden.
- Figure 35. Shaded relief map based on swath bathymetry, and core locations, Sulafjorden.
- Figure 36. Seismic profile at the location of cores NGU-2L/SC and NGU-3L/SC, Sulafjorden.

Figure 37. Cores from Sulafjorden.
Figure 38. Shaded relief map based on swath bathymetry, and core locations, Breisunddypet.
Figure 39. Cores from Breisunddypet.
Figure 40. Seismic profile at the location of core P0103029, Tafjorden.
Figure 41. Cores from Tafjorden, Midfjorden and Tingvollfjorden.
Figure 42. Core from Julsundet.
Figure 43. Seismic profile at the location of core NGU-6L/SC, Julsundet.
Figure 44. Shaded relief map based on swath bathymetry, and core locations, Halsafjorden.
Figure 45. Seismic profile at the location of core NGU-4L/SC, Halsafjorden.
Figure 46. Core from Halsafjorden.
Figure 47. Cores from Storsætervatnet.
Figure 48. Cores from Medvatnet.
Figure 49. Interpreted Storegga Slide tsunami deposit, Medvatnet.
Figure 50. Cores from Nedstevatnet.
Figure 51. Correlation of seismic data and cores, Nedstevatnet.
Figure 52. Cores from Rotevatnet.
Figure 53. Cores from Hovdevatnet.
Figure 54. Temporal and spatial distribution of Holocene, prehistoric events.
Figure 55. Geographical distribution of the 2000-2200 BP event.
Figure 56. Geographical distribution of events in the time period 2800-3200 BP.
Figure 57. Clusters of rock avalanches and gravitational bedrock fractures plotted on a base map displaying earthquakes and land uplift.
Figure 58. Area affected by landslides versus earthquake magnitude (from Keefer 1984).
Figure 59. Potential landslides areas during earthquakes of magnitude 6.5 and 7.0 at Otrøya and in Innfjorden (Berill fault).

TABLES

Table 1. Core inventory, fjords.

Table 2. Core inventory, lakes.

Table 3. ¹⁴C dating results, fjord cores.

Table 4. ¹⁴C dating results, lake cores.

Table 5. Temporal and spatial distribution of events in the investigated fjords and lakes.

APPENDIX

Appendix 1. Review report by SINTEF.

Appendix 2. Comments to Review report by SINTEF.

1. INTRODUCTION

The Ormen Lange Gas Field was discovered in the Norwegian Sea outside Møre og Romsdal in 1997. The development of this field, which is located in the area of the Storegga Slide, immediately to the northwest of the main slide escarpment, requires that the safety of the project is investigated and documented. As part of this work, the Geological Survey of Norway (NGU) and Norsk Hydro ASA, in cooperation with the University of Bergen and Sogn og Fjordane College, have carried out a project with the following main aims:

- i) Make a regional compilation of slides, avalanches and gravitational faults that may have resulted from large earthquakes or tsunamis in northwest Western Norway
- ii) Date horizons reflecting mass movements or sediment instability in fjords and lakes

The stratigraphy in 25 coastal lakes has shown that most of the Norwegian coast line was impacted by a large tsunami caused by the Second Storegga Slide about 8000 years BP (Bondevik et al. 1997a, b). The tsunami was recognized in the sedimentary record as an erosional unconformity overlain by graded or massive sand with shell fragments, followed by redeposited organic detritus. The greatest runup along the coast was found in areas most proximal to the slide scar, in Sunnmøre (10-11 m above high tide at the contemporary sea level). The tsunami wave was not significantly influenced by the local topography, suggesting a very long wave length (Bondevik 1997a).

An 8.5 m long core from Voldafjorden (Fig. 1) has shown distinct turbidites (Sejrup et al. 2001). The uppermost 3 turbidites were dated to approximately 2000 (ca. 2000 ¹⁴C BP), 8200 (ca. 7200 ¹⁴C BP) and 11 000 BP (ca. 9500 ¹⁴C BP). The two youngest have been correlated to seismic reflectors that occur at the level of extensive debrisflow deposits along the fjord margins (Longva et al. 2000, 2001a). The 8200 BP event was interpreted to be related to the Storegga Slide tsunami (Bondevik et al. 1998, Grøsfjeld et al. 1999, Sejrup et al. 2001). This suggested that the 2000 BP event could possibly be related to another large tsunami caused by an offshore mega-slide.

High resolution seismic reflection profiles from fjords along the coast between Sognefjorden and Kristiansund (Fig. 2) show reflectors that possibly can be correlated from fjord to fjord (Longva et al. 2001a) (Fig. 3). Fjords with significant sediment input from rivers have a strikingly similar seismic stratigraphy. Thresholds and local variations makes it difficult to directly trace reflectors from one fjord to another, however, four apparently regional reflectors/reflector bands were observed (Longva et al. 2001a). In some fjords, the reflectors can clearly be related to submarine debrisflow deposits or avalanches/rock fall deposits from the surrounding land areas. Such deposits may have been caused by climatic changes, earthquakes, or tsunamis generated by large submarine slides (which in turn could have been earthquake triggered). The reflectors/reflector bands are (Longva et al. 2001, Fig. 3):

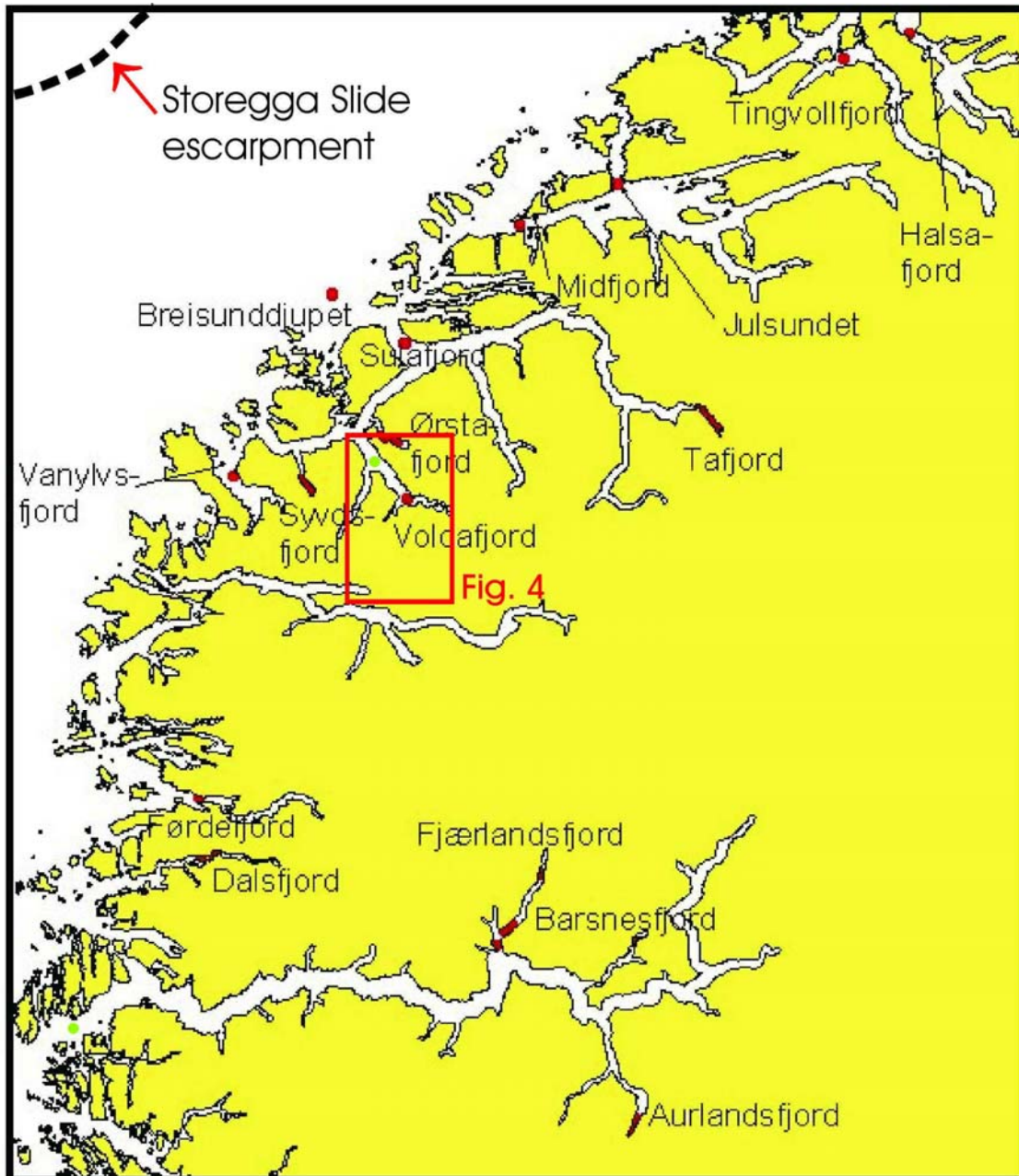


Figure 1. Map showing the investigated areas and location of fjord cores. Green dots show location of cores in Voldafjorden (Sejrup et al. 2001) and Sognesjøen (Haflidason 2002).

Violet reflector (interpreted to be ca. 12 000 ¹⁴C years old). This reflector is often diffuse. It usually occurs above a 10-30 m thick, acoustically transparent to chaotic unit, which again rests on acoustically stratified, glaciomarine deposits. In several fjords, the reflector clearly represents the upper boundary of thick debrisflow deposits. These are stratigraphically overlain by more debrisflow deposits, slide deposits or acoustically stratified sediments, followed by an acoustically transparent unit, usually less than 8 m thick. The reflector was probably formed just after the deglaciation of the fjords.

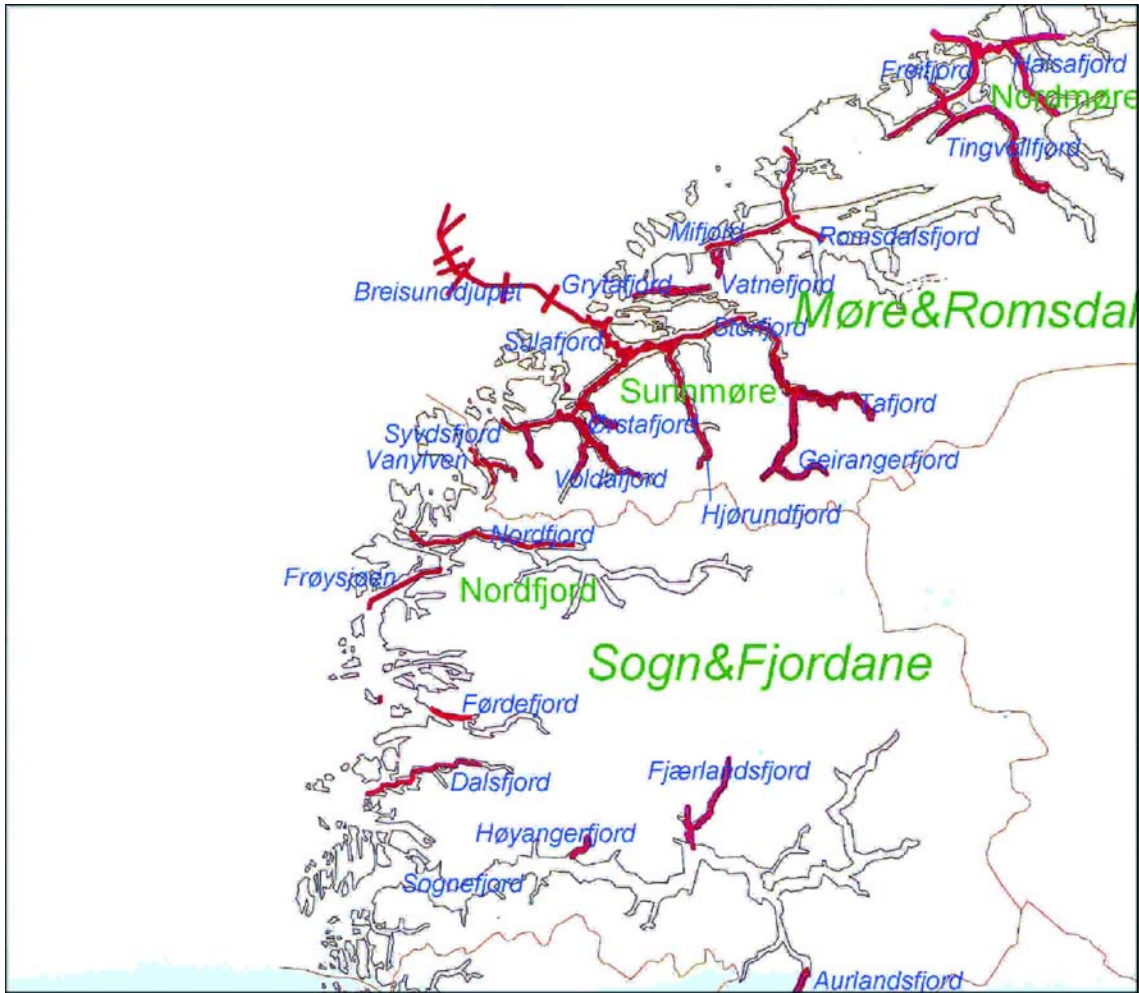


Figure 2. Index map from Longva et al. (2001a). Red lines show the coverage of seismic data.

Orange reflectors (interpreted to be 9000-11 000 ^{14}C years old). These appear as a set of three distinct, closely spaced reflectors. The lowermost one is the most pronounced, representing the upper boundary of the acoustically transparent unit deposited after the deglaciation. Occasionally there are slides/debrisflows related to these reflectors, especially in the fjords in Nordmøre.

Green reflector (interpreted to be 7200 ^{14}C years old). This reflector is the most prominent, and represents the upper boundary of an acoustically transparent (locally stratified) unit, above the orange reflectors. In most of the investigated fjords, there are large debrisflow deposits associated with the green reflector. The number of debrisflow deposits related to the reflector seems to be lower in Nordmøre than further south.

Red reflector (interpreted to be ca. 2000 ^{14}C years old). This reflector is very prominent in the southern part of Sunnmøre (and possibly in Nordfjord and Sunnfjord), but becomes very

vague towards the north. The reflector is related to slides and debrisflow deposits along the fjord margins, but occurs within a succession of acoustically transparent sediments in the central parts of the fjords.

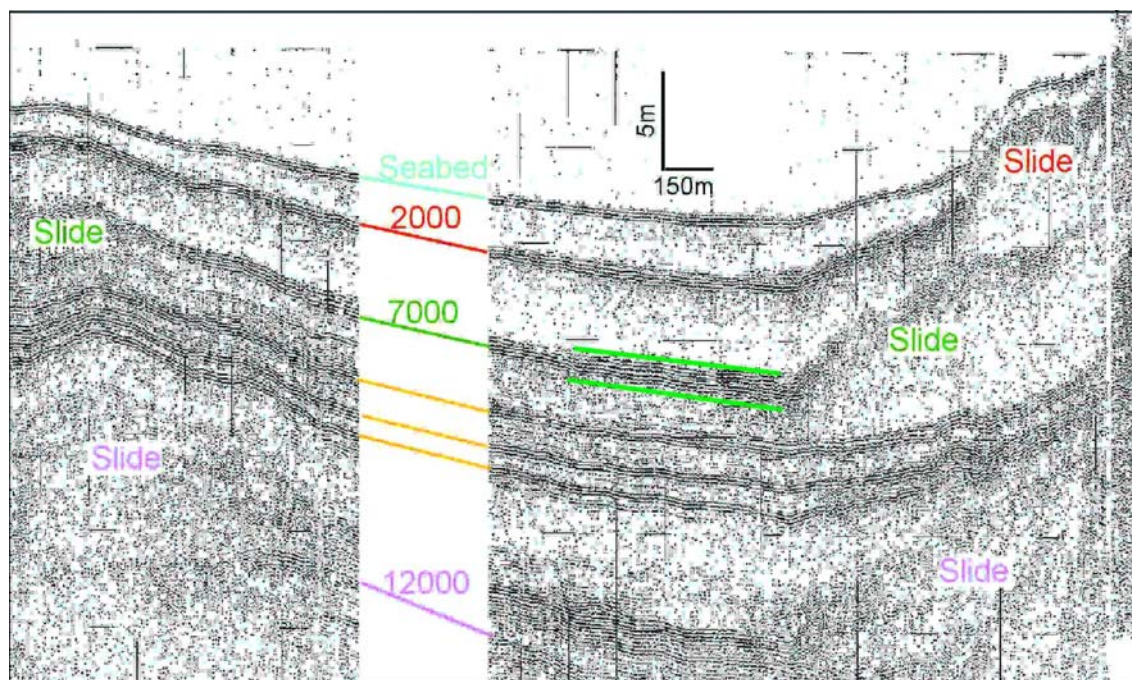


Figure 3. Seismic profile (NGU9909003) through the deepest part of Voldafjorden. The numbers on the coloured reflectors represent estimated ^{14}C -ages, based on correlation with the well-dated core from Voldafjorden (Sejrup et al. 2001). From Longva et al. (2001a). An alternative interpretation discussed here could be that the Storeegga Slide tsunami deposit occurs in the upper part of the wide reflector band (upper green line), while an older slide-related turbidite occurs in the lower part of the reflector band (lower green line).

A major task in the present project has been to investigate the interpreted red reflector and its age in all the fjords and to evaluate its cause; climatic variations, a tsunami (possibly caused by an earthquake affecting the offshore area), an earthquake only affecting parts of western Norway, or a combination of an earthquake and a tsunami. The distinction between a tsunami and an earthquake can be made by studying lake sediments at different elevations; tsunami deposits only occur in lakes reached by the tsunami wave, at low elevations. Mass-movement deposits of the same age at both high and low elevations could be interpreted as the result of local earthquakes, but not tsunamis. Also younger and older mass movements, including Storeegga Slide tsunami deposits and pre-Storeegga Slide slide and debrisflow deposits have been studied in the present project, both in fjord and lake sediments.

The work carried out during the project has been executed in several phases, described in the next chapter.



Figure 4. Map showing the location of investigated lakes in Nordfjord and Sunnmøre. R: Rotevatnet; H: Hovdevatnet; N: Nedstevatnet; M: Medvatnet; S: Storsætervatnet.

2. METHODS

2.1 Phase A1

This phase comprised interpretation of seismic data (Fig. 2) and swath bathymetry from several fjords, from Sognefjorden in the south, to Halsafjorden in the north (Fig. 1). Both NGU data and data from Norsk Hydro ASA were used. Based on the interpretations, a coring programme was proposed for dating of interpreted regional reflectors and establishing the origin of the reflectors (Longva et al. 2001a).

2.2 Phase A2

During this phase, penetration echosounder data were acquired from 5 lakes in Sunnmøre and Nordfjord (Fig. 4). The acoustic profiling was done by GeoCore as (Longva and Olsen 2001). The data were processed and interpreted at NGU, and a coring programme, aiming at sampling and dating possible mass-movement deposits, was suggested (Longva and Olsen 2001).

2.3 Phase B1

In this part of the project, a coring cruise with NGU's research vessel FF Seisma was organised. The multipurpose cruise involved testing of a newly developed vibrocorer (HYBAV) as well as sampling for stratigraphical and environmental (heavy metals and dinocysts) purposes. Stratigraphical cores were retrieved at 31 fjord locations (Fig. 1, Table 1, Longva et al. 2001b). Most of the cores were obtained at locations recommended by Longva et al. (2001a), based on the interpretation of seismic profiles. In addition, two box cores and several stratigraphical cores, that were subsampled for environmental analyses, were retrieved. The cruise also involved four days of high resolution (Topas) seismic profiling.

During a coring cruise in November 2001, Norsk Hydro collected 5 long cores from 4 localities by the coring equipment Selcore at sites selected by NGU in Halsafjorden, Julsundet and Sulafjorden (Table 1, Fig. 1) (Geoconsult 2002). In addition, we have had access to 5 Norsk Hydro cores from Ørstafjorden and 2 UiB cores from Breisunddypet (Table 1, Fig. 1).

Table 1. Core inventory, fjords.

Seismic line	Fjord	Core number	X (UTM32)	Y (UTM32)	Latitude WGS84	Longitude WGS84	Water depth (m)	Core length (m)
0002010	Aurlandsfj.	P0103001	399620	6752240	60° 53.5556'	7° 9.008474'	178	1.98
0002011	Aurlandsfj.	P0103002	398844	6750453	60° 52.58125'	7° 8.206415'	73	1.64
0002011	Aurlandsfj.	P0103003	398423	6750180	60° 52.42767'	7° 7.750053'	43	0.78
0002015	Fjærlandsfj.	P0103004	371204	6793299	61° 15.16045'	6° 35.95284'	247	2.30
0002015	Fjærlandsfj.	P0103005	372763	6794625	61° 15.90477'	6° 37.64045'	238	1.93
0002015	Fjærlandsfj.	P0103006	379027	6805562	61° 21.91132'	6° 44.21854'	172	1.60
0102001	Barsnesfj.	P0103007	399035	6791482	61° 14.67339'	7° 7.115135'	82	1.74
0102001	Barsnesfj.	P0103008	399052	6791462	61° 14.66240'	7° 7.134504'	82	1.28
0002015	Fjærlandsfj.	P0103009	369695	6790158	61° 13.43994'	6° 34.39725'	305	1.73
Dalsfj_1B	Dalsfjord	P0103011	305266	6809367	61° 22.15027'	5° 21.35081'	260	0.80
Dalsfj_1B	Dalsfjord	P0103012	308008	6810303	61° 22.74605'	5° 24.36410'	173	1.54
Dalsfj_1B	Dalsfjord	P0103013	308358	6810457	61° 22.83897'	5° 24.74616'	173	1.62
9702003	Førdefj.	P0103014	304986	6822163	61° 29.03091'	5° 20.23141'	340	0.87
0003001	Vanylvsfj.	P0103015	312358	6892247	62° 6.924362'	5° 24.15304'	297	1.64
Syvd fj_1	Syvdsfj.	P0103016	329141	6889338	62° 5.839233'	5° 43.58826'	90	1.35
Syvd fj_1	Syvdsfj.	P0103017	328359	6890251	62° 6.308899'	5° 42.63805'	99	1.44
Syvd fj_1	Syvdsfj.	P0103018	327293	6891540	62° 6.972885'	5° 41.33909'	99	1.49
Syvd fj_1	Syvdsfj.	P0103019	327293	6891555	62° 6.980896'	5° 41.33869'	100	1.58
Syvd fj_1	Syvdsfj.	P0103020	327258	6891591	62° 6.998978'	5° 41.29626'	99	1.14
9909001	Austefj.	P0103021	350294	6887354	62° 5.311890'	6° 7.967291'	317	0.40
0003010	Ørstafj.	P0103022	344780	6901079	62° 12.56035'	6° 9.148121'	172	0.69
9908007	Tafjord	P0103023	416461	6904222	62° 15.62073'	7° 23.47089'	200	0.7
9908008	Tafjord	P0103024	417194	6903270	62° 15.11787'	7° 24.34542'	150	0.95
9908004	Tafjord	P0103025	417187	6903867	62° 15.43922'	7° 24.31981'	190	0.47
9908001	Tafjord	P0103026	416628	6903998	62° 15.50217'	7° 23.67059'	197	1.27
9908009	Tafjord	P0103027	414959	6905842	62° 16.47217'	7° 21.68919'	205	1.00
9908026	Tafjord	P0103028	414892	6905970	62° 16.54015'	7° 21.60833'	207	0.3
9908006	Tafjord	P0103029	414932	6906158	62° 16.64246'	7° 21.64836'	207	1.14
9908006	Tafjord	P0103030	413383	6907603	62° 17.39845'	7° 19.81605'	217	0.83
0003023	Midfjord	P0103031	374839	6947337	62° 38.12500'	6° 33.54000'	253	0.57
SSundalsora	Tingvollfj.	P0103032	444906	6983247	62° 58.48755'	7° 54.79268'	302	0.78
0003010	Ørstafj.	Ørsta-GC1A	348212	6899623	62° 11.8617'	6° 04.9433'	136	1.48
0003010	Ørstafj.	Ørsta-GC1B	348212	6899623	62° 11.8617'	6° 04.9433'	136	1.47
0003010	Ørstafj.	Ørsta-GC2	347897	6900188	62° 12.1583'	6° 04.5517'	137	1.68
0003009	Ørstafj.	Ørsta-GC3	347244	6900268	62° 12.1850'	6° 03.7950'	141	1.92
0003009	Ørstafj.	Ørsta-GC4	346629	6900745	62° 12.4267'	6° 03.0617'	136	1.62
SBreis-Volda	Breisundd.	HM129-03	333849	6931988	62° 28.90'	5° 46.55'	246	2.52
SBreis-Volda	Breisundd.	HM129-04	334074	6931846	62° 28.83'	5° 46.82'	267	2.30
SSt-Breis4	Sulafjord	NGU-2L/SC	349480	6921298	62° 23.5500'	6° 5.2800'	446	4.0
SSt-Breis4	Sulafjord	NGU-3L/SC-1	349646	6921342	62° 23.5783'	6° 5.4700'	443	3.4
SSt-Breis4	Sulafjord	NGU-3L/SC-2	349646	6921342	62° 23.5783'	6° 5.4700'	443	2.0
SHalsafj.	Halsafj.	NGU-4L/SC	459289	6988764	63° 1.5733'	8° 11.7317'	510	7.3
0003025	Julsundet	NGU-6L/SC	395697	6956098	62° 43.2300'	6° 57.6033'	500	6.3

2.4 Phase B2

In this phase of the project, Høgskulen i Sogn og Fjordane (HSF, Sogn og Fjordane College) collected sediment cores from five lakes in Nordfjord and Sunnmøre (Fig. 4, Table 2, Sønstegeard et al. 2001). The cores were mainly taken at locations recommended by Longva and Olsen (2001), based on the interpretation of penetration echosounder profiles. 26

sediment cores, with a combined length of 70 m, were sampled with a modified 110 mm Livingstone piston corer.

Table 2. Core inventory, lakes.

Lake name	Altitude m a.s.l.	Core number	Latitude (WGS84)	Longitude (WGS84)	Time on seismic data	Water depth (m)	Core length (cm)	X-ray images	Density	Mag. suscept.
Storsetervatnet	277	S1	61 56 481	06 08 312	13:20:25	9	220	x	x	x
Storsetervatnet	277	S2	61 56 740	06 08 328	14:59:53	11	49	x		
Storsetervatnet	277	S3	61 56 778	06 08 282	15:00:47	9	234	x	x	x
Storsetervatnet	277	S4	61 56 772	06 08 302	15:00:23	9	350	x		
Storsetervatnet	277	S5	61 56 778	06 08 213	15:06:55	6	219	x	x	x
Storsetervatnet	277	S6	61 56 758	06 08 315	15:00:07	10	264	x	x	x
Storsetervatnet	277	S7	61 56 776	06 08 292	15:00:33	9	214	x		
Storsetervatnet	277	S8	61 56 798	06 08 218	14:47:50	6	251	x		
Storsetervatnet	277	S9	61 56 615	06 08 525	14:12:35	6	250	x		
Storsetervatnet	277	S10	61 56 800	06 08 249	14:47:00	6	484	x	x	x
Medvatnet	12,5	M1	62 01 929	06 02 923	12:28:58	21	154			
Medvatnet	12,5	M2	62 01 941	06 02 887	12:29:17	22	332	x	x	(x)
Medvatnet	12,5	M3	62 01 740	06 02 726	12:50:45	19	133			
Medvatnet	12,5	M4	62 01 717	06 02 650	12:51:37	19	350	x	x	x
Medvatnet	12,5	M5	62 01 700	06 02 562	12:52:48	21	210	x		
Medvatnet	12,5	M6	62 01 733	06 02 544	12:53:02	22,5	242	x	x	
Nedstevatnet	9	N1	62 02 223	06 02 833	15:50:20	17	540	x	x	x
Nedstevatnet	9	N2	62 02 217	06 02 730	15:49:21	15	383	x	x	x
Nedstevatnet	9	N3	62 02 246	06 02 934	15:51:30	17	330	x	x	x
Nedstevatnet	9	N5	62 02 209	06 02 944	15:36:25	18	313	x	x	(x)
Rotevatnet	47	R1	62 08 517	06 05 831	17:23:52	6	290	x	x	x
Rotevatnet	47	R2	62 08 524	06 05 853	15:12:02	8	231	x		
Rotevatnet	47	R3	62 08 434	06 05 928	13:14:45	12,5	290			
Hovdevatnet	73	H1	62 11 315	06 02 732	13:10:49	15	290	x	x	x
Hovdevatnet	73	H2	62 11 183	06 02 664	12:10:09	14	170	x		
Hovdevatnet	73	H3	62 11 207	06 02 666	12:10:40	14	150	x		

2.5 Phase C

All the laboratory work on cores from fjords and lakes was executed during Phase C. This included multisensor core logging (MSCL), x-ray inspection (XRI), sedimentological description, measurement of physical and geotechnical parameters, ¹⁴C dating and grain-size analysis (Lepland et al. 2002).

2.6 Phase D

This phase of the project involved a compilation of existing data on rock avalanches, gravitational bedrock fractures and neotectonic faults onshore western Norway (Blikra et al. 2002).

2.7 Phase E

This final report, which is a compilation report comprising project results and discussions.

3. CLIMATE, MASS-MOVEMENT ACTIVITY AND HUMAN INFLUENCE OVER THE PAST 11 500 YEARS (10 000 ¹⁴C YEARS)

The occurrence of floods and mass movements is influenced by many parameters, e.g. climate (precipitation), sea-level changes, human activity (agriculture/deforestation) and tectonic movements (earthquakes). The frequency of slides, debrisflows and floods on land and in fjords is generally governed by one of, or a combination of these parameters. This is important for the risk assessment of floods and slides/debrisflows today. Below, we present a short overview of the available data on climate, mass movements and flood activity over the past 11 500 years with a focus on the period after 4000 BP, in Mid-Norway.

3.1 Palaeoclimatic data

An overview of the vegetational history has been compiled by Hafsten (1987):

- The period 11 500-10 000 BP (10 000-9000 ¹⁴C BP) is characterized by pioneer vegetation partly reflecting unstable growth conditions, e.g. along river banks. Due to limited vegetation and rapid land uplift, the river banks were highly unstable.
- From 10 000 to 9000 BP (9000-8000 ¹⁴C BP) a warmer and dryer climate predominated. Large pine woods contributed to stabilisation of river valleys.
- A warmer and more humid climate characterises the period 9000-5000 BP (8000-4500 ¹⁴C BP). A diverse vegetation contributed to stabilisation of river banks.
- A cooler and more humid period started around 5000 BP (4500 ¹⁴C BP), with a reduction in the vegetation diversity as a result.
- The first traces of human activity (grazing by cattle) occur at 5000 to 4500 BP (4500-4000 ¹⁴C BP). More intense grazing and deforestation took place during 4000 to 3200 BP

(3500-3000 ¹⁴C BP). The first traces of grain harvesting occur around 2000 BP (2000 ¹⁴C BP).

Studies in other parts of Scandinavia and Britain show a similar evolution with a lowering of tree limits at ca. 5800 BP (5000 ¹⁴C BP) (Selsing and Wishman 1984, Kullman 1988, Gunnarsdóttir 1996). Vegetation and upper tree limits studies show a regional climatic deterioration from ca. 4500 BP (4000-3800 ¹⁴C BP) both in Scandinavia and in Britain (Bennet 1984, Birks 1988, 1990, Kullman 1988, 1989, 1993, Gunnarsdóttir 1996). The reason for the lowering of the three limits in mountain areas in Sweden is thought to be increased precipitation as snow and lowering of the snow line.

A general climatic deterioration since ca. 6000 BP is evident from studies of glacier fluctuations and other types of proxy records (e.g. Dahl and Nesje 1996, Gunnarsdóttir 1996, Nesje et al. 2000, Barnett et al. 2001). Neoglacial phases are recognized since 4000 BP (Karlén and Matthews 1992, Nesje et al. 1995a, Matthews et al. 2000, Nesje et al. 2000, 2001) and although the mass balance of glaciers in western Norway is controlled mainly by changes in winter precipitation (Nesje et al. 1995b), significant decrease in summer temperatures after ca. 4000 BP is indicated by tree-line data (Dahl and Nesje 1996) and the vegetation history of eastern Jotunheimen (Gunnarsdóttir 1996) and Leirdalen (Barnett et al. 2001). The division of the Holocene into a warmer and a colder period is, however, too simplistic, because there is growing evidence of short-term climatic fluctuations during the Holocene. In northern Jostedalbreen, Nesje et al. (2000) recognized 41 periods of relatively large glaciers and 36 periods of relatively small glacier, with mean return periods of 150±10 and 210±15 years, respectively.

3.2 Climatic influence on mass movements and flood activity

The frequency of snow avalanches and mudflows in Sogn og Fjordane, Møre og Romsdal and Jotunheimen has previously been studied by Blikra and Nemeč (1998), Blikra and Selvik (1998) and Sletten et al. (2002). In addition, a study of flood activity over the past 5000 years has been undertaken in Atnsjøen in eastern Norway (Nesje et al. 2001).

Blikra and Nemeč (1998) estimated the temporal frequency of Holocene debrisflows at 17 localities in western Norway. Their radiocarbon dates, though quite limited, are consistently younger than ca. 5800 BP (5000 ¹⁴C BP) and indicate an increase in debrisflow frequency after ca. 3200 BP (3000 ¹⁴C BP). This corresponds with an increase in waterflow processes in some colluvial systems (Blikra and Nemeč 1993a, b). In Leirdalen in western central Norway, Matthews et al. (1997) recognized an increase in debrisflow activity between 4400 and 2000-2200 BP (3800-2300 ¹⁴C BP) and again after 1600/1300 BP (1600 ¹⁴C BP). An adjacent locality in Leirdalen indicates an increase in slopewash processes some time after 3200 BP (3000 ¹⁴C BP) (Matthews et al. 1986). An increase in soil erosion around Vanndalsvatnet (45

km west of Leirdalen) and triggering of turbidity currents in the lake after 2000 BP was identified by Nesje et al. (1991), who attributed it to short-lived climatic events, such as heavy rainstorms and/or rapid seasonal snow or ice melting. In the Ålfotbreen area, 35 km from the coast, Nesje et al. (1995a) recognized a period of increased erosion and massflow activity around lake Grøndalsvatn in the period 3100-2700 BP. Sletten et al. (2002) studied debris-flow activity in the lake Ulvådalsvatn, south of Romsdalen, and demonstrated an increased frequency of events from ca. 2200 BP. The earliest debrisflow event in Ulvådalsvatnet is ca. 7300 years old, with another around 5200 BP. Many floods have occurred over the past 3000 years in Atnsjøen (Nesje et al. 2001), and especially during the last 1200 years.

These previous findings are from different localities and morphological settings, with varying levels of chronostratigraphic resolution, and detailed comparisons thus requires caution. However, the studies jointly indicate an increase in slope-wasting processes since ca. 5800 BP (5000 ¹⁴C BP) and particularly after 3200 BP (3000 ¹⁴C BP). At several sites there is another increase in the frequency of debrisflows around 2200 BP. A similar trend has been recognized elsewhere in Scandinavia (Jonasson 1991, 1993), suggesting a regional increase in the frequency of intense rainstorms in the latest Holocene.

3.3 Timing of high mass-movement activity

The frequency of turbidites, slide and debrisflow deposits in fjords is strongly influenced by flood activity in rivers entering the fjords and by stability of sediments along the fjords. The flood activity is influenced by precipitation (extreme rainfall), slides damming rivers and human activity. Other important factors are sea level changes and tectonic activity.

The period 11 500-10 000 BP (10 000-9000 ¹⁴C BP) was characterized by high flood- and mass-movement frequency. This was probably a period of strong earthquakes (Olesen et al. 2000, NORSAR 2001), and rapid isostatic rebound combined with an open vegetation caused extensive erosion of river banks and fjord margins.

An increase in farming and grazing opened the forest and contributed to a destabilisation of the ground after 4000 BP (3500 ¹⁴C BP). This, combined with an increase in precipitation and a higher number of large spring floods due to increased precipitation as snow (see references in Chapter 3.1 and 3.2), may have led to unstable river banks, higher sediment transport and a higher frequency of turbidity currents in the fjords. Slopewash processes and debrisflow activity seem to have been prominent in a phase after ca. 3200 BP and after 2200 BP.

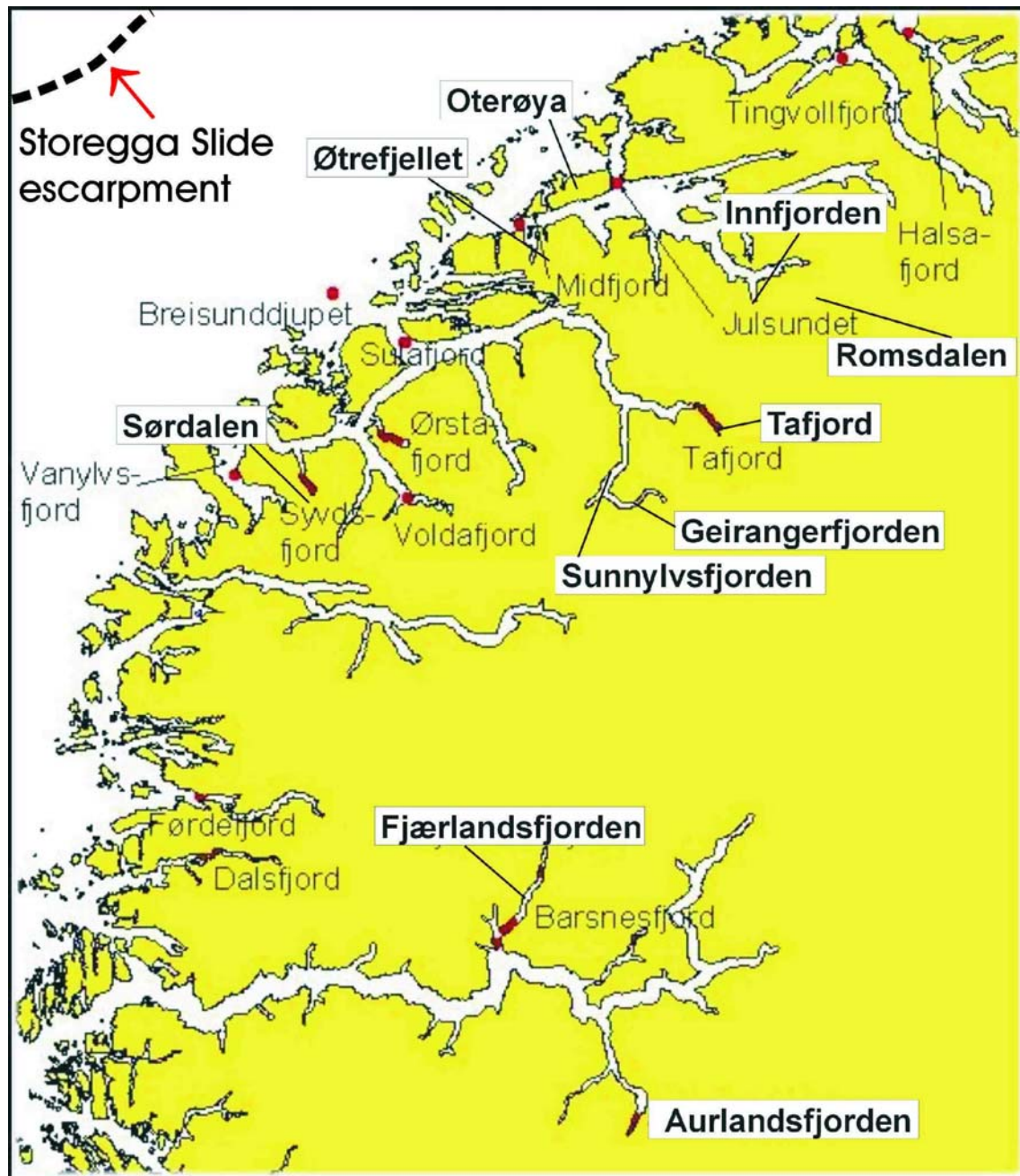


Figure 5. Map showing the location of investigated areas on land.

4. ROCK AVALANCHES, GRAVITATIONAL FRACTURES AND NEOTECTONIC FAULTS ON LAND

This chapter comprises a summary of the main results of Blikra et al. (2002b). Selected examples and an overview of the regional occurrence of gravitational slope failures in the studied areas in Møre og Romsdal and Sogn og Fjordane (Figs. 5 and 6) are presented. Geological studies show that several areas in western Norway have been affected by a

significant number of large rock avalanches throughout the postglacial period. More than 100 individual events displacing more than 1 mill. m³ of material have been located, with the largest avalanche estimated to have a volume of about 100 mill. m³, in Tafjorden. The geographic distribution of rock avalanches and gravitational bedrock fractures clearly shows a clustering in specific zones (Fig. 6), with the highest frequency in the inner fjord areas of western Norway. The highest number of such features is found in Romsdalen and Tafjord. Clusters of rock-avalanche deposits and gravitational bedrock fractures are also found in two smaller areas, around Oterøya and Syvdsfjorden, while distinct clusters of gravitational failures occur in the phyllite areas in Aurland. Fig. 7 shows the distribution of historical rock avalanches that have created tsunamis.

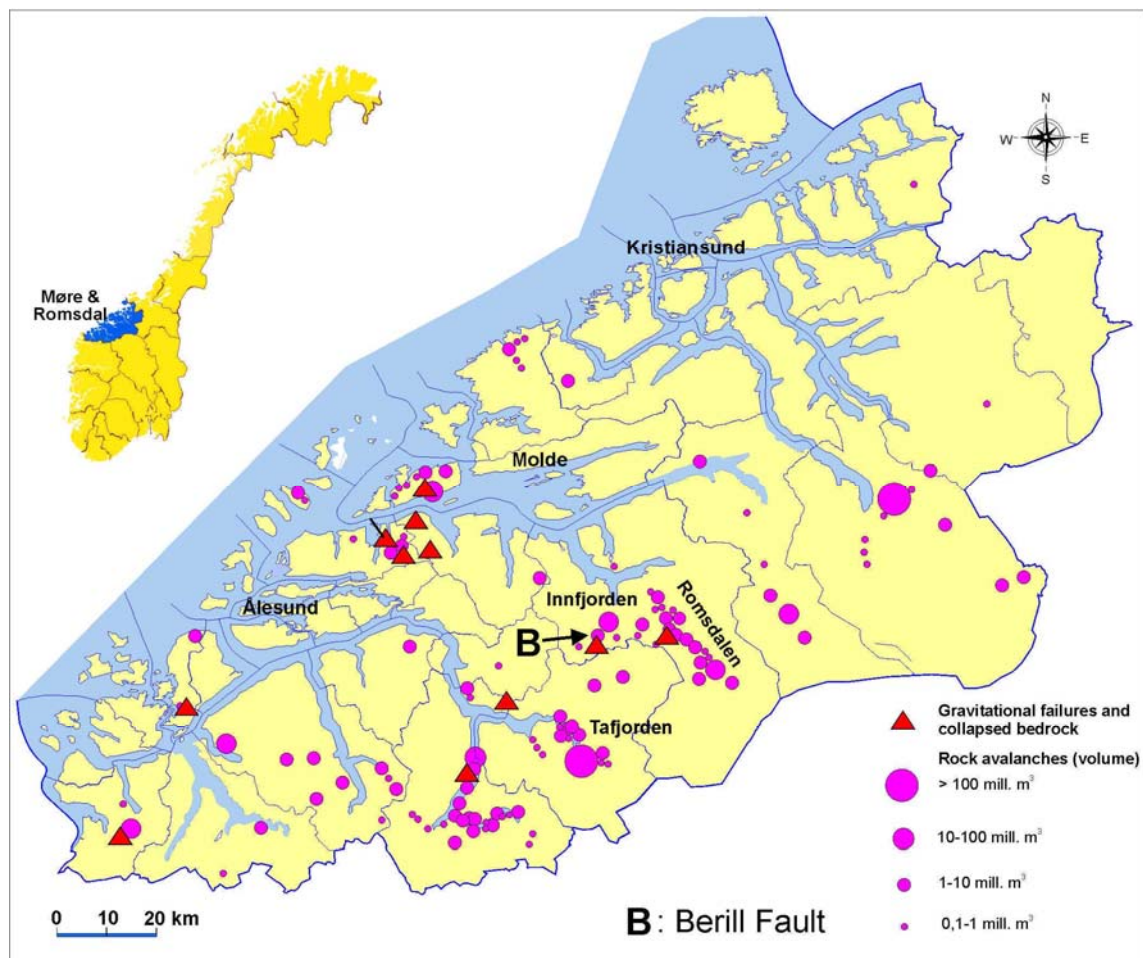


Figure 6. Rock avalanches and gravitational fractures in Møre og Romsdal.

4.1 Romsdalen and Innfjorden

One of the largest concentrations of rock avalanches on land is found in Romsdalen (Fig. 8), where more than 15 large rock avalanches cover almost the entire valley floor over a distance of 25 km. Debrisflow deposits, generated by the rock-avalanche impact on the valley floor,

are often found outside the bouldery rock-avalanche deposits. A large rock avalanche occurs at Venje. Coal below the avalanche deposits has been radiocarbon dated and ages of 1992-1882 BP and 1413-1352 BP have been obtained. The elevation of the deposits, only 10 meters above the present sea level, also indicates a young age. Many of the rock-avalanche deposits in Romsdalen are situated below the marine limit, but are unaffected by later fluvial erosion or marine sedimentation, showing that they were formed on land after 5000 BP, when this area became dry land.

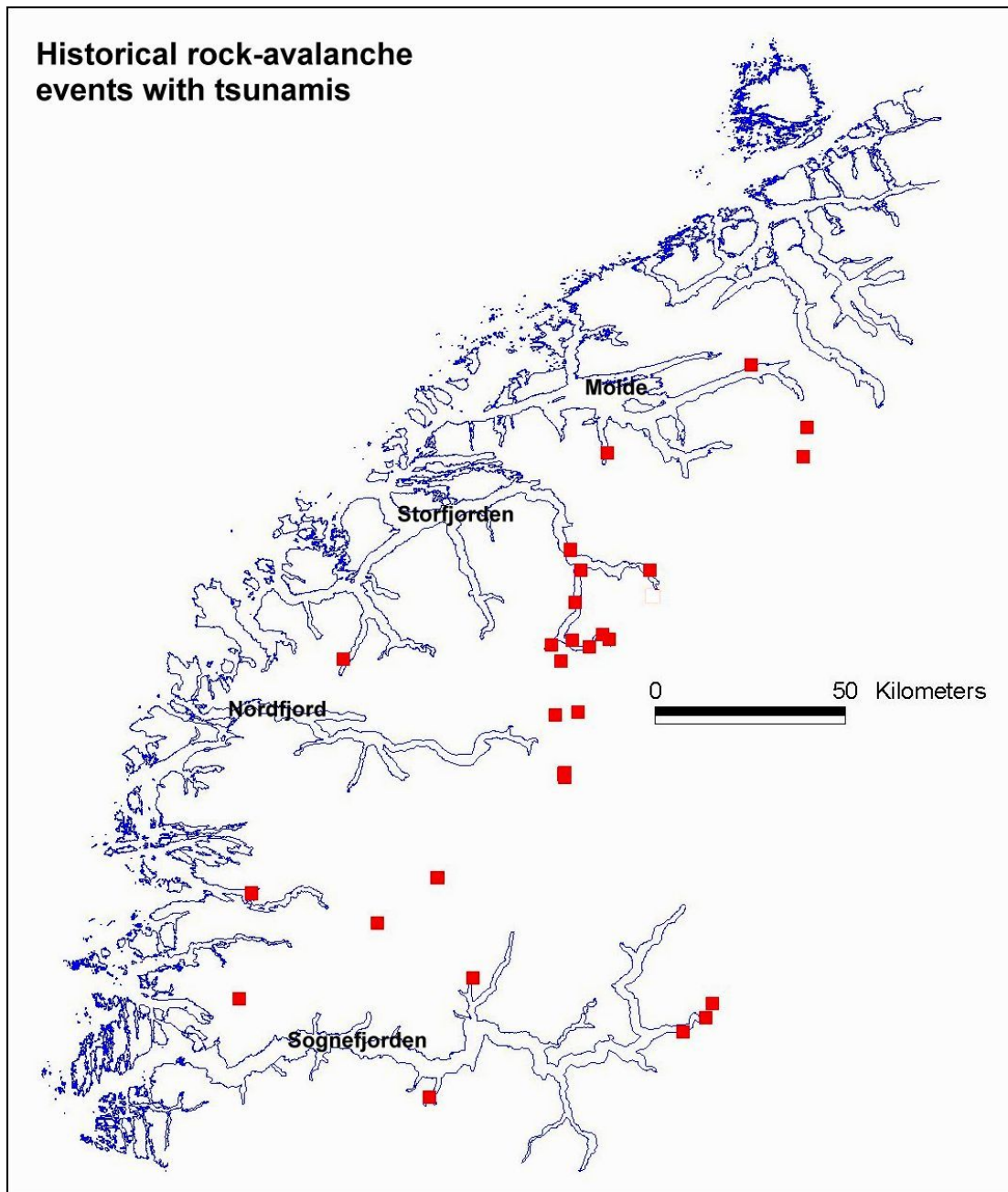


Figure 7. Historical rock-avalanche events with related floodwaves/tsunamis in Møre og Romsdal and Sogn og Fjordane. Source: historical database (NGU/Astor Furseth).

Several mountain slopes with significant instability and faulting have been observed in this region. One of the largest is a 2 km long area at Børa (Fig. 9). Typical deformation features include more than 20 m deep crevasses, demonstrating considerable horizontal displacement (Fig. 10). Rock avalanches from this area are deposited in the Romsdalen valley (Fig. 8). The largest has nearly crossed the valley and formed distinct concentric ridges by deforming the underlying valley-fill sediments. A radiocarbon date in peat above this deposit gave an age of 5919-5763 BP (5118 ± 43 ^{14}C BP), which is a minimum age of the event.

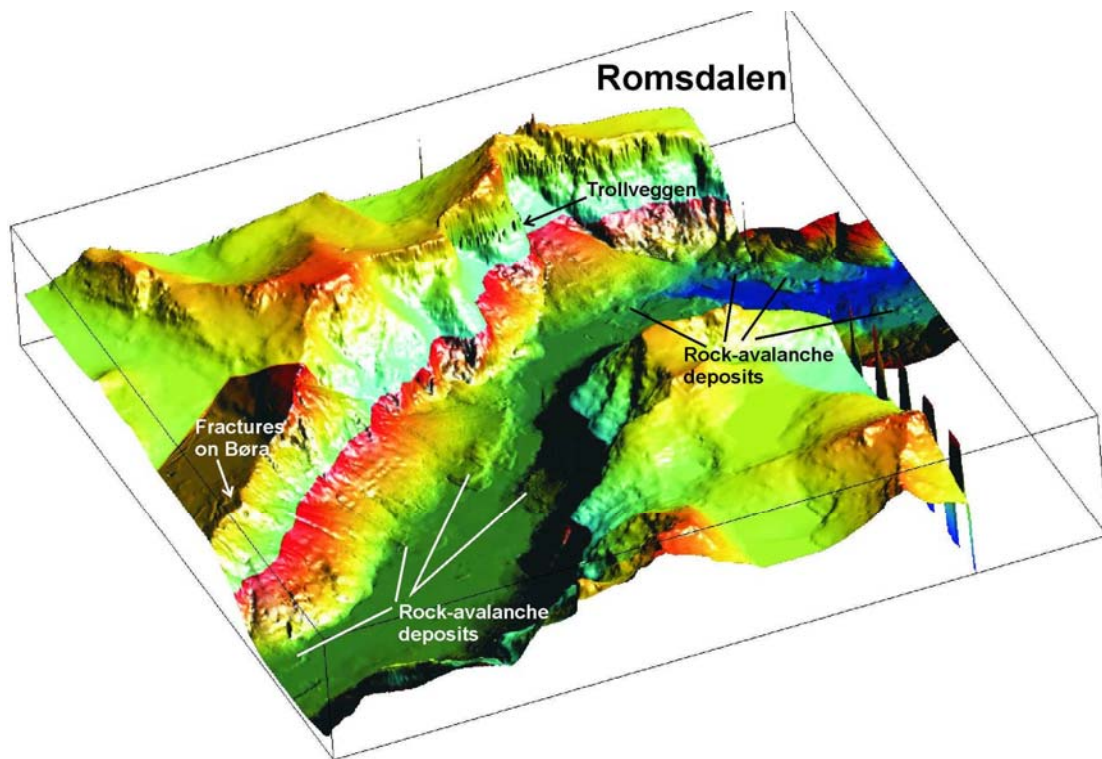


Figure 8. 3D image from Romsdalen based on topographic data in scales 1:50 000 (above 600 m a.s.l.) and 1:5000 (up to 600 m a.s.l.). Note that large parts of the valley is affected by rock avalanches, shown by lobes and irregular surfaces.

The Berill fault in Innfjorden is the first example of a neotectonic fault in southern Norway (Blikra et al. 2002b, Anda et al. 2002) (Fig. 11). The observed lineament is ca. 2 km long, but probably it has a continuation towards the south. The fault escarpment trends SSW-NNE, and is up to 6 m high (generally 2-4 m). This indicates an aspect ratio of less than 10^{-3} , which is at least a factor of ten too large (ratios in the range 10^{-4} to 10^{-5} are common), indicating that only a small part of the fault trace reaches the surface. Moreover, reverse faults like this one are more easily "hidden" in rugged topography than elsewhere. The fault can be traced from about 400 m a.s.l., close to the valley floor, upslope across a relatively steep mountain side and across a mountain ridge ca. 1200 m a.s.l. The structure cuts through till in the lowermost

part, and truncates avalanche-dominated colluvial fans higher on the slope. The till, and especially the colluvial fan, are offset by several meters along the fault. The colluvial fan at this location is interpreted to be formed by snow-avalanches, active at present. Snow avalanches post-dating the actual faulting have not modified the fault scarp significantly. This implies that the faulting is young, at least younger than the Younger Dryas.

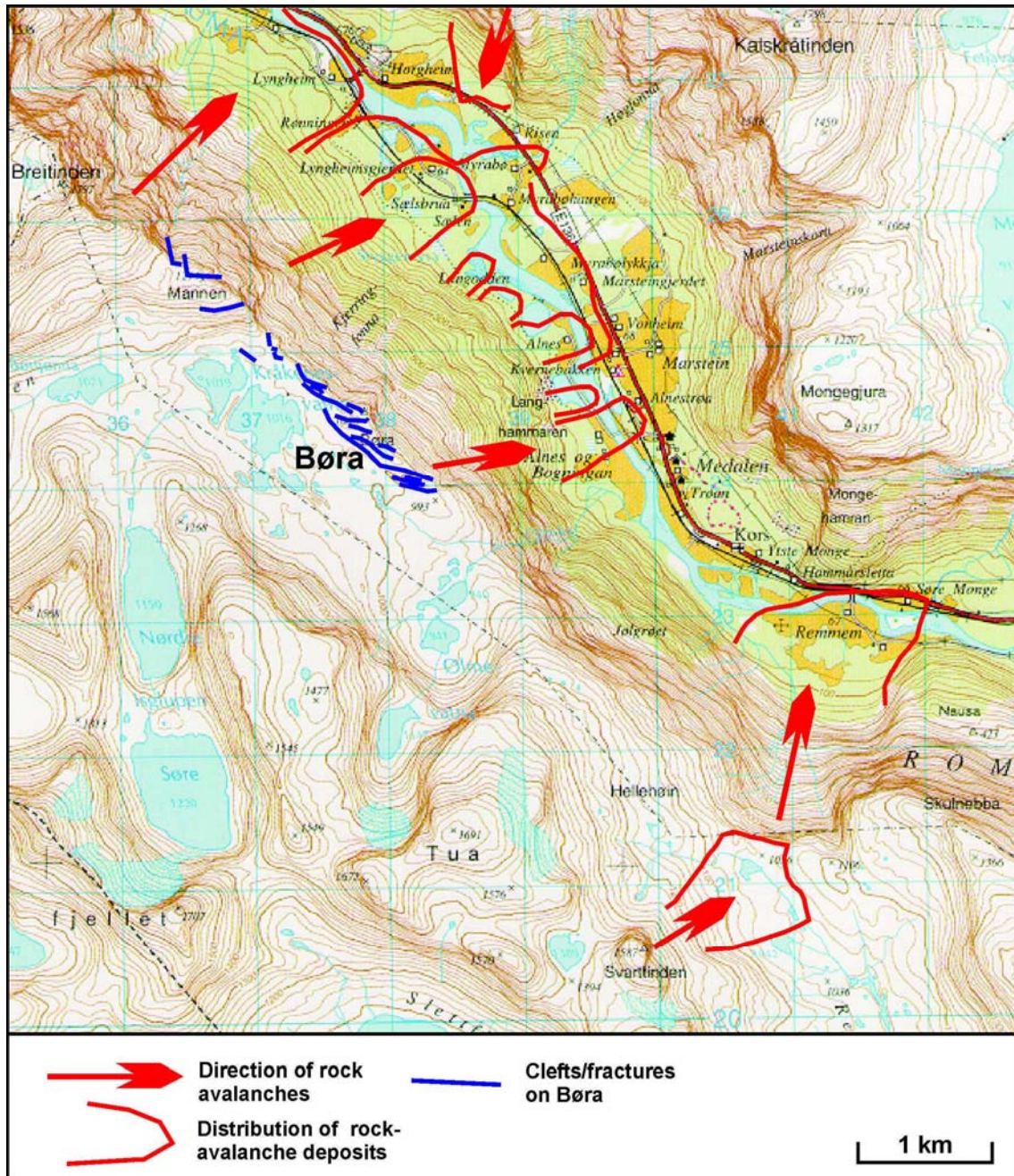


Figure 9. Topographic map from Romsdalen showing fractures on Børa and distribution of rock-avalanche deposits.



Figure 10. The unstable mountain plateau on Børa in Romsdalen seen from a helicopter. Note the deep and long fractures, cutting into glacial till and bedrock. View towards the northwest.

The moderate modification of the fault scarp may indicate that the faulting occurred during the second half of the Holocene. The Berill fault occurs in an area characterised by a high number of rock-avalanches (Fig. 6). A series of rock avalanches and fractures have been mapped in the nearby Romsdalen valley, 15-20 km to the east. At least 4 large rock avalanches occur 4-6 km down-valley from the Berill area, and at least one of them triggered a major, secondary debrisflow, which descended several kilometres down the valley. Excavations and dating results have demonstrated that the debrisflow is younger than 3800 BP. Furthermore, there are historical indications of a large rock-avalanche in 1611 AD. It is reasonable to believe that the high number of rock-avalanches in this region are controlled and triggered by relatively young seismic events. This implies that large earthquakes and local surface deformation can occur today (as supported also by other arguments, see NORSAR 2001), possibly triggering failures both on land and in the fjords. It is worth noting that Innfjorden is situated in the area of the highest present uplift gradient in western Norway (Dehls et al. 2000).

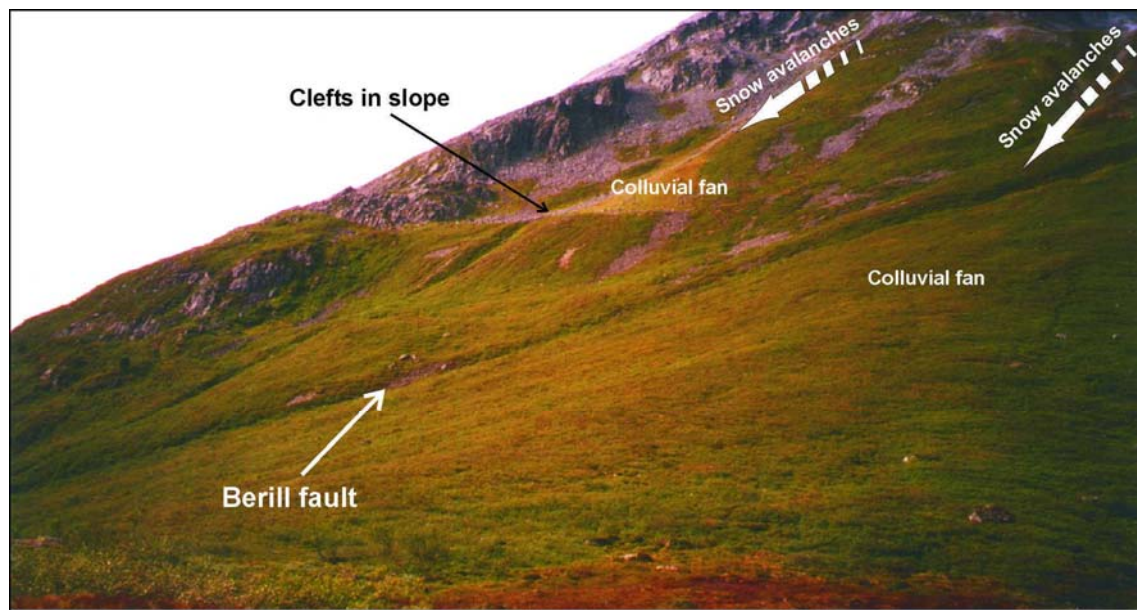


Figure 11. The postglacial Berill fault. Note that the fault clearly truncates the colluvial fan and displaces it several meters (up to the right). See Fig. 6 for location of the fault.

4.2 Tafjord-Geirangerfjord-Sunnylvsfjord

About 3 million m³ of rock and talus avalanched into Tafjorden in 1934, and the tsunami generated by the slide reached a maximum height of 62 m above sea level, killing 40 persons. The geological mapping reveals a high number of slide scars in the fjord sides, and about 10 large rock-avalanche lobes are recorded in the fjord (Figs. 12-13).

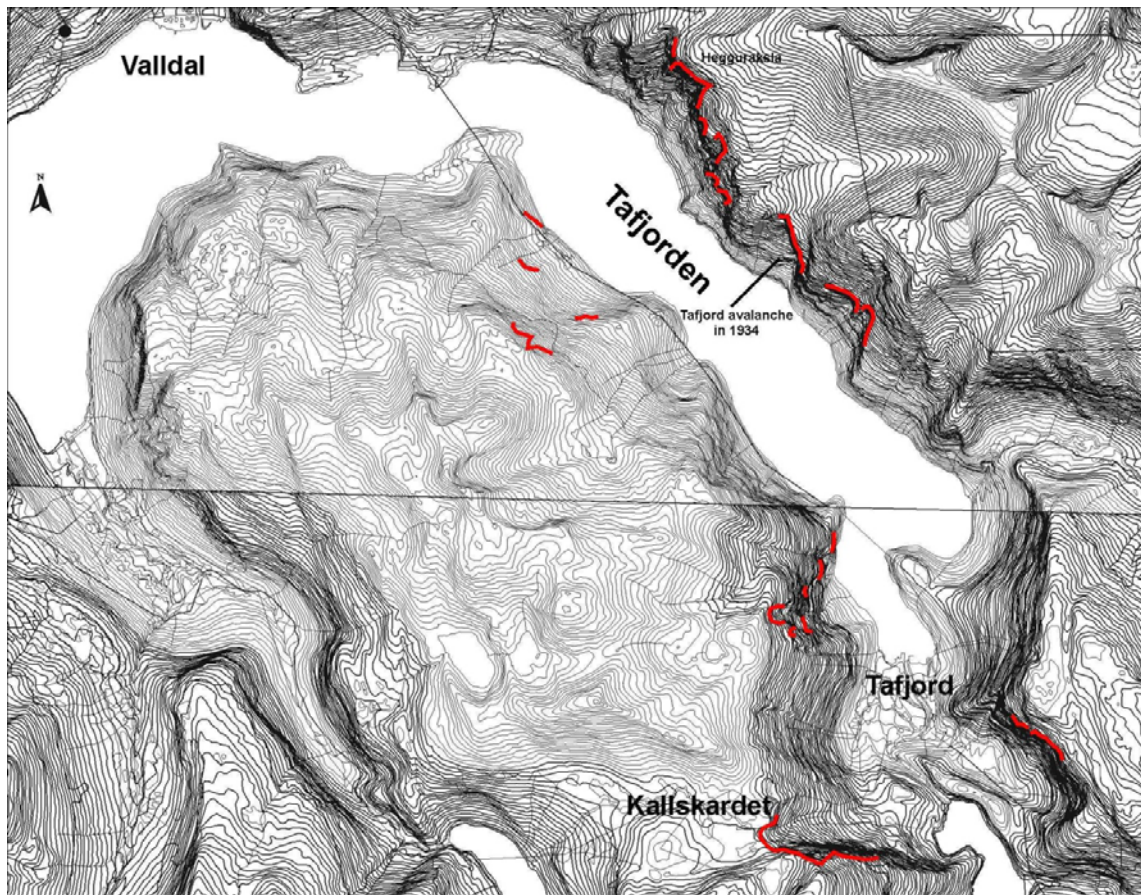


Figure 12. Topographic map of the Tafjorden area. The most prominent slide scars are shown.

Swath bathymetry shows the morphology of individual deposits (Fig. 13). The seismic data (Fig. 14) and lithostratigraphy (see chapter on fjord investigations), demonstrates that events are spread throughout the postglacial time, particularly in the second half of the Holocene. Older, more voluminous rock-avalanche deposits are identified below the 1934 slide deposits. The 1934 event is illustrated in Fig. 15. An enormous rock avalanche, which is estimated to be more than 100 million m³, occurs at Kallskardet (Fig. 12) The avalanche debris can be traced into the fjord with an outrun distance of more than 2 km along the fjord bottom.

Swath bathymetry and seismic data have also been acquired in Geirangerfjorden and Sunnlyvsfjorden (Fig. 5), demonstrating a high number of rock-avalanches in these fjords. Large areas of Geirangerfjorden are covered by bouldery rock-avalanche deposits, but they are generally smaller than in Tafjorden. No cores have been obtained, and the seismic stratigraphy is yet to be studied.

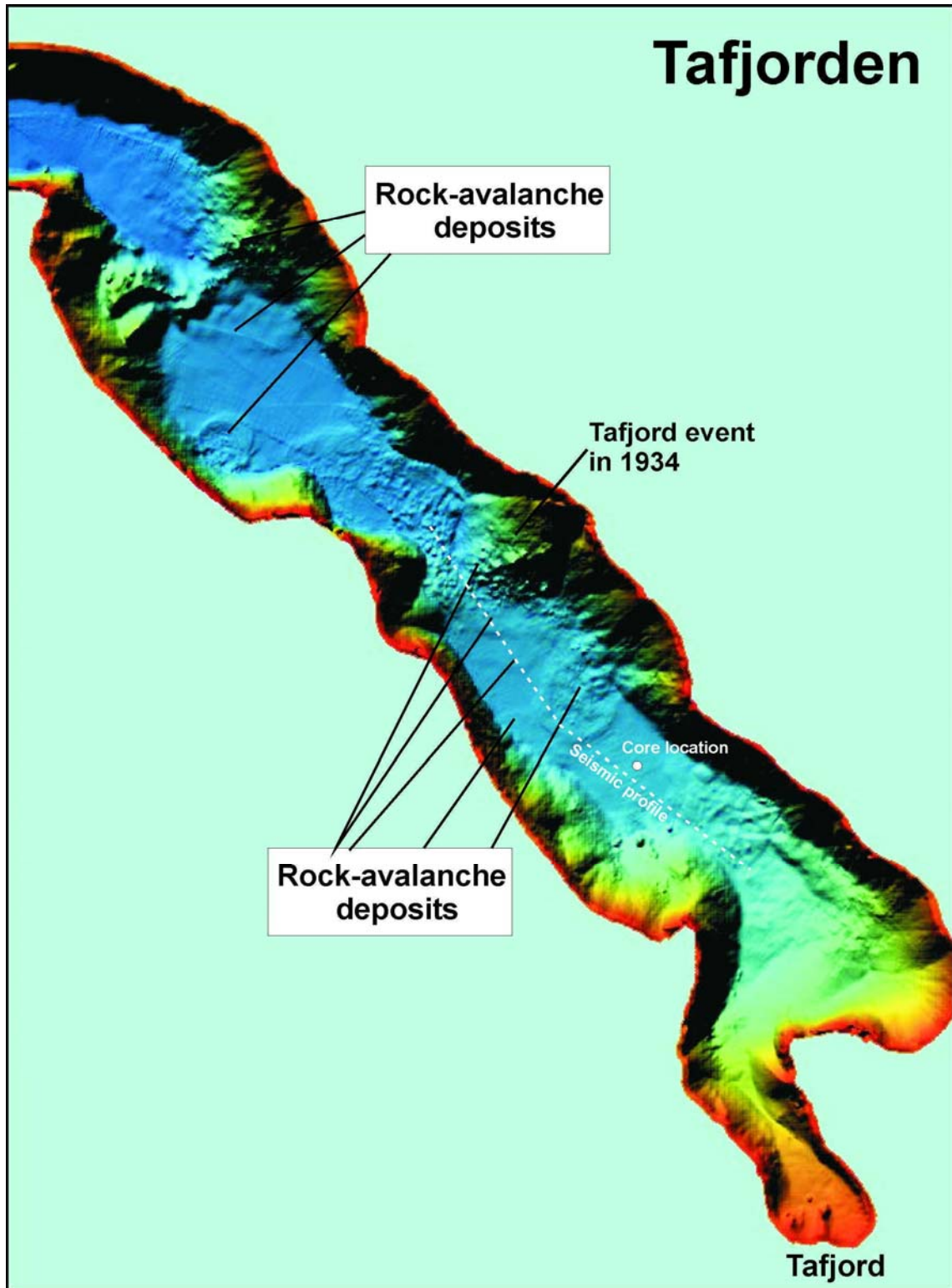


Figure 13. Shaded relief map from Tafjorden based on swath bathymetry. The location of the seismic profile in Fig. 14 is shown.

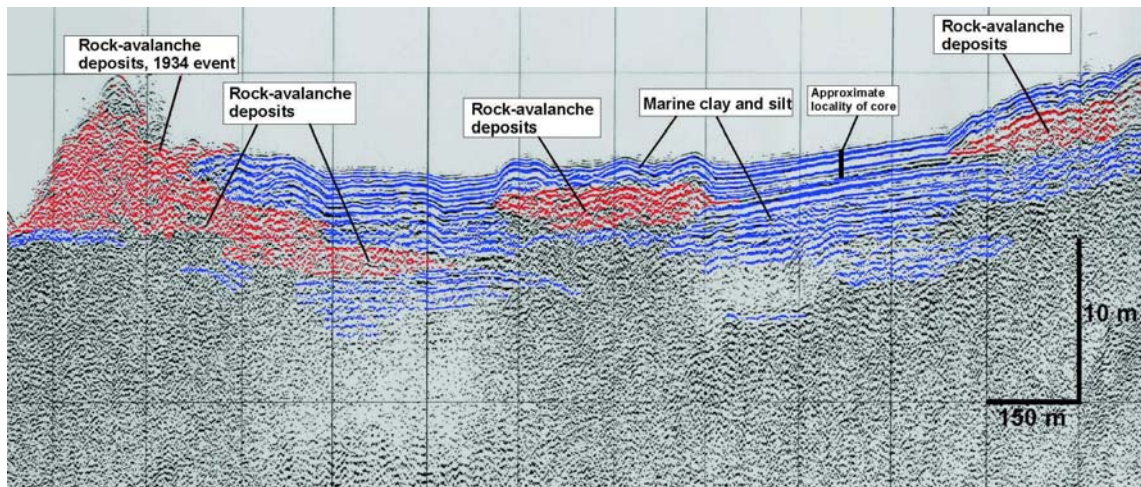


Figure 14. Seismic profile from Tafjord showing the relationship between rock-avalanche deposits and finer-grained marine sediments. See location of seismic profile in Fig. 13.

4.3 Øtrefjellet, Oterøya and Sjørdalen

Øtrefjellet is situated on the peninsula northeast of Ålesund (Fig. 5). A bedrock ridge is cut by fractures and clefts oriented in two main directions; sub-parallel to the ridge (SSW-NNE), and almost transverse to the ridge (E-W). The ridge is surrounded by a series of large rock-avalanche deposits. Bedrock failures with well-defined slide scars have developed into large rock avalanches with well-defined frontal lobes. The features observed on Øtrefjellet are postglacial since they occur far below the upper limit of the maximum Weichselian ice sheet. Parts of the mountain slopes on Øtrefjellet are probably too gentle to initiate slope failures by gravitation alone, and a large magnitude earthquake is therefore called for in this case. Cores from a lake downslope show that the bedrock failures occurred prior to the end of the Younger Dryas.

Several rock-avalanche deposits occur on the northern part of Oterøya (Fig. 5), and an unstable mountainside has been reported at Opstadhornet, along the southern slope of the island (Robinson et al. 1997, Blikra et al. 2001). Open crevasses and clefts, reflecting block sliding, are found in a 1 km wide area, from the sea level up to an elevation of 700 m. Several mega-blocks are identified. Some have moved downslope 10-30 m (Fig. 16). On the plateau around Opstadhornet, 1-2 m deep clefts in the soil and moraine indicate reactivation of fractures. In the lowland, near the foot of the mountain-side, at least two clefts show that blocks have been downfaulted by 2-5 m. They indicate that the entire slope down to sea level has experienced or experiences movements.

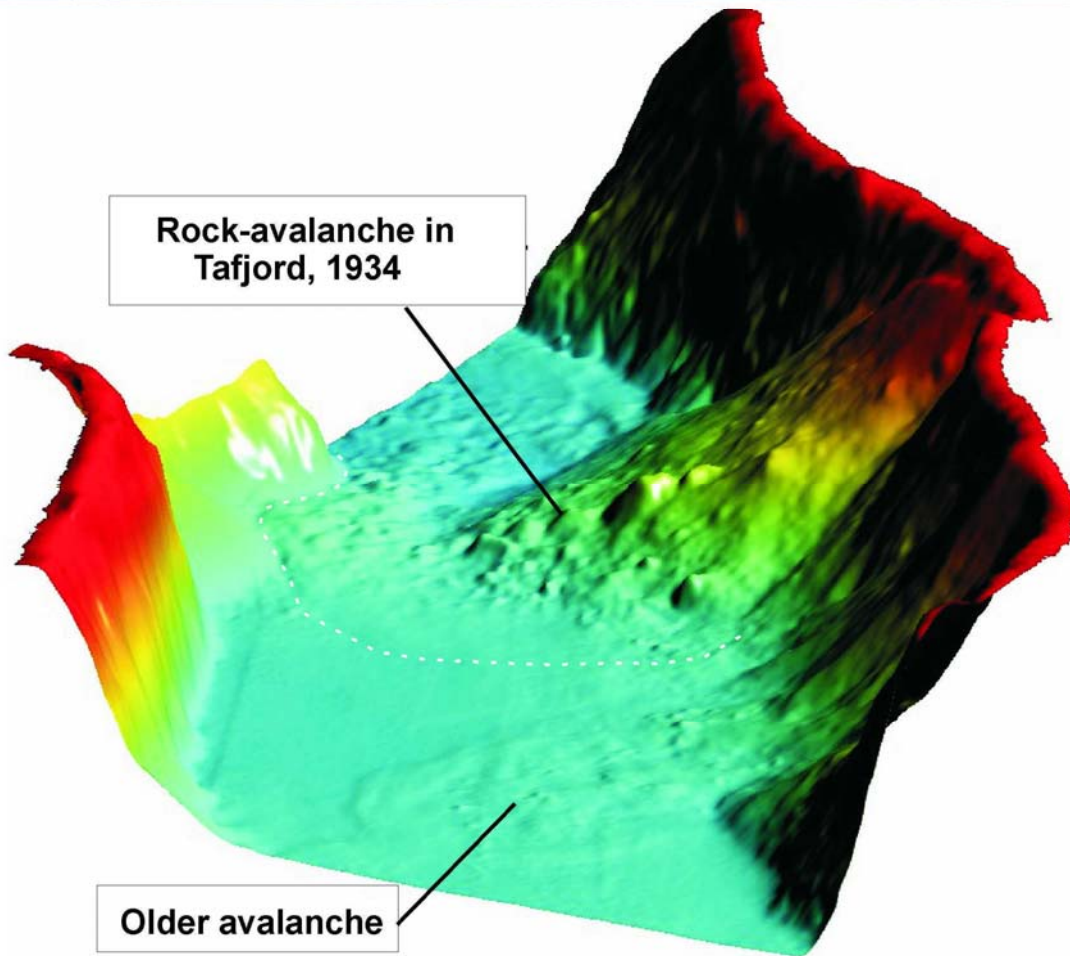
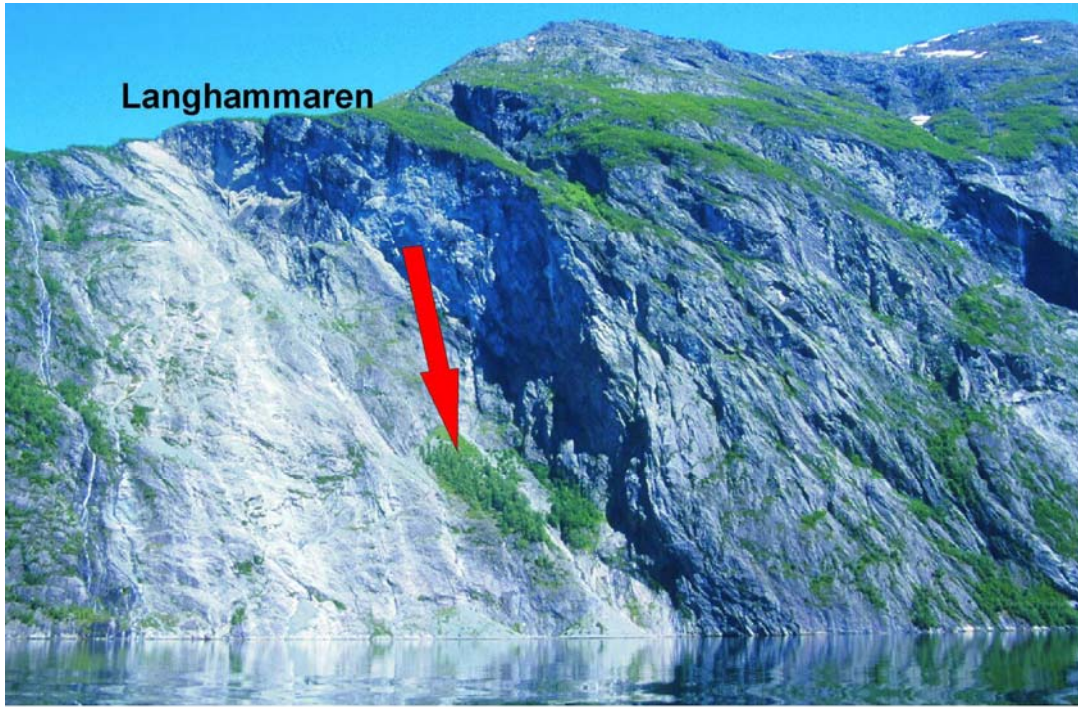


Figure 15. Langhammaren in Tafjord, with the slide scar of the 1934 event. The 3D image shows the rock-avalanche deposits in the fjord. View towards the north.



Figure 16. Oppstadhornet. View from the north, showing the master fault in the back of the collapse field, and a major, wide-open cross-crevasse (from Blikra et al. 2001).

A series of fractures occur on the mountain Storhornet south of Syvdsfjorden (Fig. 5). A large, potential slide block is sitting on the flank of the mountain. Several rock avalanches have been initiated on this unstable mountain slope, and the entire southern part of the Sjørdalen valley is covered by bouldery and hummocky rock-avalanche deposits. Also the northern part shows distinct ridges with large blocks. Excavations show that only the upper meter seems to comprise mass-movement deposits. The sea level-stand was no higher than 10 m during deposition of the rock-avalanche deposits, which occur 12 m above the present sea level, without signs of reworking by fluvial processes. This shows that the event is younger than the Younger Dryas.

4.4 Sogn og Fjordane and Hordaland

A reconnaissance study based on interpretations of aerial photos in a 20 km wide zone from Odda in Hardanger to Aurland in Sogn was carried out by Blikra et al. (2000a). More than 20 areas of gravitational faults and/or large rock avalanches were observed (Fig. 17). These occur along a SSW-NNE trend from Odda to Aurland, and include the gravitational fractures and

rock avalanches described from Flåmsdalen and Aurlandsfjorden (see below). Many rock avalanches also occur in Nærøyfjorden, Fjærlandsfjorden, the inner fjord system of Sognefjorden (Lustrafjorden-Fortun) and in the inner Nordfjord area.

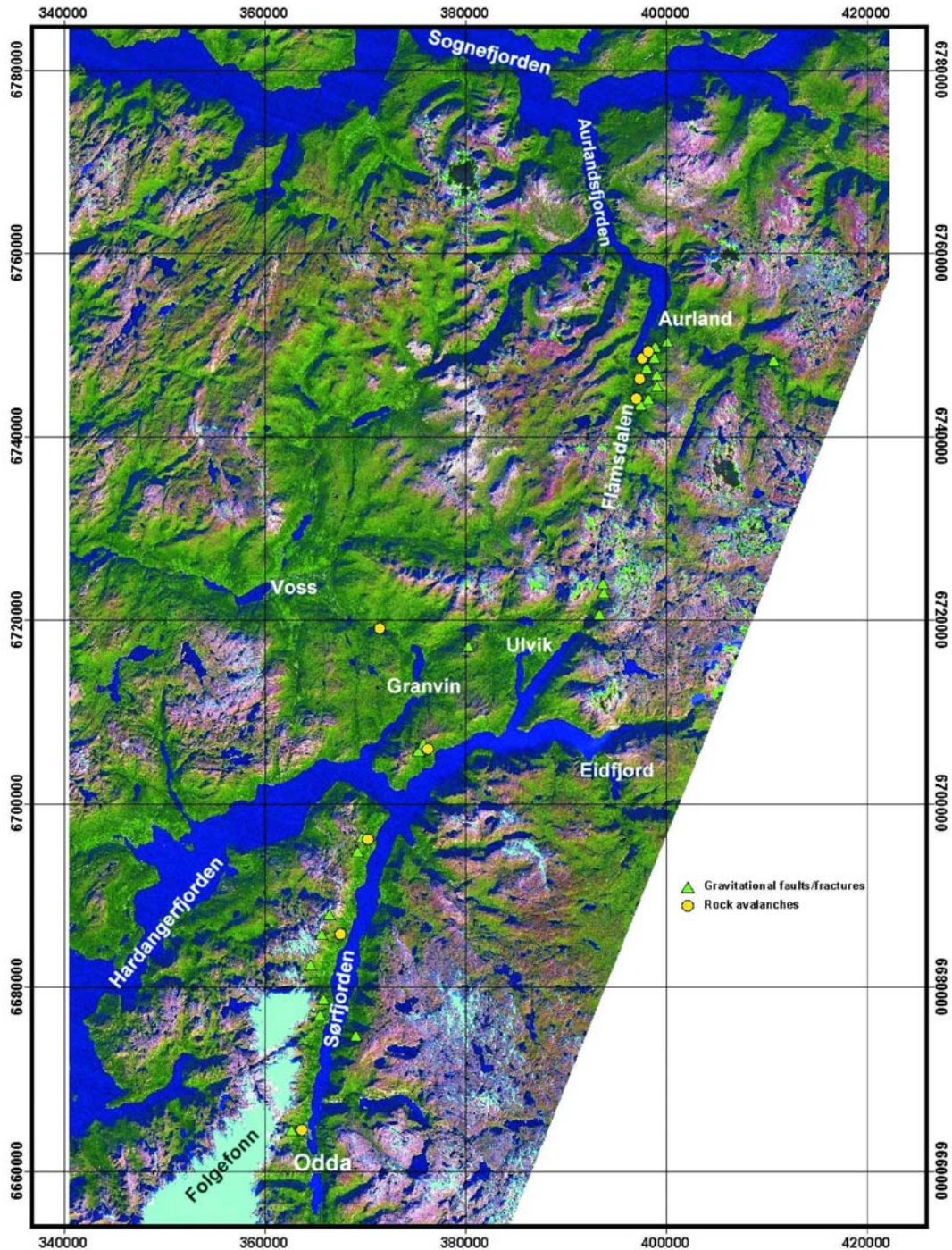


Figure 17. Satellite image showing locations of gravitational-slope failures in an area from Odde in Hardanger to Aurland in Sogn. An interpretation of aerial photos has been done in a 20 km wide area from Odde to Aurland. The line spacing is 20 km. From Blikra et al. (2000a).

4.4.1 Aurlandsfjorden

A range of instability features have been mapped in the phyllite areas of the Aurland-Flåm region (Figs. 17 and 18) (Blikra et al. 2002a, b). Geological mapping demonstrates that a series of rock avalanches, creep features and gravitational bedrock fractures occur in a SSW-NNE zone 11 km long (Fig. 19).

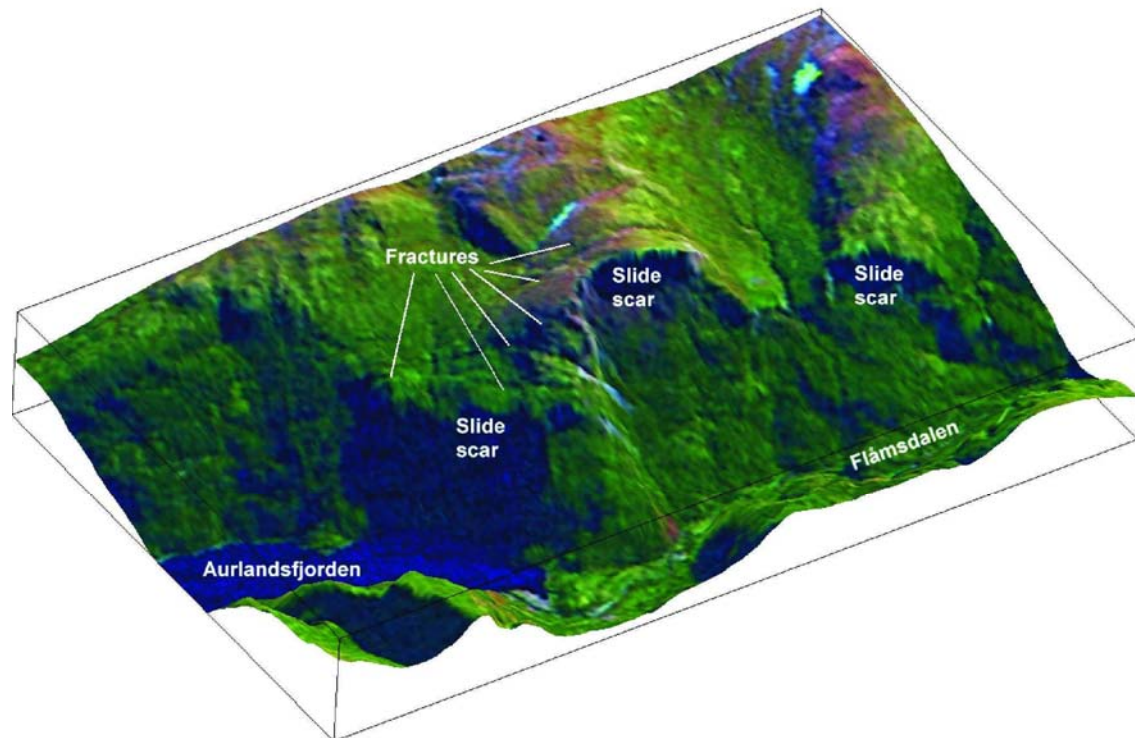


Figure 18. Gravitational fractures and slide scars in Flåmsdalen and Aurlandsfjorden. 3D model based on satellite and topographic data. View towards the southeast.

Instability features are evidenced by normal faults along the eastern margin of Aurlandsfjorden/Flåmsdalen (Fig. 19). In the northern part of the area, slides in bedrock and glacial till are associated with a normal fault. The northern part of the mountain Ramnanosi is characterised by several N-NW trending faults and joints, which are cut by a series of transverse fractures, parallel to the steep mountain side above Aurlandsfjorden. The entire mountain area has been downfaulted several metres. If the thickness of the downfaulted rock masses are 300-500 metres, the total volume is 900-1500 mill. m³. Rock avalanches along Flåmsdalen and in Aurlandsdalen are not included in this estimate. The system is most probably gravitationally controlled, rather than of tectonic origin.

A series of slide scars are prominent along the eastern mountains of Flåmsdalen and Aurlandsfjorden (Figs. 18 and 19). A large area of the eastern slope of Flåmsdalen is covered by 100-700 m wide bouldery tongues, interpreted to have formed by creep in previously

formed rock-avalanche deposits (Blikra et al. 2002a). Similar features also occur along Aurlandsfjorden.

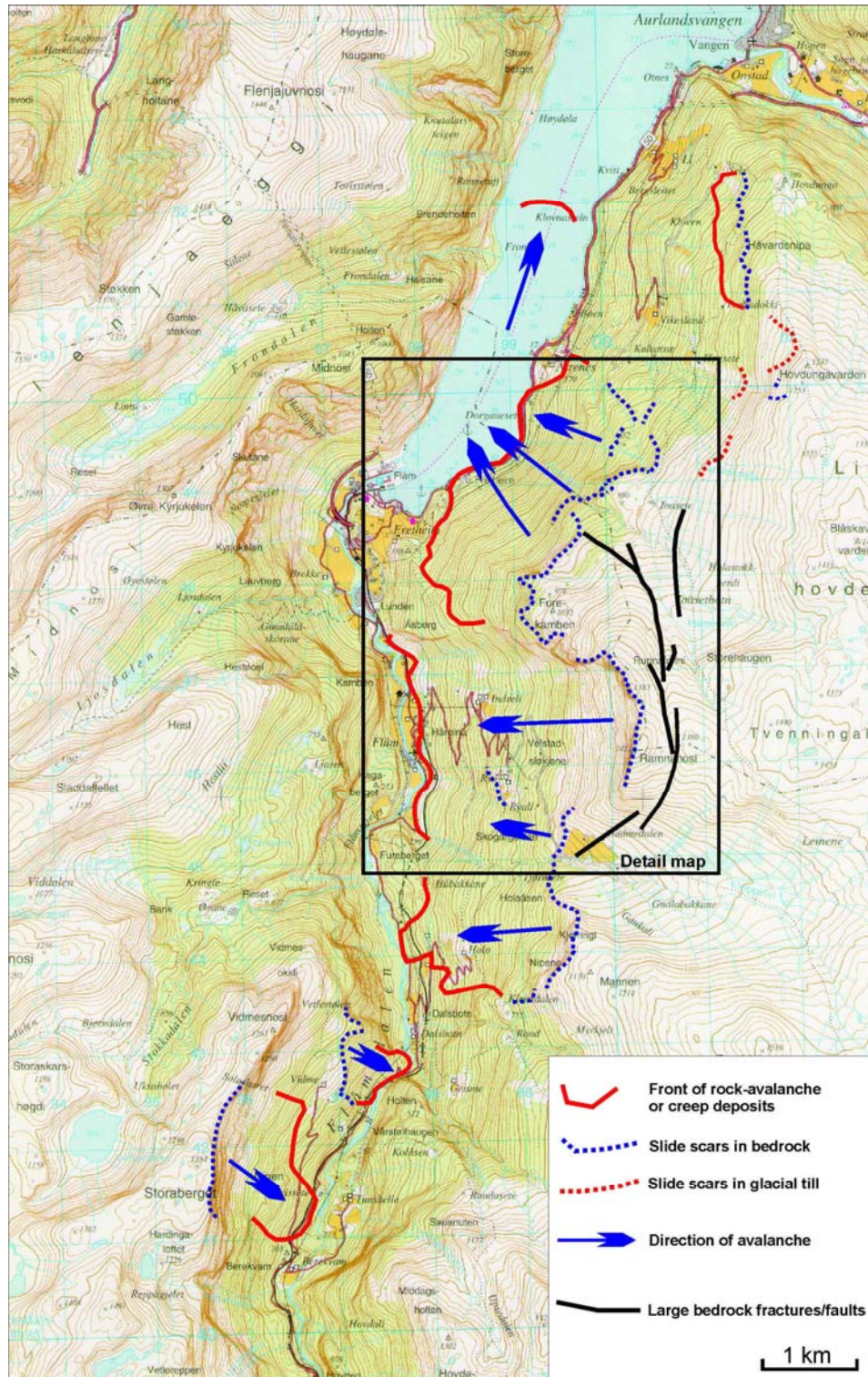


Figure 19. Study area in Flåmsdalen and Aurland (Blikra et al. 2002a). Major fractures and the main distribution of rock-avalanche and creep deposits are shown.

The morphology in Aurlandsfjorden shows large ridges, basins and hummocky relief at the seabed (Fig. 20). Several rock avalanches have originated from the mountains to the east (Fig. 18). Sediment core data from the fjord (see below) indicate that the youngest rock avalanche is ca. 3000 years old. The gravitational faulting and large rock avalanches in Flåmsdalen and along Aurlandsfjorden may have occurred shortly after the deglaciation.

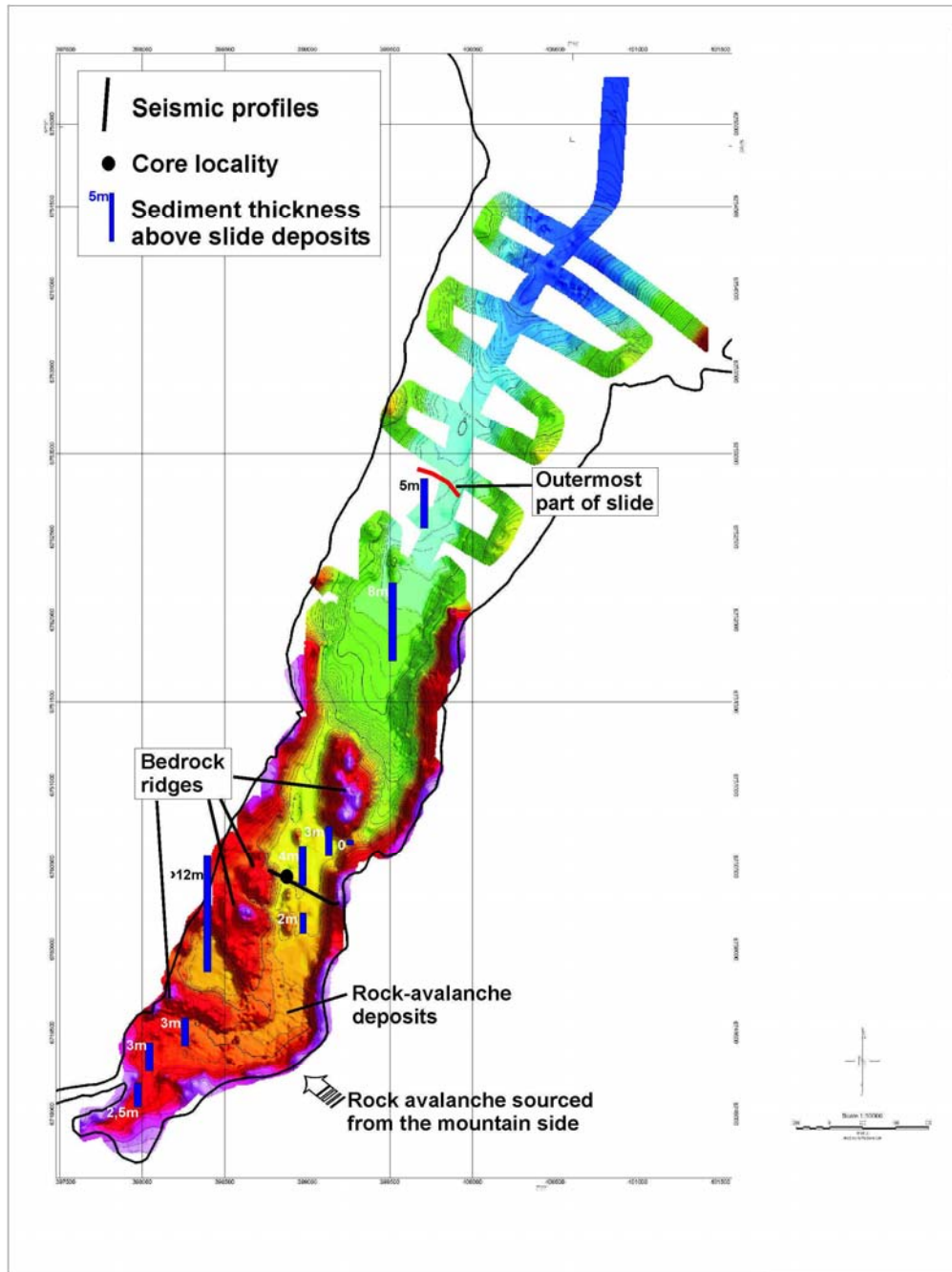


Figure 20. Bathymetric data from Aurlandsfjorden showing the main geomorphic features and sediment thicknesses above slide deposits. The location of the dated core is shown (modified from Blikra et al. 2002a).

4.4.2 Fjærlandsfjorden

Several rock-avalanche deposits have been mapped on land, close to Fjærland (Fig. 5), and a seismic survey has demonstrated a series of rock avalanches in the fjord (see below). The largest was found in the Berrfjøttene area, where a large and well-defined slide scar occurs in the mountain side. A rock avalanche occurs at the delta in the inner part of Fjærlandsfjorden. Georadar data indicate that this event is probably younger than 1000 years (Lauritsen and Elvebakk 2001).

5. FJORD INVESTIGATIONS

5.1 Sogn

The seismic investigations in Aurlandsfjorden, Fjærlandsfjorden and Barsnesfjorden were carried out under the projects "Fjellskredkartlegging i Sogn og Fjordane" and "Fyllittprosjektet i Aurland". Due to the many slide deposits in these fjords, a coring programme was carried out also in the inner part of Sognefjorden.

5.1.1 Aurlandsfjorden

A dense grid of seismic profiles was acquired in order to map stratigraphy and slide/debrisflow deposits in Aurlandsfjorden (Blikra et al. 2002a). The seismic data demonstrate that a large part of the inner fjord basin is filled by such deposits. Only 2-4 m of younger sediments cover these (Fig. 20). Further out in the fjord, fine-grained sediments above slide/debrisflow deposits are 5-8 m thick. Normally, the sediment thickness would decrease away from the delta area (in Flåm), which is the main sediment input to the system. This indicates that the slide/debrisflow deposits further out in the fjord are the oldest.

Three cores (Table 1) were obtained from Aurlandsfjorden (Fig. 1). P0103001 (1.98 m long) was intended to reach the top of interpreted slide/debrisflow deposits, while the purpose of P0103002 (1.64 m long) and P0103003 (0.78 m long) was to date sediments on top of interpreted rock-avalanche deposits. Based on the seismic data and the MSCL and XRI data (Lepland et al. 2002), only P0103002 was opened and examined in detail.

The core consists of homogenous, bioturbated, dark grey silty clay with some isolated clasts at ca. 1.2 m depth (Fig. 21). Slide or other mass-movement deposits are thus not present in this core. The core was not taken at exactly the intended position, but the acoustic signature at

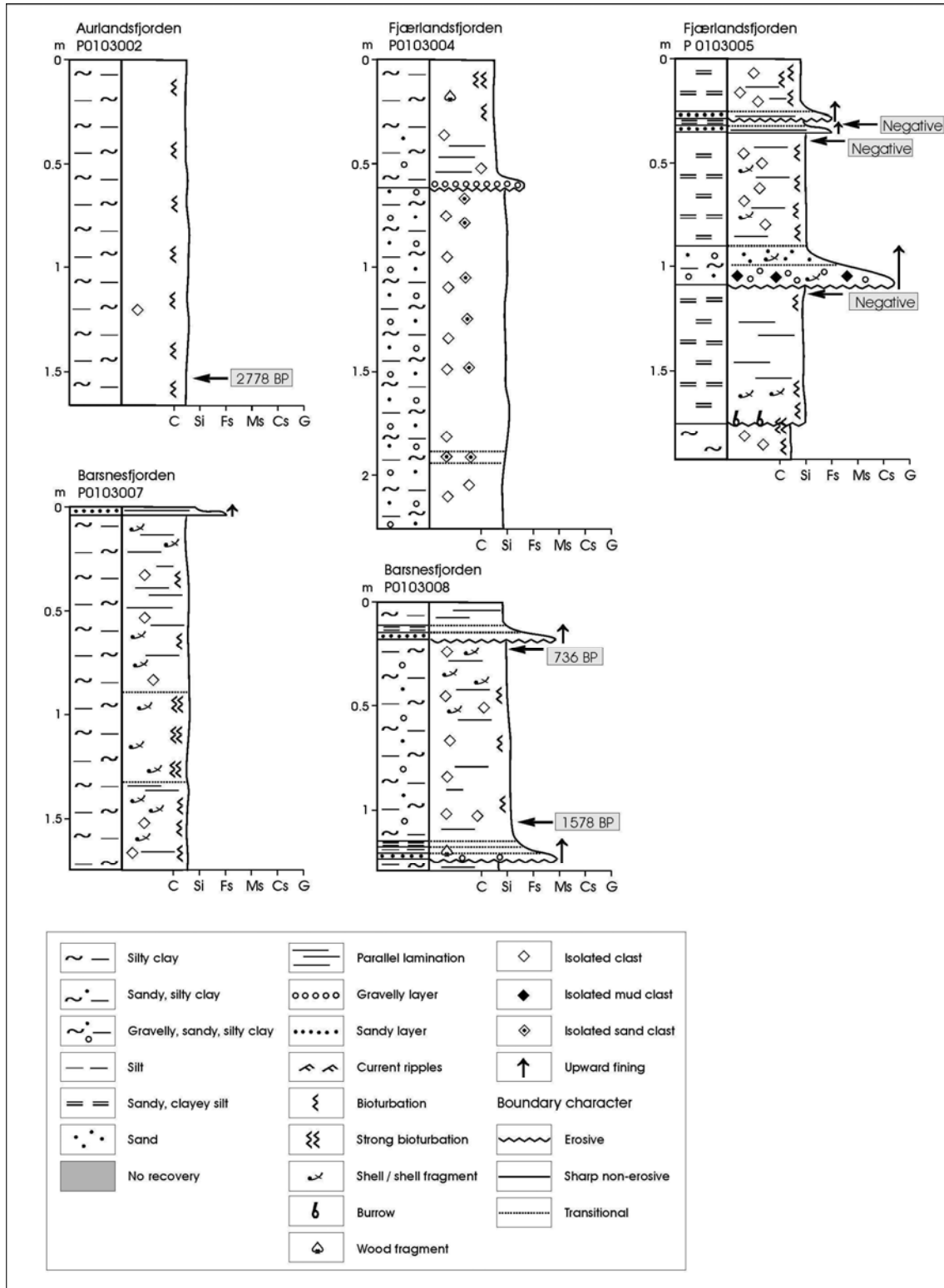


Figure 21. Cores from Aurlandsfjorden, Fjærlandsfjorden and Barsnesfjorden.

the coring site is quite similar to the signature at the intended position. The chaotic acoustic signature in the seismic data may possibly be due to shallow gas in the sediments. A sample from the lowermost part of the core (1.50-1.55 m) gave an age of 2778 BP (2640 ± 70 ^{14}C BP) (Table 3), showing that in this part of Aurlandsfjorden, there is no trace of mass-movement deposits younger than that. The age of 2778 BP indicates that the slide/debrisflow deposit below is approximately 3000 years old.

Table 3. ^{14}C radiocarbon dating results, fjord cores.

Fjord	Core ID	Depth (m)	Sample No.	Lab. No.	Species	Sample weight (mg)	Uncorrected ^{14}C age (BP)	$\delta^{13}\text{C}$ (‰) V-PDB	Reservoir corrected ^{14}C age (BP)	Calendar-year age (BP)
Barsnesfjorden	P0103008	0.18-0.23	2001-6	ETH-25050	<i>Globobulimina</i> sp., <i>Uvigerina (peregina) mediterranea</i>	8,5	1215 ± 65	1.0 ± 1.2	815 ± 65	736 (824-672)
Barsnesfjorden	P0103008	1.06-1.11	2001-7	ETH-25051	<i>Nonion labradoricum</i>	5,2	2030 ± 60	1.6 ± 1.2	1630 ± 60	1578 (1681-1514)
Dalsfjorden	P0103012	1.37-1.42	2001-10	ETH-25053	<i>Globobulimina</i> sp., <i>Cibicides</i>	5,5	8905 ± 90	1.0 ± 1.2	8505 ± 90	9458 (9765-9108)
Dalsfjorden	P0103013	0.92-1.02	2001-11	ETH-25492	Mixed benthic foraminifers	9,1	2600 ± 55	0.2 ± 1.2	2200 ± 55	2297 (2331-2182)
Førdesfjorden	P0103014	0.55-0.6	2001-13	ETH-25054	<i>Uvigerina (peregina) mediterranea</i> , <i>Hyalinea baltica</i>	11,2	2640 ± 55	-0.7 ± 1.2	2240 ± 55	2320 (2348-2285)
Vanylvsfjorden	P0103015	1.14-1.19	2001-14	ETH-24864	<i>Uvigerina (peregina) mediterranea</i> , <i>Hyalinea baltica</i>	11	3190 ± 55	1.3 ± 1.2	2790 ± 55	2962 (3064-2881)
Sydsfjorden	P0103019	1.5-1.55	2001-15	ETH-24865	<i>Globobulimina</i> sp.	14	2665 ± 50	1.1 ± 1.2	2265 ± 50	2333 (2359-2301)
Taffjorden	P0103026	0.28-0.33	2001-16	ETH-24866	<i>Globobulimina</i> sp., <i>Bulimina marginata</i> , <i>Uvigerina (peregina) mediterranea</i>	8,6	1090 ± 55	2.7 ± 1.2	690 ± 55	647 (679-616)
Taffjorden	P0103026	0.86-0.91	2001-18	ETH-25055	<i>Globobulimina</i> sp., <i>Uvigerina (peregina) mediterranea</i> , <i>Hyalinea baltica</i>	9,4	3300 ± 70	1.0 ± 1.2	2900 ± 70	3141 (3239-3021)
Aurlandsfjorden	P0103002	1.5-1.55	2001-21	ETH-25056	<i>Globobulimina</i> sp., <i>Uvigerina (peregina) mediterranea</i>	7,5	3040 ± 70	2.0 ± 1.2	2640 ± 70	2778 (2866-2736)
Breisunddjupet	HM129-03	1.58-1.63	2001-22	ETH-24867	<i>Uvigerina (peregina) mediterranea</i> , <i>Hyalinea baltica</i>	9,5	3480 ± 60	0.8 ± 1.2	3080 ± 60	3352 (3419-3297)
Breisunddjupet	HM129-03	1.41-1.46	2001-23	ETH-24868	<i>Uvigerina (peregina) mediterranea</i> , <i>Hyalinea baltica</i>	11	7775 ± 65	-2.1 ± 1.2	7375 ± 65	8204 (8321-8156)
Ørstaafjorden	ØrstaGC1A	0.76-0.81	2001-24	ETH-24869	<i>Globobulimina</i> sp.	9,2	2760 ± 60	1.8 ± 1.2	2360 ± 60	2454 (2605-2345)

Table 3. Continued

Fjord	Core ID	Depth (m)	Sample No.	Lab. No.	Species	Sample weight (mg)	Uncorrected ¹⁴ C age (BP)	δ ¹³ C (‰) V-PDB	Reservoir corrected ¹⁴ C age (BP)	Calendar-year age (BP)
Julsundet	NGU-6L/SC	0.71-0.75	2001-27	ETH-25317	<i>Hyalinea balthica</i>		3365 ± 55	0.2 ± 1.2	2965 ± 55	3222 (3313-3148)
Julsundet	NGU-6L/SC	2.64-2.65	2001-28	ETH-25301	<i>Astarte sp. (Astarte sulcata)</i>		8885 ± 65	-0.2 ± 1.2	8485 ± 65	9447 (9753-9106)
Julsundet	NGU-6L/SC	5.07-5.11	2001-30	ETH-25318	<i>Melonis barleeanum</i>		10650 ± 75	1.9 ± 1.2	10250 ± 75	11900, 11839, 11723 (12269-11493)
Halsafjorden	NGU-4L/SC	1.51-1.55	2001-32	ETH-25319	<i>Hyalinea balthica</i>		3650 ± 50	2.2 ± 1.2	3250 ± 50	3548 (3621-3464)
Halsafjorden	NGU-4L/SC	3.71-3.75	2001-33	ETH-25302	Shell fragments		7930 ± 75	0.3 ± 1.2	7530 ± 75	8374 (8429-8322)
Halsafjorden	NGU-4L/SC	6.51-6.55	2001-36	ETH-25320	<i>Melonis barleeanum, Nonionellina labradorica</i>		12080 ± 80	3.6 ± 1.2	11680 ± 80	13484 (13806-13413)
Sulaifjorden	NGU-2L/SC	3.04-3.08	2001-37	ETH-25321	<i>Uvigerina (perigrina) mediterranea</i>		7660 ± 65	1.3 ± 1.2	7260 ± 65	8111 (8172-8012)
Sulaifjorden	NGU-2L/SC	1.82-1.86	2001-38	ETH-25322	<i>Hyalinea balthica</i>		4665 ± 55	0.5 ± 1.2	4265 ± 55	4851 (4949-4819)
Halsafjorden	NGU-4L/SC	4.98-5.02	2001-39	ETH-25493	<i>Melonis barleeanum, Nonionellina labradorica, Globobulimina sp.</i>	31.2	10560 ± 75	-4.0 ± 1.2	10160 ± 75	11657 (11913-11355)
Julsundet	NGU-6L/SC	0.45-0.50	2001-42	ETH-25667	<i>Mixed benthic foraminifers and gastropods</i>		3875 ± 60	2.2 ± 1.2	3475 ± 60	3828 (3906-3725)
Ørstaafjorden	ØrstaGC1A	0.49-0.52	2001-43	ETH-25669	<i>Globobulimina sp.</i>		2120 ± 50	0.1 ± 1.2	1720 ± 50	1695 (1769-1615)
Breisunddjupet	HM129-03	0.25-0.30	2001-45	ETH-25670	<i>Uvigerina perigrina</i>		4720 ± 55	0.8 ± 1.2	4320 ± 55	4940 (5026-4847)
Breisunddjupet	HM129-03	2.29-2.34	2001-46	ETH-25668	Shells (whole with perios)		6530 ± 65	0.1 ± 1.2	6130 ± 65	7011 (7147-6934)
Sydsfjorden	P0103019	0.84-0.88	2001-47	ETH-25671	<i>Globobulimina sp.</i>		2185 ± 50	-2.6 ± 1.2	1785 ± 50	1780 (1837-1701)

5.1.2 Barsnesfjorden

In the original schedule, it was not planned to visit Barsnesfjorden (Fig. 1). However, seismic data (Topas) collected in 2001 indicated the presence of acoustically chaotic debrisflow deposits along the northwestern margin of the fjord (Fig. 22), and it was decided to sample these. P0103007 (1.74 m long) (Table 1) comprises olive grey to very dark grey, bioturbated and laminated silty clay with shells (Fig. 21). A 4 cm thick, fine sand turbidite occurs in the

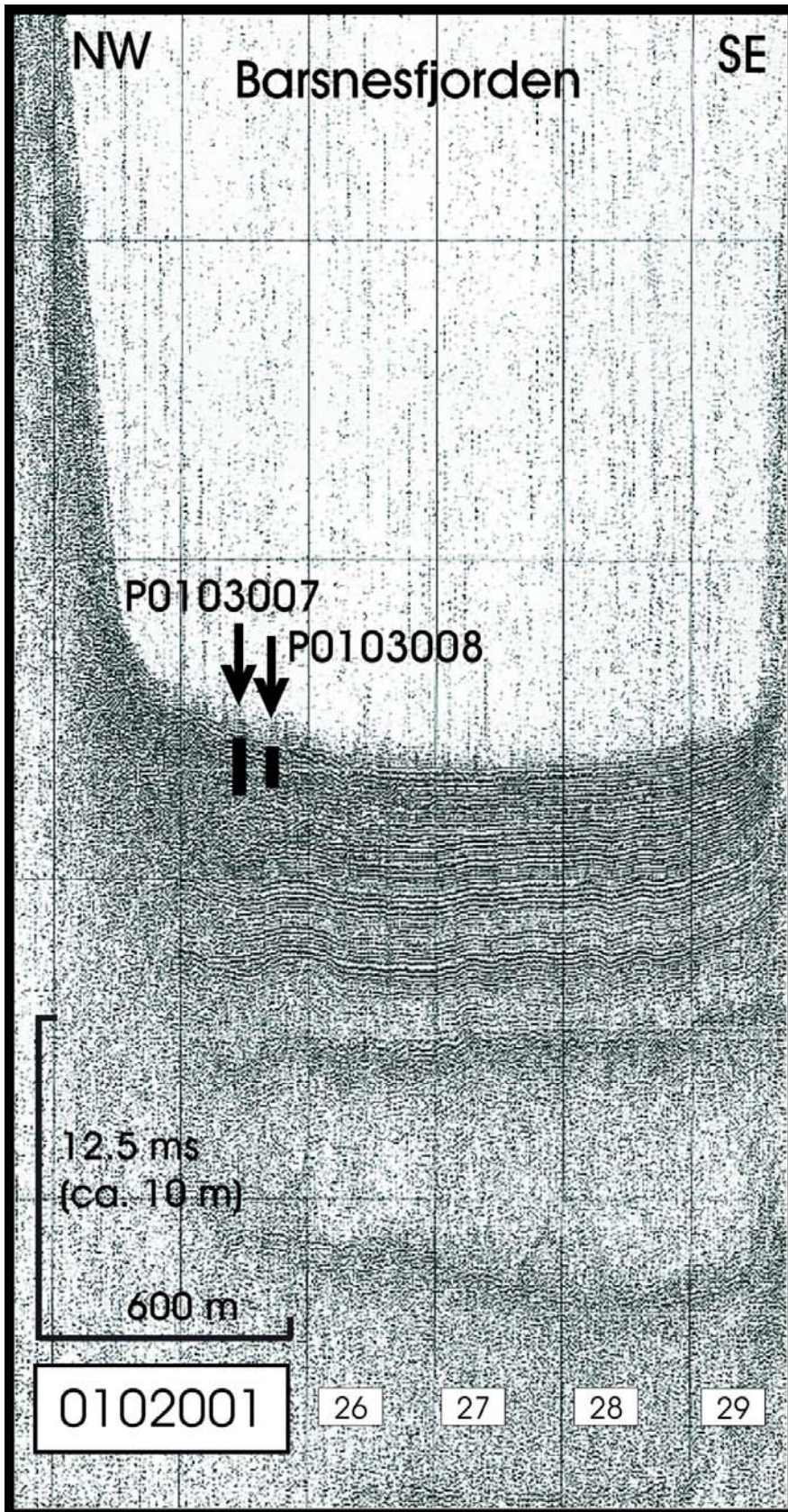


Figure 22. Seismic profile at the location of cores P0103007 and P0103008, Barsnesfjorden.

uppermost part. P0103008 (1.28 m long) comprises silty and sandy, laminated clay with shells. The core contains two normally graded and erosively based medium sand turbidites, at 0.12-1.8 m and 1.14-1.24 m depth. The lowermost turbidite contains a silt/sand layer rich in plant fragments, at 1.18-1.22 m depth. The uppermost turbidite can probably be correlated with the turbidite in the uppermost part of P0103007.

A sample from immediately below (0.18-0.23 m depth) the uppermost turbidite in P0103008 gave an age of 736 BP (815 ± 65 ^{14}C BP) (Table 3). This age represents a maximum age for that turbidite. A sample from above (1.06-1.11 m depth) the lowermost turbidite gave an age of 1578 BP (1630 ± 60 ^{14}C BP), which represents a minimum age for the lowermost turbidite. The apparently disturbed and chaotic nature of the sediments observed in the Topas data (Fig. 22) was not verified by the sampling. It is thus not likely that thick debrisflow deposits occur as a continuous carpet in this area. The acoustically chaotic nature of the sediments may be due to a locally hummocky sea bed shaped by small debrisflows and density currents.

5.1.3 Fjærlandsfjorden

Several rock-avalanche deposits have been mapped on land, close to Fjærland (Fig. 1), and a seismic survey has indicated a series of rock-avalanches in the fjord. The largest was found in the Berrfjøttene area, where a large and well-defined slide scar occurs in the mountain side. This was also observed by Aarseth et al. (1989). The seismic data show that the avalanche has crossed the fjord. Laterally, it can be traced about 4 km to the SW. Five cores were obtained from Fjærlandsfjorden (Fig. 1, Table 1). The cores are located above relatively young slide/debrisflow deposits as well as between slide/rock avalanche lobes. The aim was to date the mass-movement deposits. Based on the seismic and the MSCL and XRI data (Lepland et al. 2002), two cores from the outer part of the fjord (P0103004-005) were opened and examined in detail.

P0103004 (2.30 m long) comprises an upper, 0.63 m thick bed of olive grey silty clay (Fig. 21). The lower part of the bed is normally graded, and it has an erosive lower boundary. Below the boundary comes a structureless, dark grey to blue-grey, silty, sandy and gravelly clay with numerous sand clasts up to 5 cm in diameter. We interpret this lower bed as redeposited glaciomarine sediments or, perhaps more likely, glaciomarine sediments pushed up by a rock avalanche from the southeast into glaciomarine sediments. The seismic data indicate chaotic sediments at this level (Fig. 23). The core did not contain material suitable for dating of mass movements.

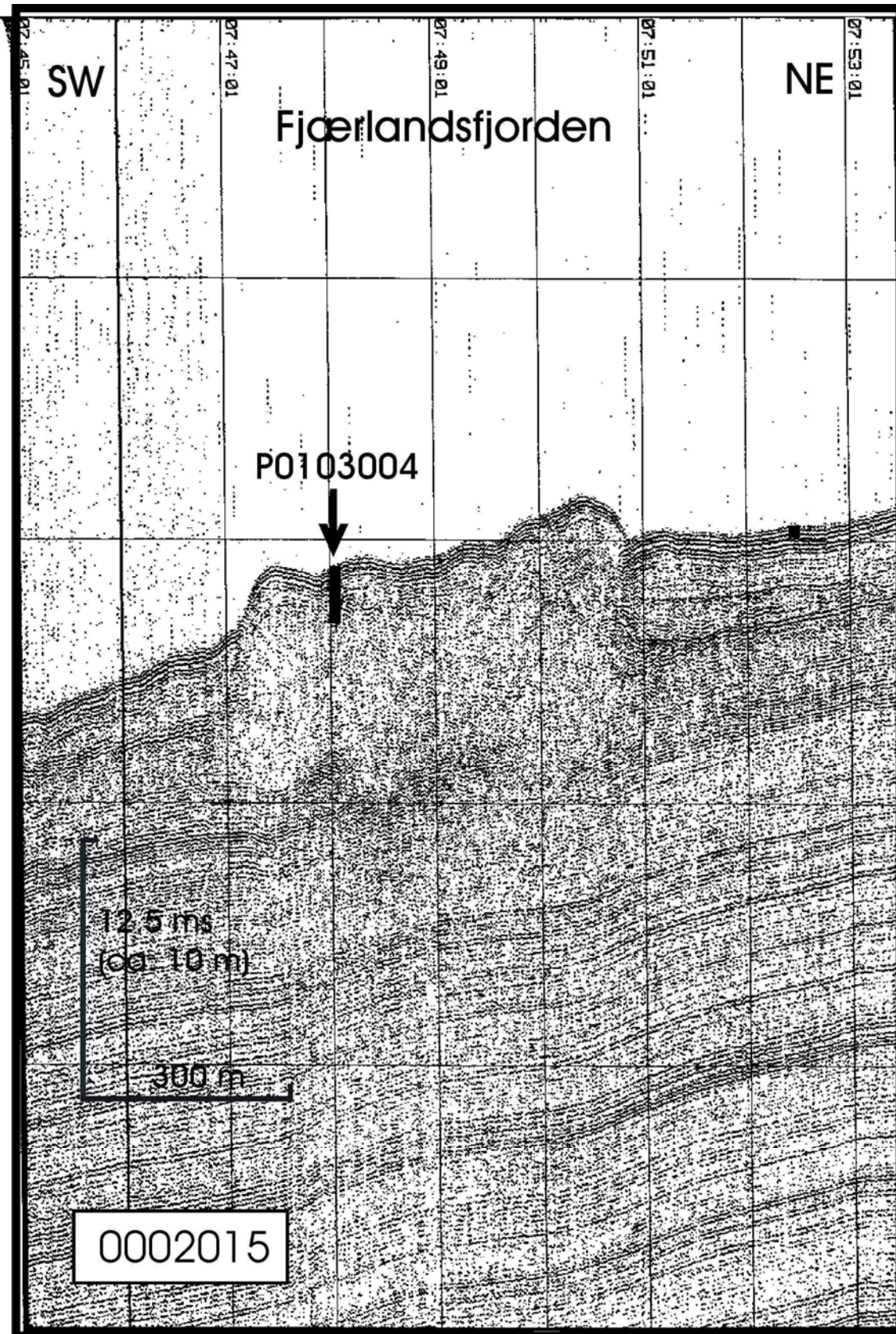


Figure 23. Seismic profile at the location of core P0103004, Fjærlandsfjorden.

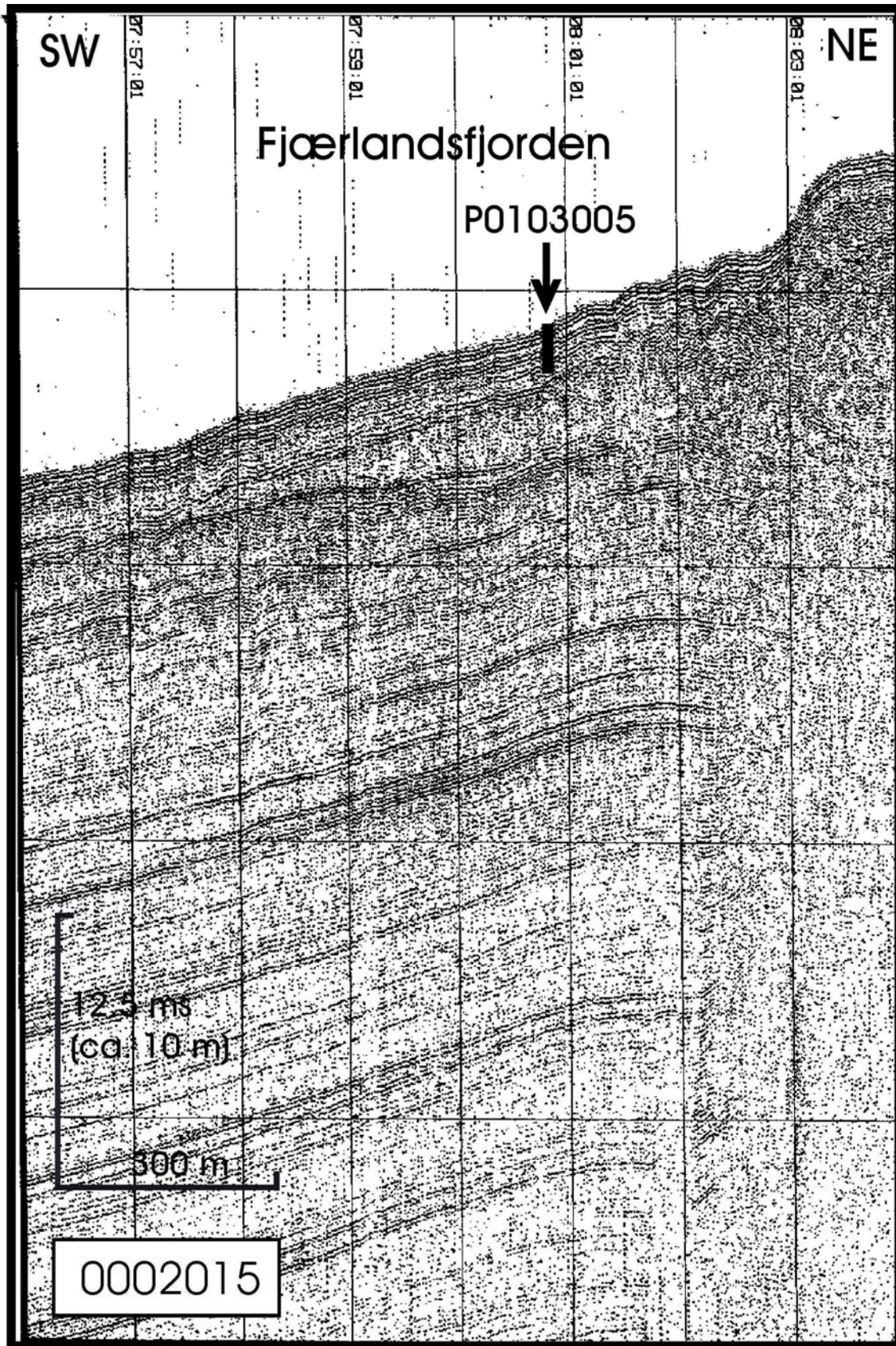


Figure 24. Seismic profile at the location of core P0103005, Fjærlandsfjorden.

P0103005 (1.93 m long) comprises bioturbated olive grey to grey sandy and clayey silt (Fig. 21). Fine sand turbidites occur at 0.28-0.32 m and 0.36-0.39 m depth. At 0.90-1.08 m depth, an upward fining deposit with an erosive lower surface occurs. This deposit comprises pebbles up to 3 cm, shells up to 1 cm and blue-grey clay clasts in the lower part. We interpret these sediments as a debrisflow deposit derived from the southeastern fjord slope. Samples from below the two turbidites (0.32-0.36 and 0.39-0.44 m) and below the more coarse-grained debrisflow deposit (1.11-1.16 m) did not contain enough foraminifers for ^{14}C dating. Therefore, it is unknown when these mass movements occurred. At 1.78 m depth, there is a sharp, undulating boundary towards structureless, bioturbated blue-grey pebbly clay, in the lowermost part of the core. The seismic data (Fig. 24) show that these sediments probably represent slide deposits or glaciomarine sediments strongly disturbed by nearby slide activity. The upper part of the unit was bioturbated prior to deposition of the unit above.

5.2 Sunnfjord

5.2.1 Dalsfjorden

In Dalsfjorden (Fig. 1), several debrisflow deposits occur at the levels of the interpreted red, green and violet reflectors (Longva et al. 2001). Three cores were obtained from this fjord (Fig. 25) (Table 1).

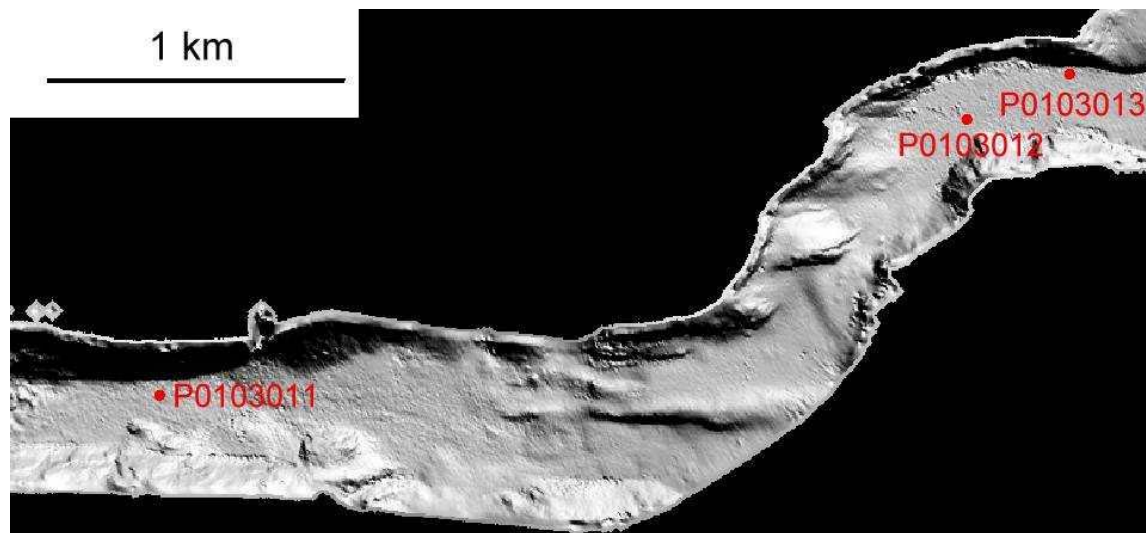


Figure 25. Shaded relief image from swath bathymetry and core locations, Dalsfjorden.

P0103011 (0.80 m long) was aimed to penetrate the interpreted red reflector and reach the interpreted green debrisflow level at ca. 2.2 m depth. The core comprises homogeneous,

bioturbated, dark grey silty clay with a layer of shell sand and gravel at 0.32 m depth (Fig. 26).

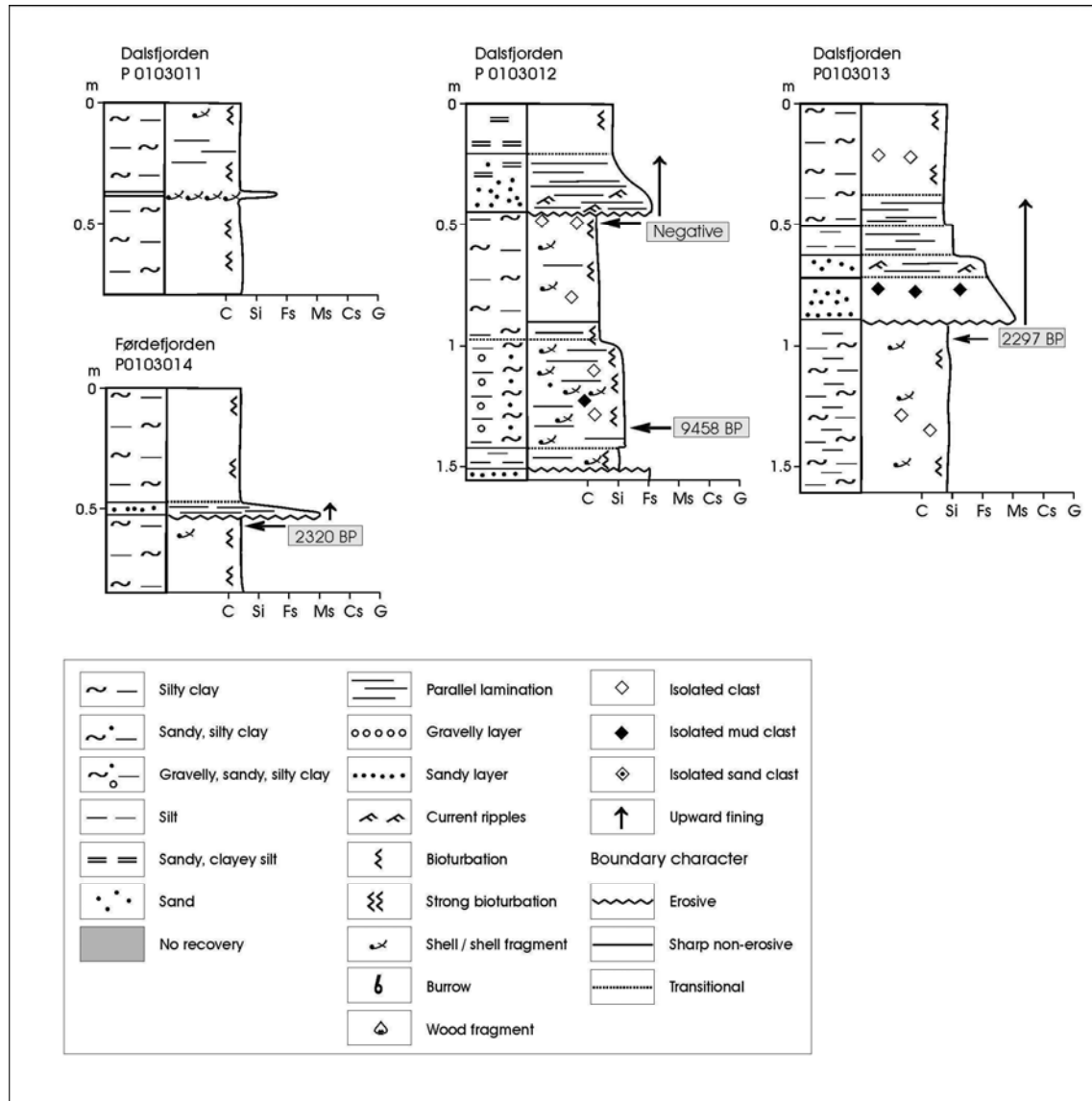


Figure 26. Cores from Dalsfjorden and Førdefjorden.

P0103012 (1.57 m long) was aimed to reach the interpreted red mass-movement level at ca. 0.5 m depth. The core comprises bioturbated, dark grey clayey silt in the uppermost 0.2 m (Fig. 26). This is underlain by an erosively based, normally graded turbidite with planar lamination and current ripples, at 0.20-0.43 m. Bioturbated, homogeneous silty clay with a few shells and isolated clasts occurs at 0.43-0.95 m depth. A sample for dating at 0.45-0.50 m depth did not contain enough foraminifers for dating. Bioturbated, diffusely banded, dark grey, gravelly sandy silt with shells and brown clasts of clayey silt occurs at 0.95-1.43 m depth. The bed is clayey at 0.95-1.05 m. A sample from the lowermost part of this poorly

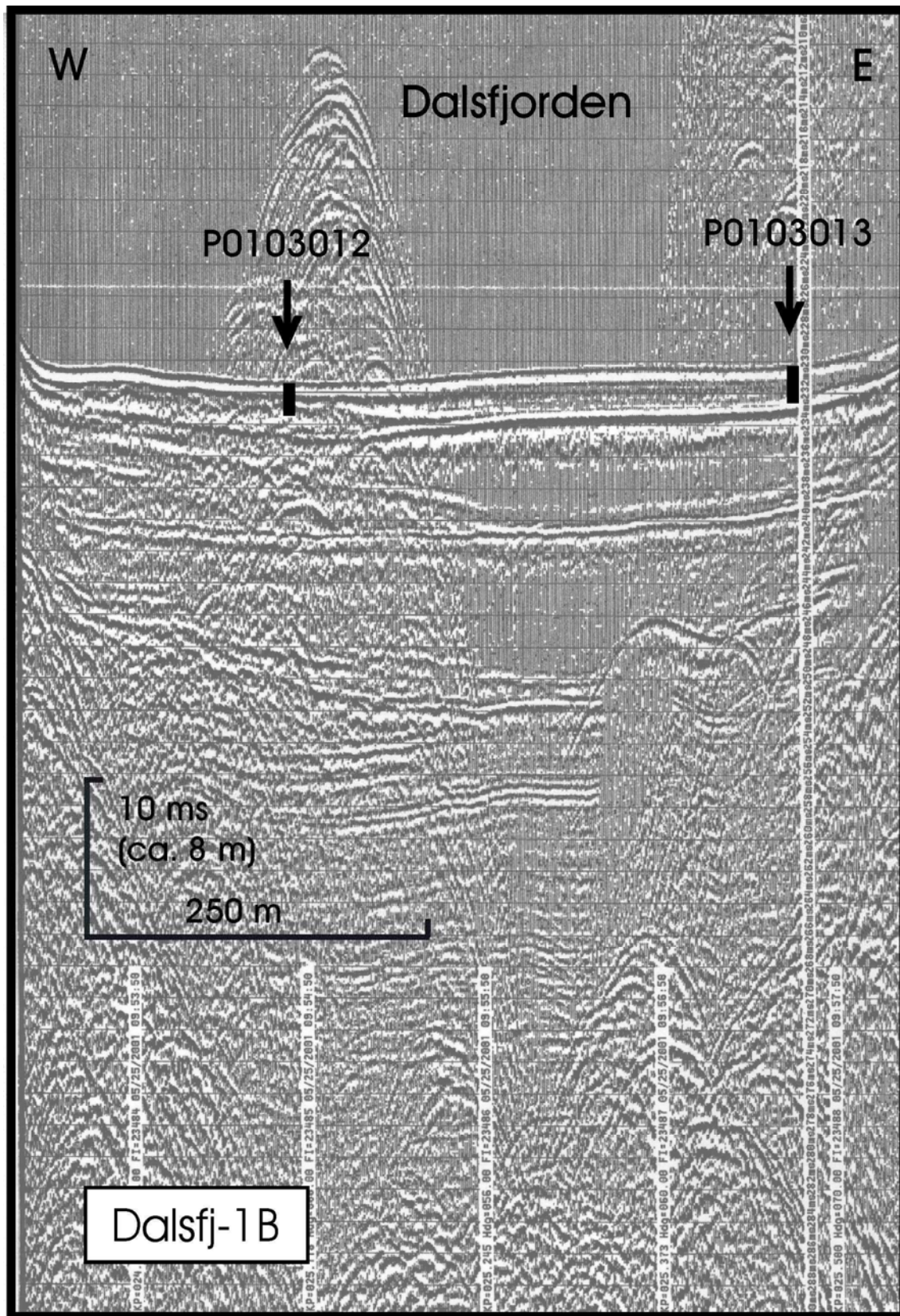


Figure 27. Seismic profile at the location of cores P0103012 and P0103013, Dalsfjorden.

sorted silt bed (1.37-1.42 m) gave an age of 9458 BP (8505 ± 90 ^{14}C BP) (Table 3). A massive, grey silt layer and massive, grey, fine sand, separated by an erosive boundary, occur in the lower part of the core. The poorly sorted silt bed and massive silt and sand beds in the lower part of P0103012 are evident in the seismic data (Fig. 27) as a wedge of acoustically chaotic sediments, probably representing several debrisflow events.

P0103013 (1.63 m long) was aimed to reach the interpreted red reflector at ca. 2.2 m depth. The core comprises bioturbated, dark grey clayey silt with shells and isolated clasts (Fig. 26). A classical Bouma-type turbidite occurs at 0.38-0.91 m depth. This has an erosive lower boundary, exhibits planar lamination and ripples, and is normally graded (medium sand-silty clay). The sandy, lower part contains clasts of brown clay. A sample from below the erosive boundary (0.92-1.02 m depth) gave an age of 2297 BP (2200 ± 55 ^{14}C BP) (Table 3). This represents a maximum age for the turbidite.

Seismic data suggest that the turbidite in the upper part of P0103012 can be correlated with the turbidite in core P0103013 (which is 2000-2200 years old, accounting for an erosion at its base), and possibly with the sand layer in P0103011. This correlation implies that the coarse-grained deposits in the lower part of P0103012, i.e. the wedge of chaotic deposits seen in the seismic data and interpreted to be related to the 2000 event (red reflector) by Longva et al. (2001a) (Fig. 27), is older than the turbidite. The age of 9458 BP probably reflects old sediments redeposited by a younger event, but we do not know the age of that.

5.2.2 Førdefjorden

P0103014 (0.85 m long) from Førdefjorden (Table 1, Fig. 1) is not located along the track of a seismic line. The core comprises bioturbated, olive grey clayey silt, with a turbidite at 0.47-0.54 m depth (Fig. 26). The turbidite has an erosive lower boundary, fines up from medium to fine sand, and exhibits planar lamination. A sample (0.55-0.60 m depth) from immediately below the turbidite gave an age of 2320 BP (2240 ± 55 ^{14}C BP) (Table 3). This represents a maximum age for the turbidite.

5.3 Sunnmøre

5.3.1 Vanylvsfjorden

P0103015 (1.64 m long) in Vanylvsfjorden (Table 1, Fig. 1), was aimed to penetrate the interpreted red and green reflectors at ca. 2.0 m and ca. 3.2 m depth, respectively. The core comprises homogeneous, bioturbated, very dark grey and olive grey silty clay/clayey silt with a turbidite at 0.96-1.13 m depth (Fig. 28). A sample for dating from above the turbidite (0.80-

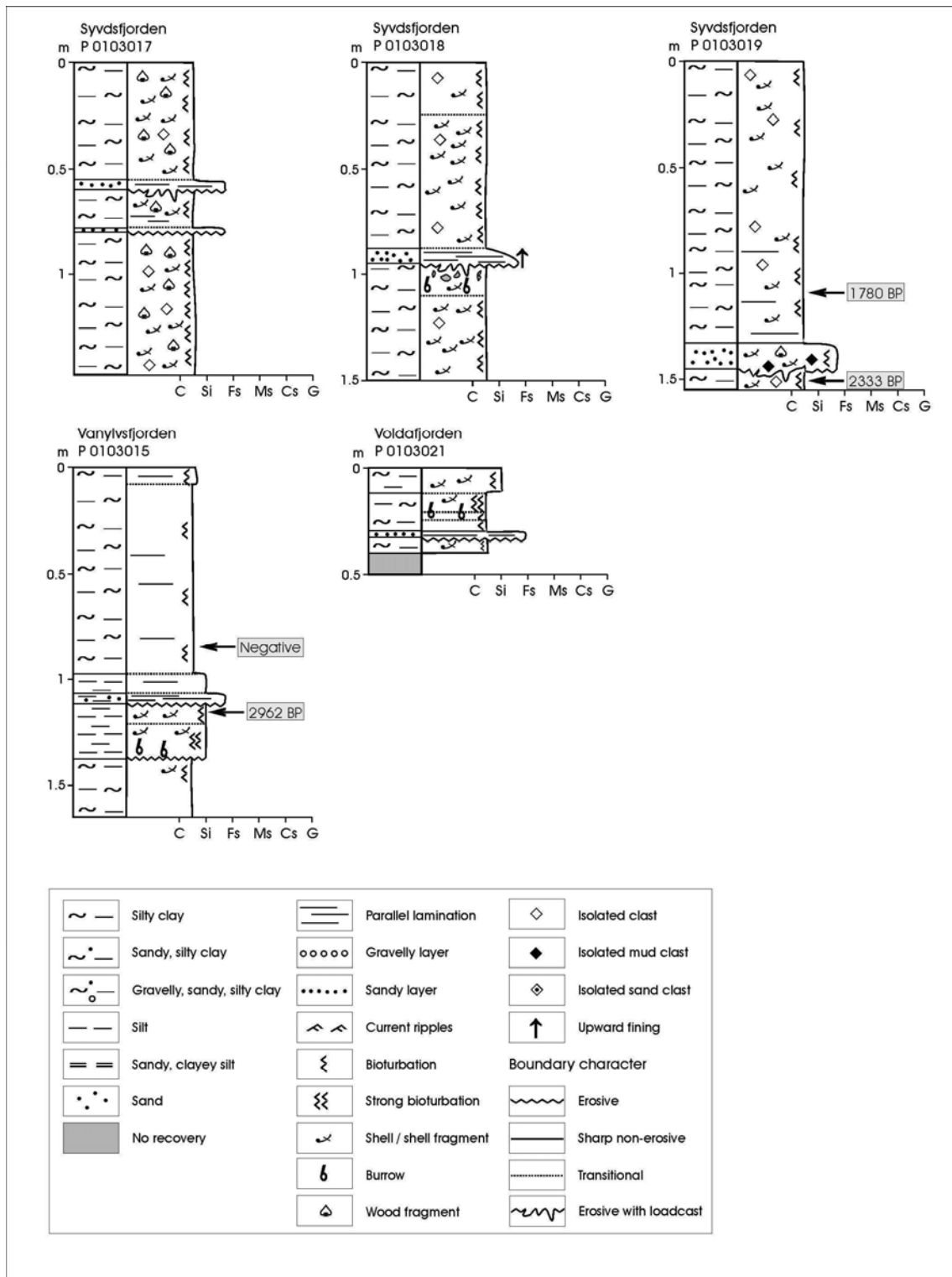


Figure 28. Cores from Vanylvsfjorden, Syvdsfjorden and Voldafjorden.

0.85 m depth) did not contain enough foraminifers for dating. An erosively based and strongly bioturbated silt bed at 1.13-1.37 m depth may possibly represent an older mass-movement

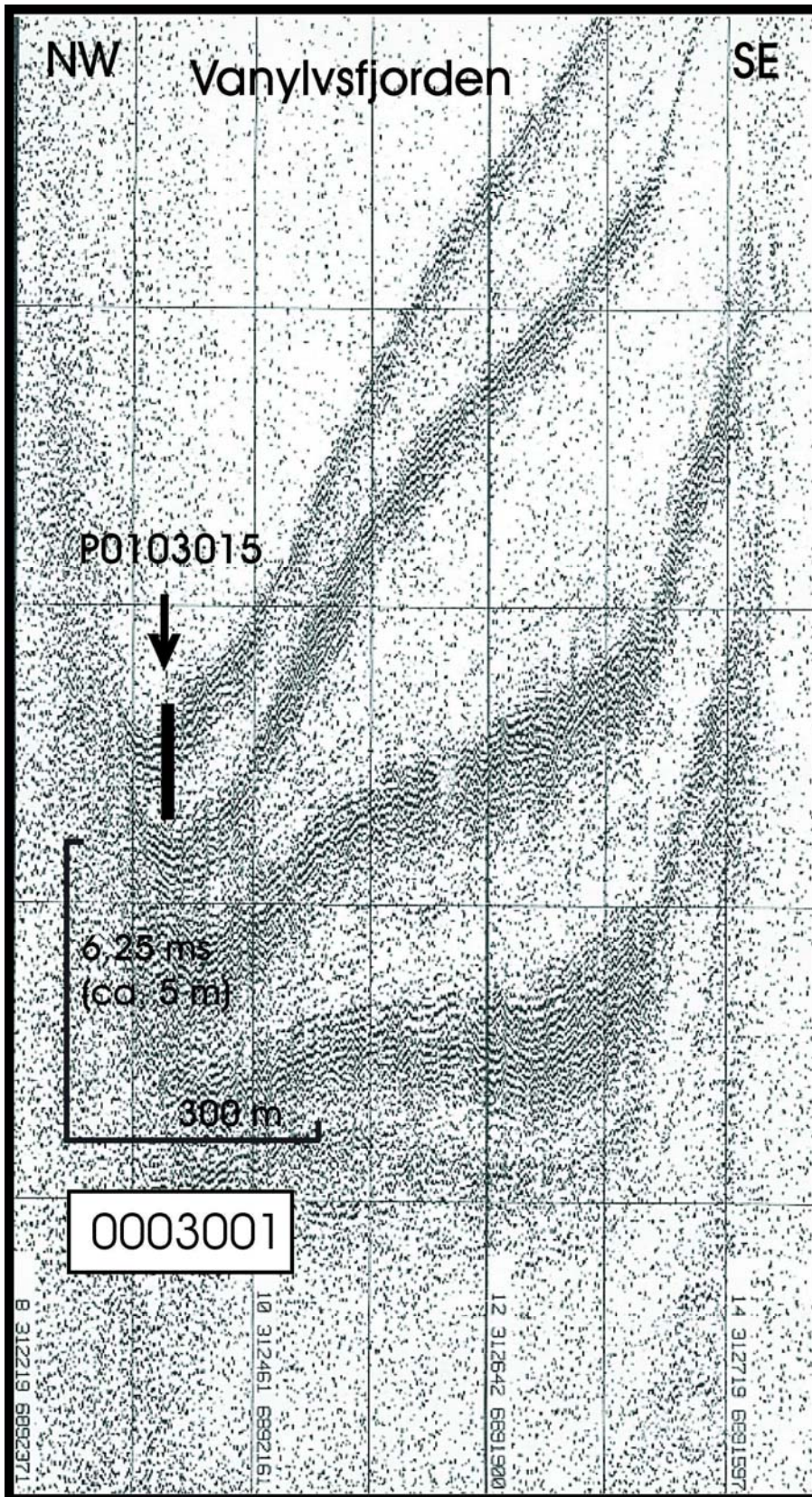


Figure 29. Seismic profile at the location of core P0103015, Vanylvsfjorden.

event. A sample from the upper part of this silt bed (1.14-1.19 m) gave an age of 2962 BP (2790 ± 55 ^{14}C BP) (Table 3). This represents a maximum age of the upper turbidite and indicates that the interpreted red reflector in Vanylvsfjorden (Fig. 29) might be older than the interpreted red reflector in Voldafjorden. We do not think that there has been significant erosion at the lower boundary of the uppermost, thin turbidite, which would have implied a younger age of the turbidite. It is worth noticing, however, that the age is from a silt bed, which may represent another mass-movement deposit with redeposited, older shells. If that is the case, the age of the overlying turbidite may be younger than suggested by the dating.

5.3.2 Syvdsfjorden

In Syvdsfjorden (Fig. 1), swath bathymetry (Fig. 30) and seismic data show slide and debrisflow deposits (and associated reflectors) at several stratigraphic levels. Mass-movement lobes show sediment transport from both the northeastern and the southwestern fjord margin as well as axially along the fjord, towards the northwest. Slide/debrisflow deposits of various ages are frequently stacked, although separated by intervening layered sediments (Fig. 30, Longva et al. 2001). This indicates repeated mass movements from the same source areas.

Five cores were obtained in Syvdsfjorden (Table 1). P0103016 (1.35 m long) was intended to penetrate a 3 m thick condensed section, with all interpreted reflectors to be present. P0103017 (1.44 m long) was aimed to reach the interpreted red slide level, at ca. 1.5 m depth. P0103018 (1.48 m long) and P0103019 (1.58 m long) were intended to penetrate the interpreted red reflector at ca. 1.7 m depth, outside the toe of the slide, while P0103020 (1.14 m long) was aimed to reach the toe of the slide, at ca. 1.5 m depth. Based on the seismic data and the MSCL and XRI data (Lepland et al. 2002), three cores (P0103017-019) were opened and examined in detail. All cores comprise bioturbated silty clay/clayey silt with shells and various clast (Fig. 28). P0103017 contains two thin turbidites. Only one turbidite occurs in P0103018, while a debrisflow deposit with shells, wood fragments and mud clasts occurs in P0103019.

The turbidite in P0103018 and the debrisflow deposit in P0103019 can be correlated. The depth difference of the deposits may partly be attributed to the coring and core handling technique. However, the fact that one core contains a turbidite, while the other contains a debrisflow deposit is probably due to variation in sediment type, thickness and depositional mechanism along the toe of a debrisflow (Figs. 30 and 31). This debrisflow corresponds to the interpreted red level in Longva et al. (2001a). A dating immediately below the debrisflow deposit, at 1.50-1.55 m in P0103019, gave an age of 2333 BP (2265 ± 50 ^{14}C BP) (Table 3). This represents a maximum age for the deposit. A dating above the debrisflow deposit, at 1.08-1.13 m in P0103019, gave an age of 1780 BP (1785 ± 50 ^{14}C BP), which represents a minimum age for the deposit. The debrisflow deposit is thus ca. 2000 years old. Based on the seismic data and the sedimentological descriptions, we think that the turbidites in P0103017

represent events that are younger than the mass-movement deposit in P0103018 and P0103019. Assuming similar sedimentation rate, they could be around 1000 years old.

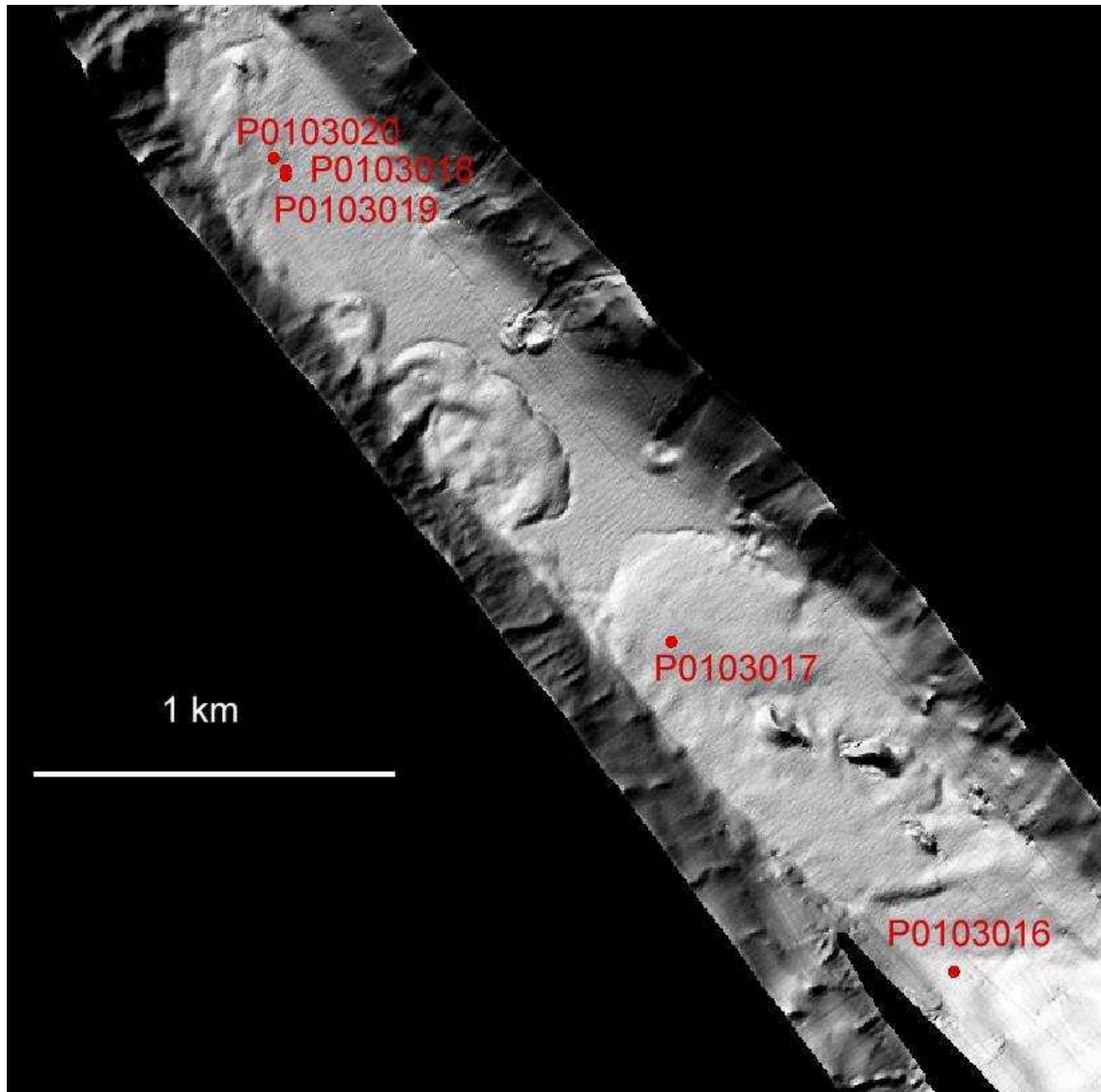


Figure 30. Shaded relief image from swath bathymetry and core locations, Syvdsfjorden.

The swath bathymetry allowed Longva et al. (2001a) to suggest that mounds at the sea bed, in the inner part of Syvdsfjorden represent large blocks derived from the subaerial fjord slopes at the time of the formation of the green reflector. In November 2001, this area was investigated by ROV (Geoconsult 2002). The video documentation shows that the mounds comprise piles of rounded cobbles and boulders surrounded by more fine-grained sediments. These observations suggest that the seabed comprises moraine, which locally pierces through a thin cover of younger sediments. Reinterpretation of the seismic data shows that a morainal ridge most probably crosses the fjord in this area. The ridge is covered by hemipelagic sediments

and thin turbidites, but the crest of it locally pierces through the silty clay/clayey silt at the sea bed. We thus conclude that the mounds do not represent rock-avalanche deposits from the fjord slopes.

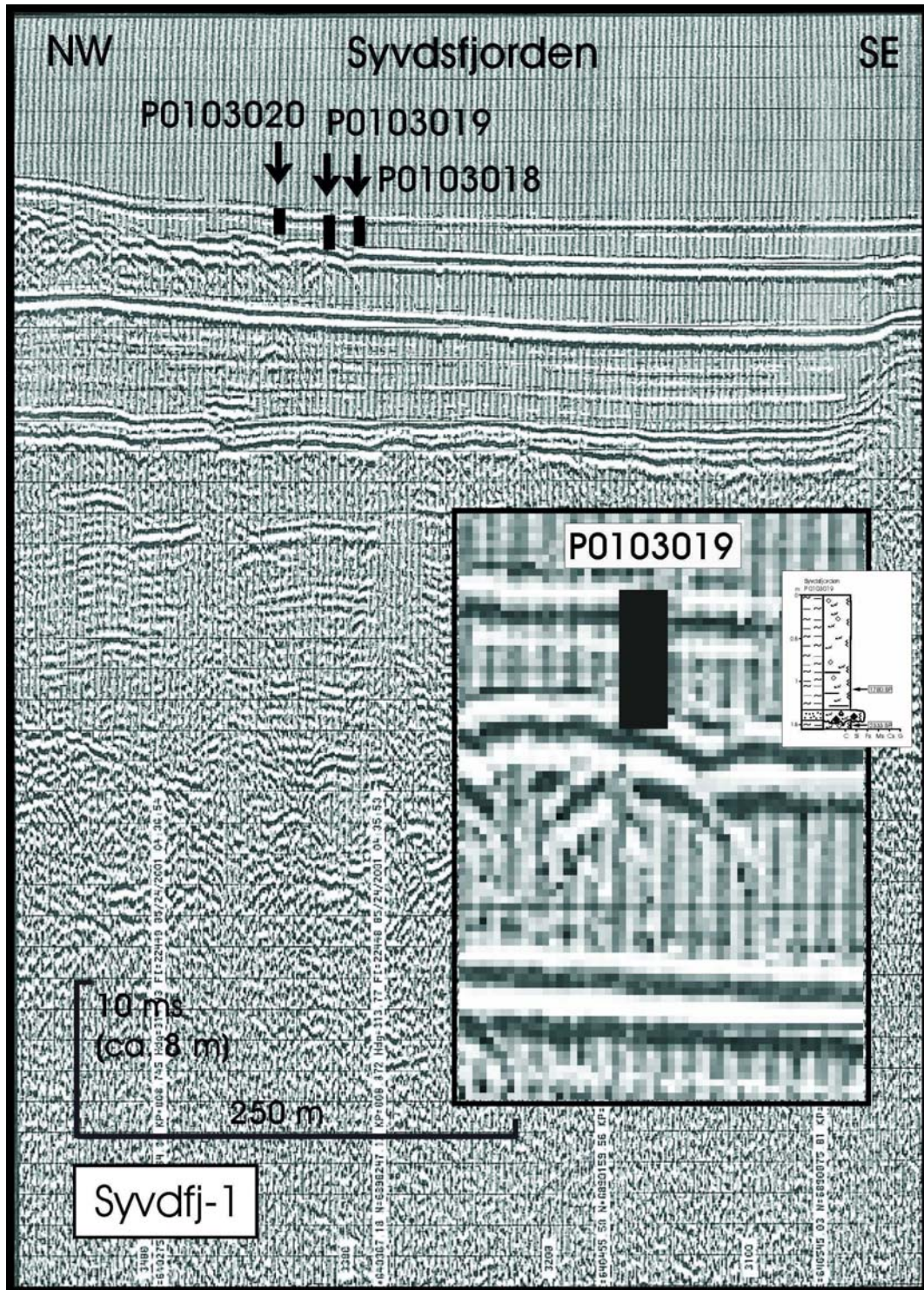


Figure 31. Seismic profile at the location of cores P0103018, -019 and -020, Syvdsfjorden. See Fig. 28 for lithological details.

5.3.3 Voldafjorden

Swath bathymetry and seismic data show that major debrisflow deposits occur at three stratigraphic levels along the margins of Voldafjorden (Fig. 3). The volume of the debrisflow deposits appears to decrease with age, however, prominent reflectors associated with all of them can be traced across the fjord basin. Two relatively young, small slide scars are evident in the swath bathymetry (Longva et al. 2000).

An 8.5 m long core was investigated by Sejrup et al. (2001), who found it to contain several turbidites, of which the three uppermost were interpreted to be ca. 2000, 8200 and 11 000 years old. Longva et al. (2000, 2001) correlated the two youngest of these to seismic reflectors at the level of the two uppermost debrisflow deposits along the fjord margin. Several cores were attempted taken in Voldafjorden to confirm this correlation, but without success. The 8200 years BP event was interpreted to be related to the Storegga Slide tsunami (Bondevik et al. 1998, Grøsfjeld et al. 1999, Sejrup et al. 2001). This led Longva et al. (2000, 2001) to suggest that the 2000 years BP event could possibly be related to another large tsunami caused by an offshore mega-slide, or a large earthquake. The lowermost major debrisflow deposit was not reached by the core.

Core P0103021 (0.40 m long) is from Voldafjorden (Table 1, Fig. 1). At this site, the aim was to obtain a core ca. 1.5 m long, and to reach the interpreted violet reflector. The sediment comprises alternating layers of bioturbated clayey silt, silty clay and silty and clayey sand (Fig. 28). Due to the short core length and the resulting difficulty to trace the sediment layers in the seismic data, this core was not dated.

In Voldafjorden, Longva et al. (2000) had problems correlating core data and seismic reflectors. The red reflector associated with the upper fjord margin debrisflow deposits was apparently situated deeper in the seismic data than in the core described by Sejrup et al. (2001). Several causes for this were discussed, e.g. overpenetration by the corer. In the core, the stratigraphic thickness between the 2000 BP and the 8200 BP events is ca. 2 m, while in the seismic data it is ca. 3.5 m. The green reflector associated with the middle fjord margin debrisflow deposits was apparently situated at the level of the ca. 11 000 BP turbidite in the core described by Sejrup et al. (2001). One possible cause for this could be sediment compaction. An alternative interpretation could be that the middle (green) fjord margin debrisflow deposit in Voldafjorden can in fact be correlated with the ca. 11 000 years old turbidite, and that the Storegga Slide tsunami is not generally associated with extensive fjord margin debrisflow deposits, as previously thought. One problem with the alternative interpretation is that Storegga Slide tsunami deposits are not recognized with certainty in the seismic data from Voldafjorden, although the upper part of the green reflector band (Fig. 3) may possibly reflect Storegga Slide tsunami deposits.

5.3.4 Ørstafjorden

Both the swath bathymetry and the seismic data show the presence of mass-movement deposits in Ørstafjorden (Fig. 1). Small slide and debrisflow lobes occur along the margin of the fjord, especially along its northeastern margin (Fig. 32). In the outer part of Ørstafjorden, mass-movement deposits occur at the level of the interpreted red reflector/directly above the red reflector, at ca. 2.4 m depth. In the innermost part of Ørstafjorden, a northwestward thinning sediment wedge, presumably debrisflow deposits, occurs directly above the red reflector. Six cores from five different locations have been studied (Table 1). The aim of the cores was to penetrate the interpreted red reflector, which occurs at 1.5-2.5 m depth at the coring sites. One core was taken by NGU with the vibrocorer in the central part of Ørstafjorden, while five gravity cores, from the inner, shallower part of the fjord, were supplied by Norsk Hydro. Based on the seismic data and the MSCL and XRI data (Lepland et al. 2002), three cores were opened and examined in detail. It is clear that none of the obtained cores have reached the level of the interpreted red reflector (e.g. Fig. 33).

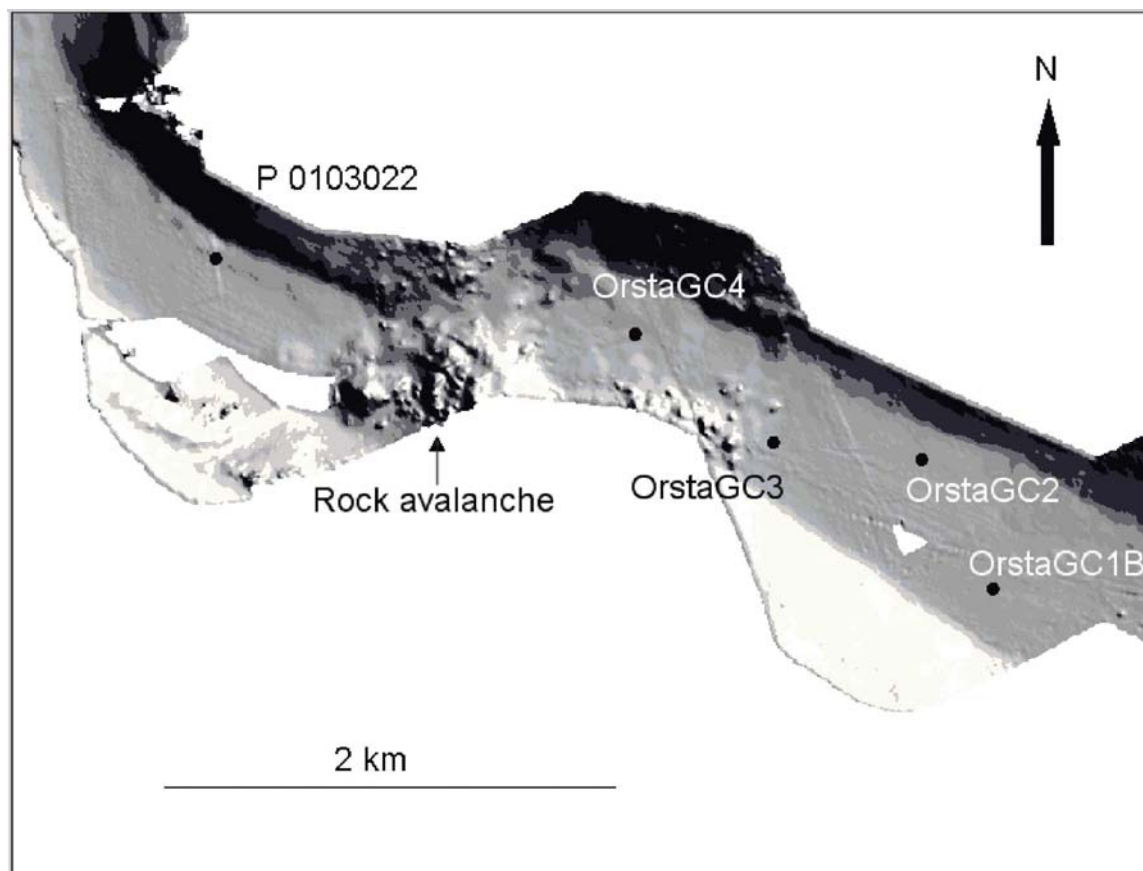


Figure 32. Shaded relief image from swath bathymetry and core locations, Ørstafjorden.

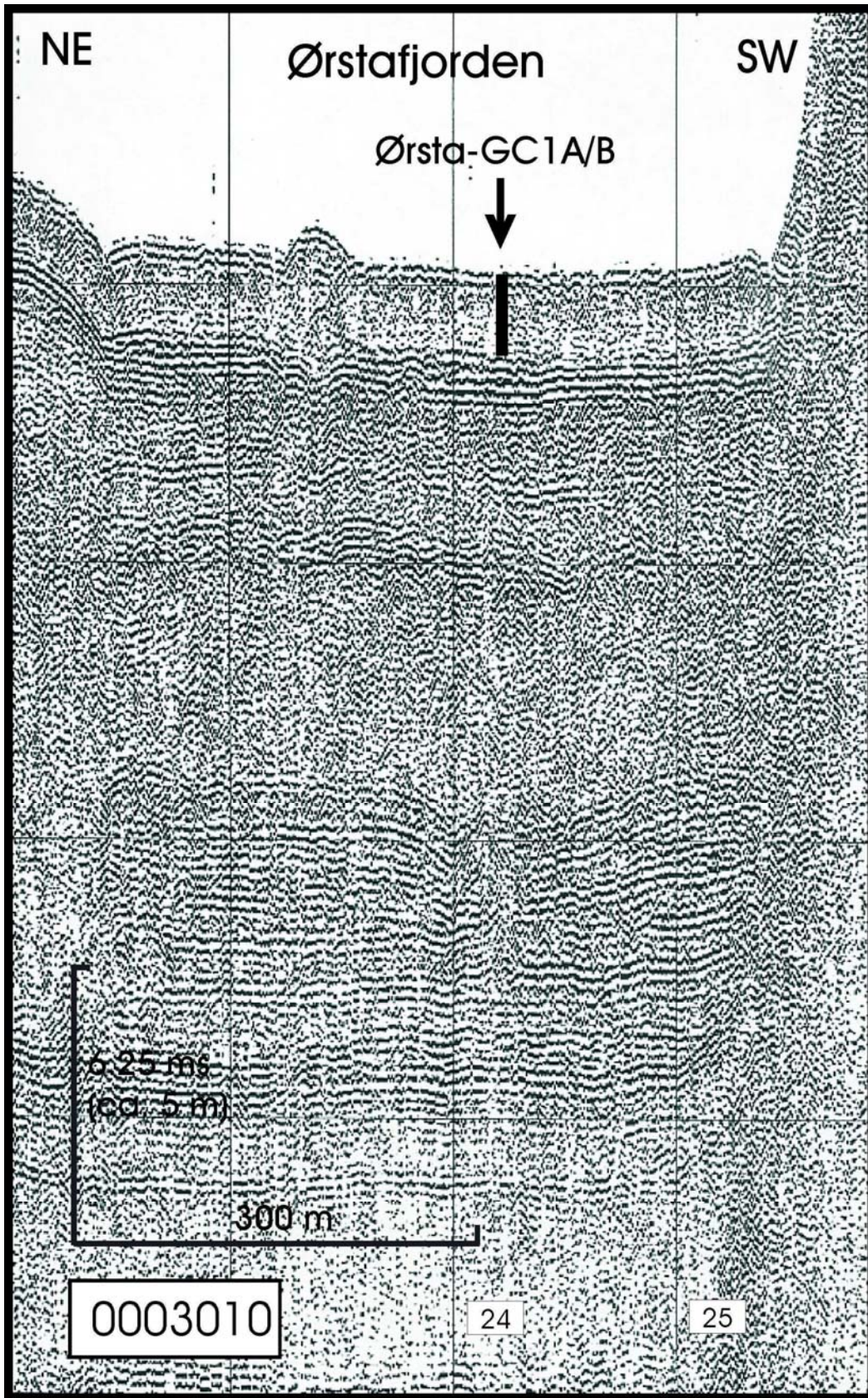


Figure 33. Seismic profile at the location of core Ørsta-GC1, Ørstaffjorden.

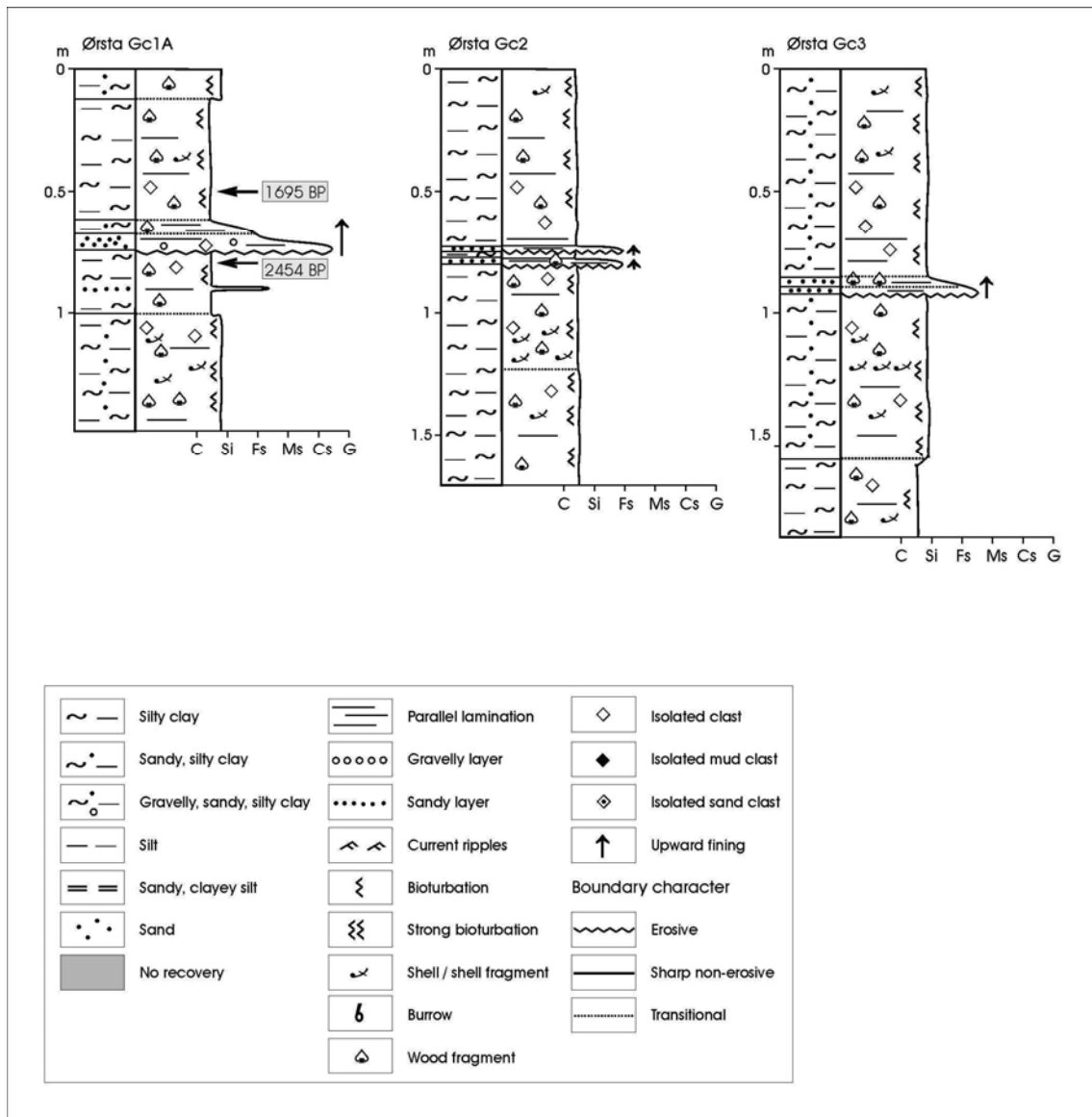


Figure 34. Cores from Ørstaffjorden.

The sedimentary succession comprises approximately 2 m of very dark grey silty and sandy clay rich in organic material/fragments (Fig. 34). Turbidites occur at 0.62-0.74 m depth in Ørsta-GC1A (1.48 m long), 0.73-0.75 m and 0.78-0.80 m depth in Ørsta-GC2 (1.68 m long), and 0.84-0.93 m depth in Ørsta-GC3 (1.92 m long). The seismic data indicate that the turbidites in Ørsta-GC1A and Ørsta-GC3 can be correlated with one of the turbidites (possibly the lowermost one, which contains wood fragments) in Ørsta-GC2. The turbidite is recognized as a very weak reflector in the middle of the uppermost, semitransparent unit. Dating of a sample (0.76-0.81 m) below the turbidite in Ørsta-GC1A gave an age of 2454 BP (2360 ± 60 ^{14}C BP) (Table 3), which represents a maximum age for the event. A sample (0.48-0.53 m) above this turbidite gave an age of 1695 BP (1720 ± 50 ^{14}C BP) (Table 3). This is a minimum age for the event, which probably occurred ca. 2000 years ago. The turbidite is

thickest and coarsest in the inner, southeastern part of Ørstafjorden, suggesting that it has originated from that area. The dating result as well as the seismic data indicate that in Ørstafjorden, the interpreted red reflector is older than the ca. 2000 BP estimated by Longva et al. (2001).

5.3.5 Sulafjorden

Several large slide/debrisflow deposits occur along both margins of Sulafjorden (Figs. 1 and 35). All mass movements identified in the swath bathymetry and the seismic data were interpreted to represent an old (green) event (Longva et al. 2001a), while the red reflector was interpreted to be weak and partly missing. Two sites, ca. 200 m apart, were cored (Geoconsult 2002). NGU-2L/SC (4.0 m long, penetration 6.65 m) (Table 1) was aimed to reach the interpreted green reflector at approximately 6.8 m depth (assuming a compressional wave velocity in the sea bed sediments of 1600 m/s), while NGU-3L/SC-1 (3.55 m long, penetration 4,55 m) and NGU-3L/SC-2 (2.0 m long, penetration 4,65 m, at the same site as NGU-3L/SC-1) were aimed at reaching the top of the corresponding green slide/debrisflow deposits, at ca. 5 m depth. Detailed analysis has been carried out on core NGU-2L/SC, as this core has the greatest length and contains an upward fining interval in its lower part.

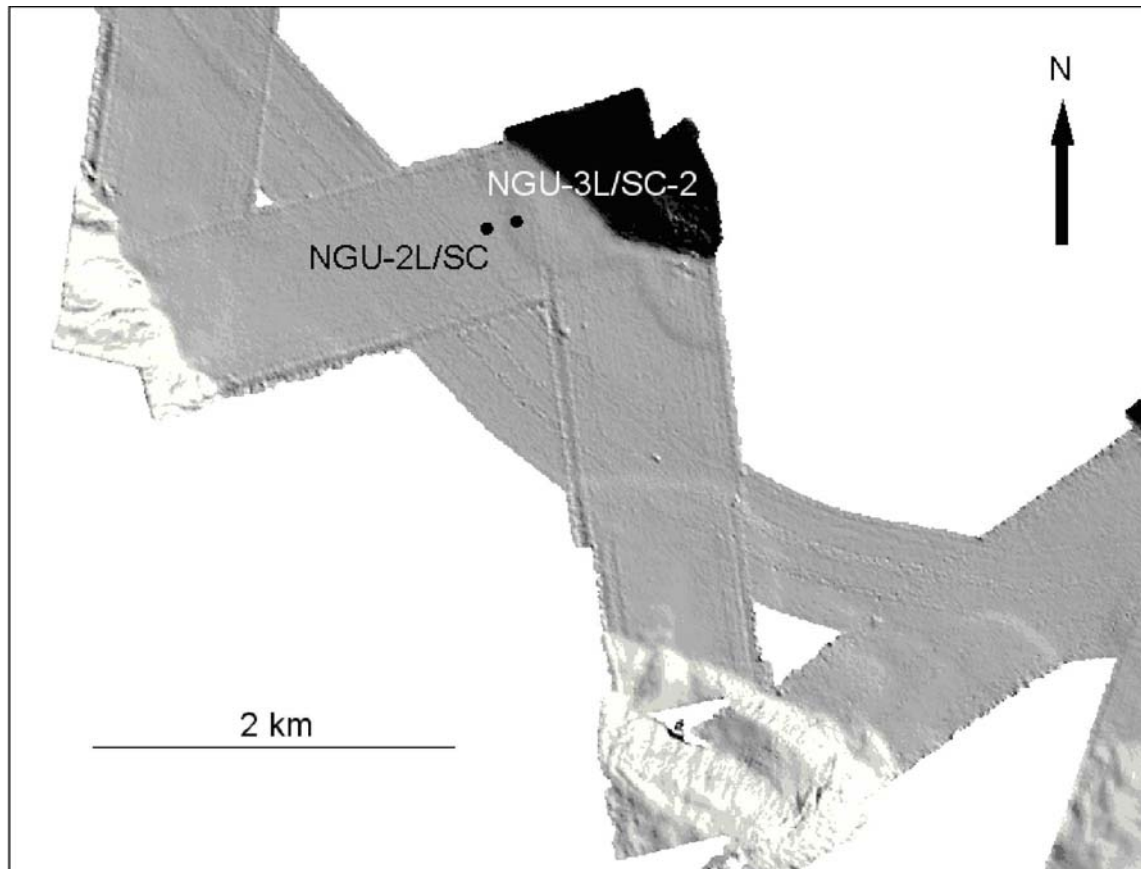


Figure 35. Shaded relief image from swath bathymetry and core locations, Sulafjorden.

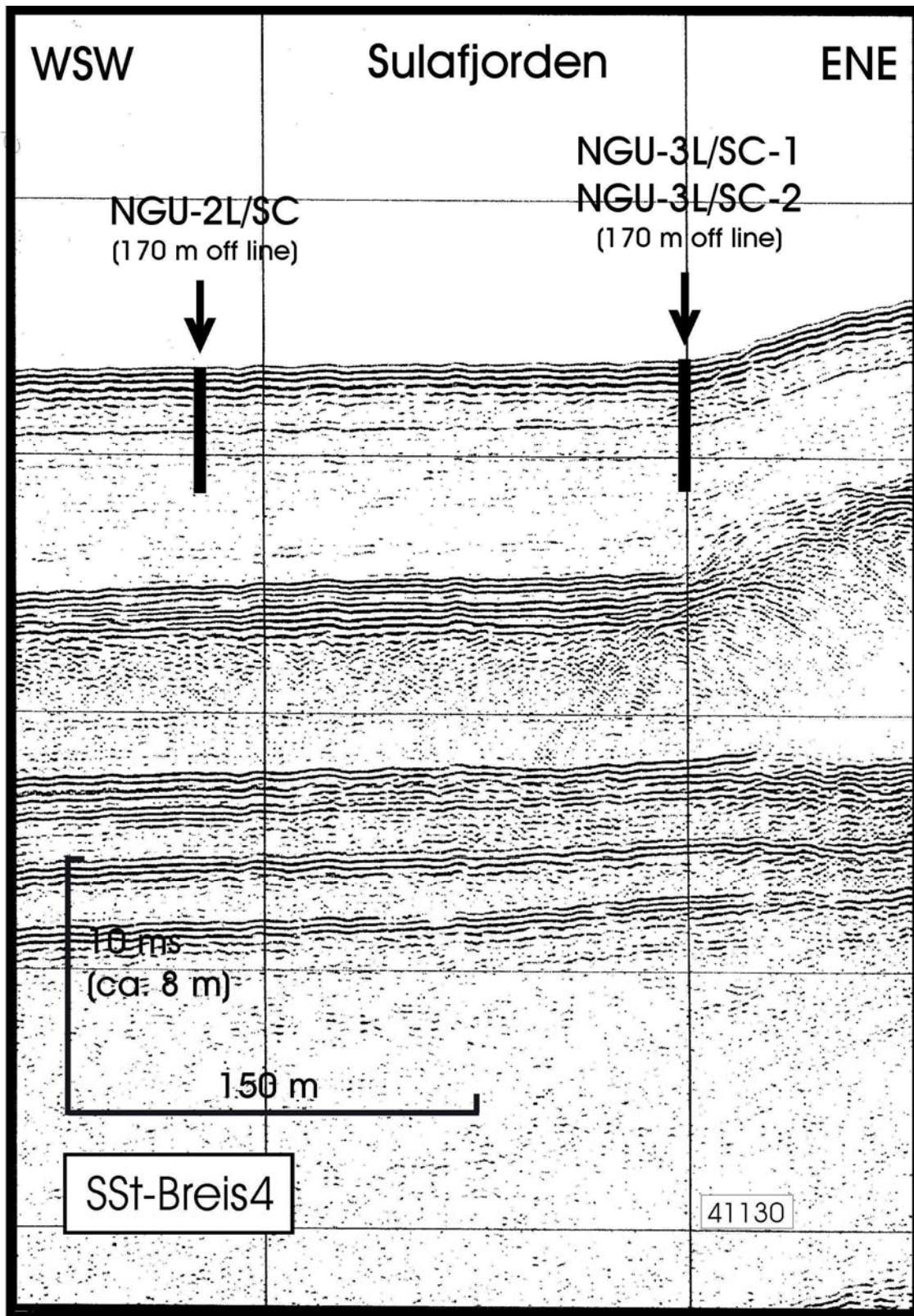


Figure 36. Seismic profile at the location of cores NGU-2L/SC and NGU-3L/SC, Sulafjorden.

MSCL data from the three cores display very similar features, but at different depths (Lepland et al. 2002). A pronounced increase in magnetic susceptibility occurs at 1.7 m depth in NGU-2L/SC, at 2.7 m depth in NGU-3L/SC-1, and at 1.0 m depth in NGU-3L/SC-2. According to the seismic data (Fig. 35), we would have expected this increase to occur at greatest depth in NGU-2L/SC and at shallower (but similar) depth in the two other cores. The discrepancy can probably be explained by strongly variable sediment compaction during coring. An increase in magnetic susceptibility at ca. 0.7 m depth in NGU-2L/SC (Lepland et al. (2002) may possibly be correlated with an increase in magnetic susceptibility and grain size 2200-2500 years ago, recorded in a core further southeast in Sulafjorden (Mikalsen 1999). The increase in magnetic susceptibility and grain size was interpreted to reflect increased snow avalanche activity due to a colder and wetter climate at that time. If the correlation is correct, this suggests that the upper part of the sedimentary succession at the coring site is present in NGU-2L/SC. If the sedimentation rate has been relatively constant after the Storegga Slide event, as suggested by our dating results (ca. 0.38 mm/year, see below), this suggests that the upper part of the stratigraphic section is preserved in the core.

The Selcore barrel length was 12 m (Geoconsult 2002). The reasons for the relatively low core recovery (core length/penetration) may be several, e.g. sediment compaction, that the uppermost part of the seabed sediments did not enter the corer, that sediments in the lowermost part of the cored section did not enter the corer, or that the lowermost part of the cored section was lost during retrieval. In our interpretations, we have assumed that the cores are from the seabed and downwards (Fig. 36). If this assumption is incorrect, our interpretations of major slides and debrisflow deposits at the 11 000-11 700 BP level, and not at the 8200 BP level, would probably have to be changed (see below). It could also imply that a possible 2000-2200 BP event, in the upper part of the stratigraphy, has not been preserved in the core (see discussions later).

Cores NGU-3L/SC-1, NGU-3L/SC-2 and the uppermost 3.15 m of core NGU-2L/SC comprises olive grey, homogeneous, strongly bioturbated clayey silt/silty clay with many shells and shell fragments smaller than 1 mm and some up to 1 cm in diameter (Fig. 37). Also the seismic data show that homogeneous sediments should be expected over this interval (Fig. 36). A seismic reflector that occurs further north can be traced towards the coring site, where it should have occurred at ca. 2 m depth. There is, however, no change in sediment type at this depth. A radiocarbon dating at 1.82-1.86 m depth gave an age of 4851 BP (4265 ± 55 ^{14}C BP), showing that the reflector, further north, is probably significantly older than 2000 years, and that there is no trace of a ca. 2000 BP event in this part of Sulafjorden. This conclusion is based on the assumption that the core represents the interval from the seabed downwards.

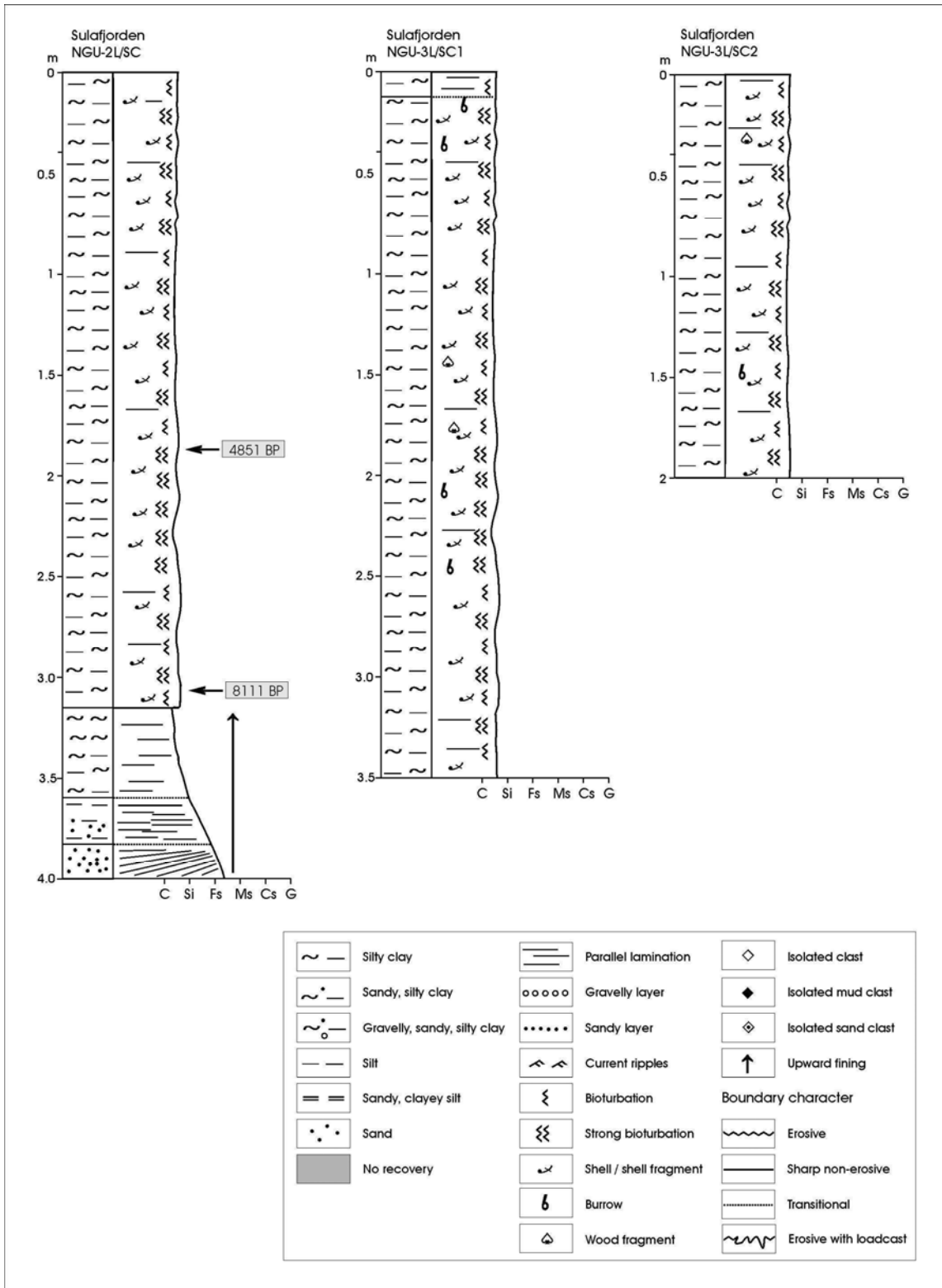


Figure 37. Cores from Sulafjorden.

The lower part of core NGU-2L/SC comprises an upward fining unit. Homogeneous grey clay occurs at 3.15-3.60 m, upward fining, planar laminated very fine sand to silt occurs at 3.60-3.82 m, while upward fining, planar and cross laminated fine to very fine sand occurs at 3.82-3.99 m. A dating at 3.06-3.10 m depth (immediately above the upward fining unit) gave an age of 8111 BP (7260 ± 65 ^{14}C BP) (Table 3), showing that this is most probably a tsunami deposit related to the Storegga Slide. The change in sediment type and density at 3.6 m depth (Lepland et al. 2002, Fig. 37), i.e. at the top of the tsunami deposit, is not reflected in the seismic data (assuming that the core extends from the seabed downwards).

We do not know how thick the tsunami deposit is, however, if the core extends from the seabed downwards, we find it unlikely that its base is at the green reflector interpreted by Longva et al. (2001a) (ca. 6.8 m depth, Fig. 36), which would give an enormous volume of tsunami sediments in Sulafjorden. It is likely that the tsunami deposit is underlain by silty clays and further by slide deposits (seen along the fjord margins) at a deeper level. This interpretation is supported by data from Hagen (1981), who described an interval, at 1.87-3.45 m depth, of alternating coarse- and fine-grained layers in a piston core obtained not far from NGU-2L/SC, at 444 m water depth in Sulafjorden. His descriptions show that this is a typical tsunami deposit (see below), and the stratigraphical distribution of benthonic foraminifera strongly suggests that it can be related to the Storegga Slide.

5.3.6 Breisunddypet

Breisundet (Fig. 1) is the offshore extension of Storfjorden-Sulafjorden. The trough cuts approximately 100 m into the shelf and ends abruptly a few kilometres before it reaches the shelf edge. The swath bathymetry (Fig. 38) shows several slide/debrisflow lobes along the margins of the trough. Large areas seem to be covered by coral mounds, in the northwestern part of the trough. Two gravity cores were obtained by the University of Bergen (Table 1). According to the swath bathymetry (Fig. 38), core HM129-03 (2.52 m long) was taken close to the outer (southeastern) boundary of a relatively young slide, with a rugged surface morphology.

The aim was to reach a reflector at 1.6 m depth. A sharp and undulating, erosive boundary was encountered at this depth exactly (Fig. 39). Below the boundary, the sediment consists of bioturbated, sandy silt with numerous shells and shell fragments. A dating from the uppermost part (1.58-1.63 m depth) of this bed gave an age of 3352 BP (3080 ± 60 ^{14}C BP) (Table 3), which represents a maximum age of the boundary. A dating from the lowermost part (2.29-2.34 m depth) of the bed gave an age of 7011 BP (6130 ± 65 ^{14}C BP) (Table 3) and a sedimentation rate during this time interval of 0.2 mm/year.

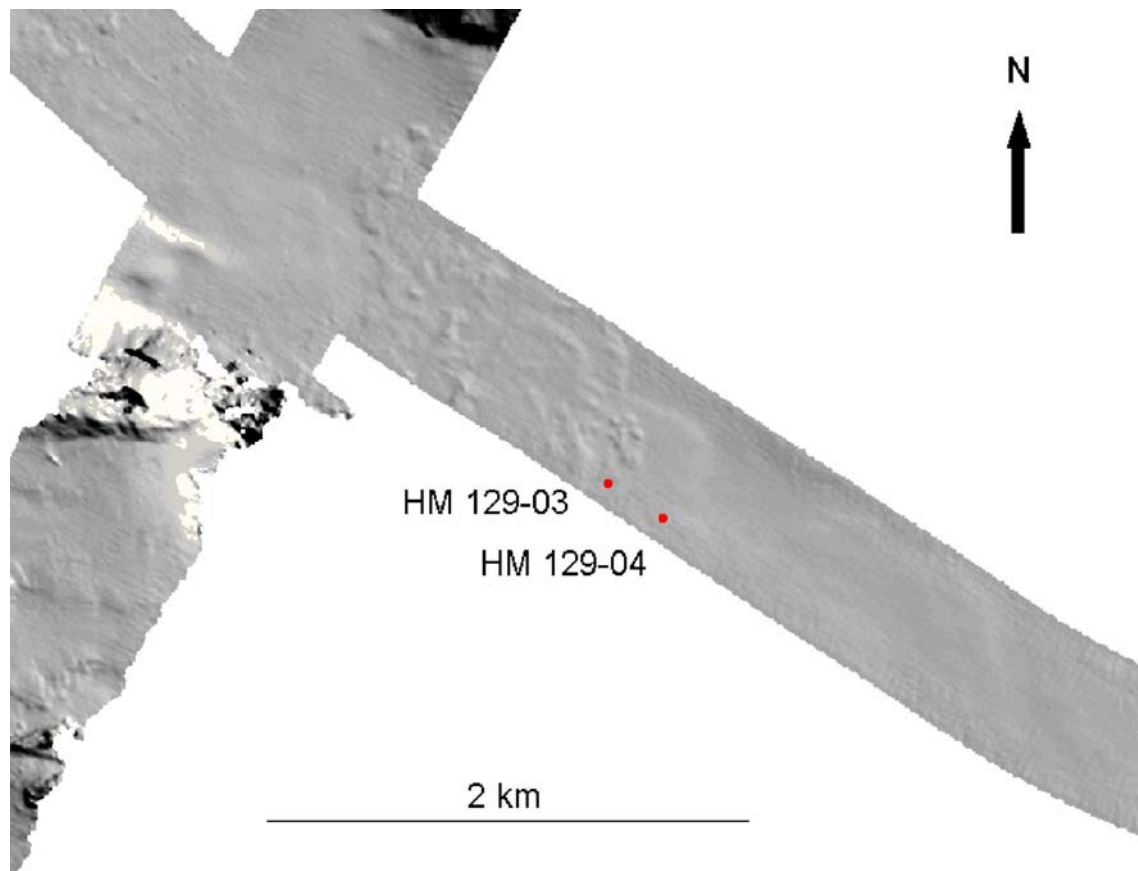


Figure 38. Shaded relief image from swath bathymetry and core locations, Breisunddypet.

Above the boundary at 1.6 m depth, the sediment comprises bioturbated and laminated silty and clayey sand. Immediately above the boundary, however, there is a clast of very dark grey silty clay similar to the sediment found in the lowermost part of the core. There are also two layers, at 1.49-1.50 m and 1.52-1.56 m depth, of light grey bioclastic sand with clasts of sandy silt similar to the sediment below the boundary. Dating of a sample above (1.41-1.46 m depth) the bioclastic sand layers gave an age of 8204 BP (7375 ± 65 ^{14}C BP) (Table 3), while a sample (0.23-0.30 m) from the upper part of the core gave an age of 4940 BP (4320 ± 55 ^{14}C BP) (see interpretation below).

Core HM129-04 (2.30 m long) was obtained ca. 300 m southeast of core HM129-03. The swath bathymetry shows that the sea bed has an even surface at this location, but the eastern boundary of underlying old slide/debrisflow deposits (with their upper boundary at ca. 2.4 m depth) is well defined to the east of the coring location (Fig. 38). A transitional boundary was found in the core at 1.15 m depth (Fig. 39). This boundary, separating silty clay/clayey silt (below) from sandy silt (above), can probably be correlated with the boundary at 2.37 m depth in HM129-03, which, according to the dating results, has a minimum age of 7011 BP. The boundary can not be seen as a reflector in the seismic data, but it is younger than the upper boundary of the old slide deposits below. If the correlation is correct, these could possibly be

related to the Storegga Slide tsunami, ca. 1000 years earlier. The bed of sandy silt is 35 cm thinner in core HM129-03 than in HM129-04. This could imply that there has been erosion of the bed at the site of HM129-03.

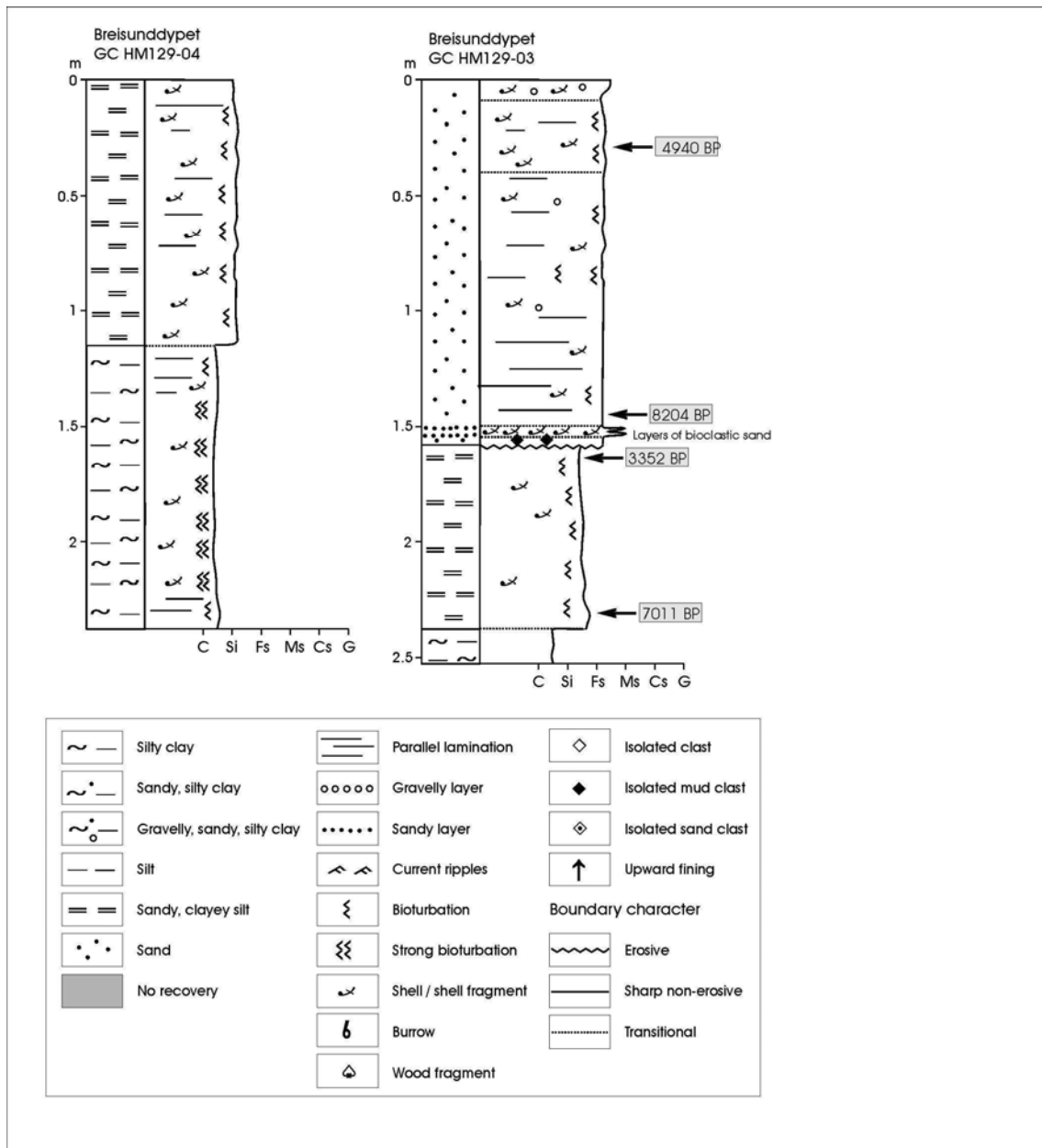


Figure 39. Cores from Breisunddypet.

The dating results, lithology and presence of relatively young slide deposits, west of the core locations, suggest that the sediments above the erosion surface in HM129-03 are redeposited, older sediments. The presence of rip-up clasts and well sorted carbonate sand layers indicate currents and erosion into the underlying units. It is possible that this may reflect a period of strong ocean currents and marine erosion. Other possibilities are relation to either slides or a

tsunami. Our dating results do not allow us to determine when this may have occurred, although it has to be younger than 3352 BP. Above the level of rip-up clast and well-sorted sand layers, lamination and bioturbation suggest normal marine sedimentation although the sediments most probably represent redeposited slide material, as indicated by the old age in the top of the core. There is a possibility that the dated section above the erosive boundary in HM129-03 may represent a slide block. If that is the case, the age of 8204 BP may suggest that the bioclastic sand layers, above the erosion surface, are related to the Storegga Slide tsunami.

5.3.7 Tafjorden

The swath bathymetry and seismic data (see above) show extensive mass-movement deposits in Tafjorden (Fig. 1). Debrisflow lobes and large cones of rock-avalanche debris occur along the northeastern and southwestern margins of the fjord (Fig. 13). Eight cores were collected from Tafjorden (Table 1). The main aim of the coring was to sample sediments above slide/debrisflow deposits and in the top of these, down to 1.2 m depth. The work in this fjord was co-ordinated with another project on slides and mass movements in fjords. Thus, 8 coring sites were visited instead of the 2 planned. Based on the seismic data and the MSCL and XRI data (Lepland et al. 2002), three cores (P0103026, P0103029 and P0103030) were opened and examined in detail. The three cores are located between major cones of rock-avalanche debris observed in the seismic (Fig. 40) and bathymetric data (Fig. 13).

All cores contain mass-movement deposits in a background sediment of bioturbated silty clay/clayey silt with clasts, shells and wood fragments (Fig. 41). P0103026 (1.27 m long), from the inner part of Tafjorden, contains 4 turbidites. A sample (0.28-0.33 m) from below the uppermost and thickest turbidite gave an age of 647 BP (690 ± 55 ^{14}C BP) (Table 3), which represents a maximum age of that turbidite. Accounting for an erosion at the base, the turbidite may be 400 years or younger. If there was significant erosion during deposition of the turbidite, it may be much younger. Thin hemipelagic deposits on top of the turbidite point to a young age, possibly the 1934 event (see below). A sample from below (0.86-0.91 m) the lowermost and thinnest turbidite gave an age of 3141 BP (2900 ± 70 ^{14}C BP) (Table 3), which represents a maximum age of that turbidite. No dating was undertaken to determine the ages of intervening turbidites in P0103026. From sedimentation rates, it is estimated that one very small event occurred around 1700 BP, and one larger event around 2500 BP. The ages are very approximate.

The studied cores are separated by several kilometres, and a correlation of turbidites from core to core would therefore be very speculative. The topography of the surrounding mountains as well as the swath bathymetric data (Fig. 13) indicate that most of the turbidites are locally derived and possibly related to mass-movement activity on the fjord slopes (above and below sea level).

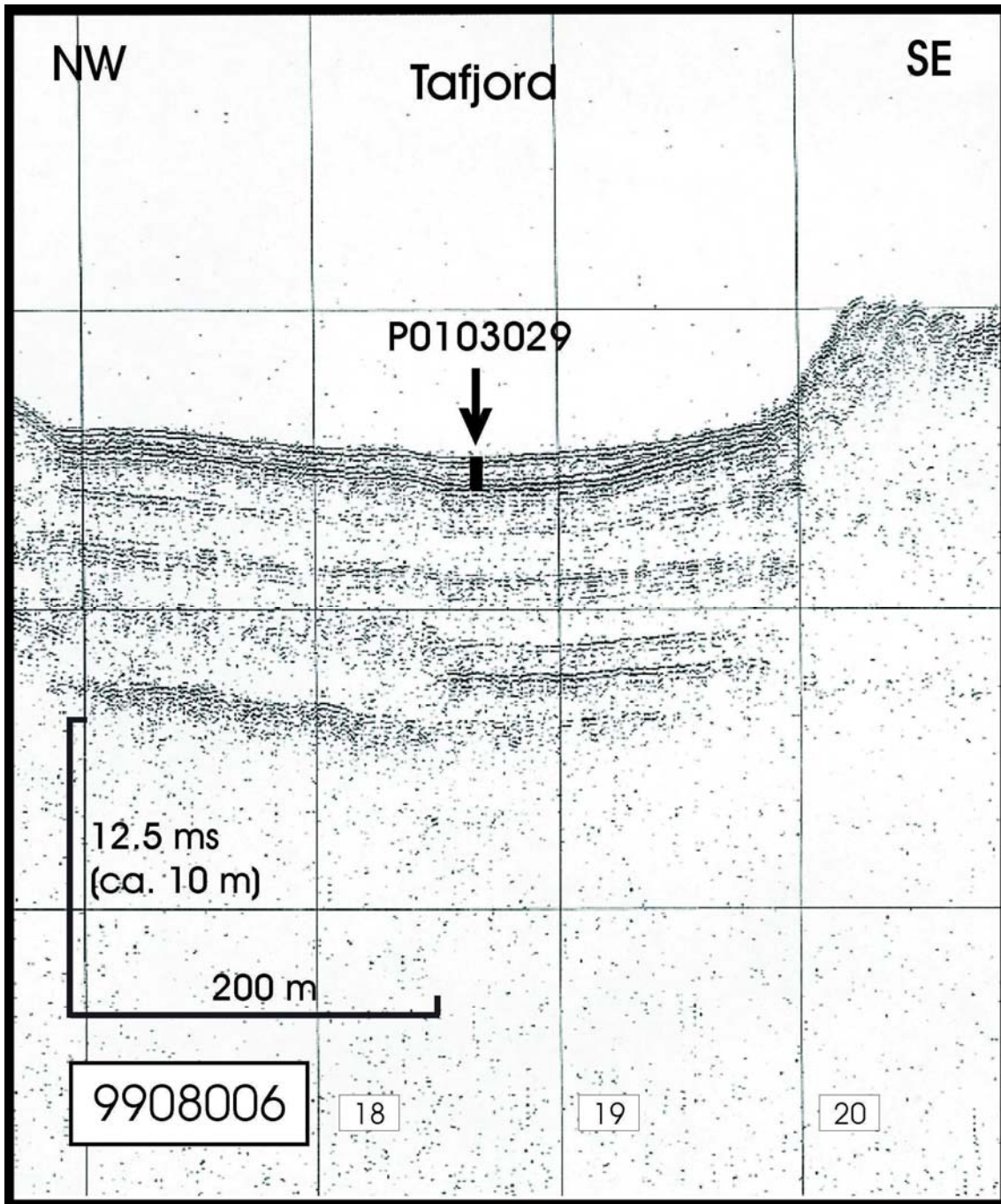


Figure 40. Seismic profile at the location of core P0103029, Tafjorden.

5.4 Romsdal

5.4.1 Mifjorden

Core P0103031 (0.57 m long) was obtained in Midfjorden (Table 1, Fig. 1). At this site, the aim was to reach the interpreted green reflector, at ca. 1.5 m depth. The retrieved sediment

comprises homogenous, bioturbated, olive silty clay with shells and fecal pellets (Fig. 41). Due to the short core length and the homogenous nature of the sediment, it was decided not to date this core.

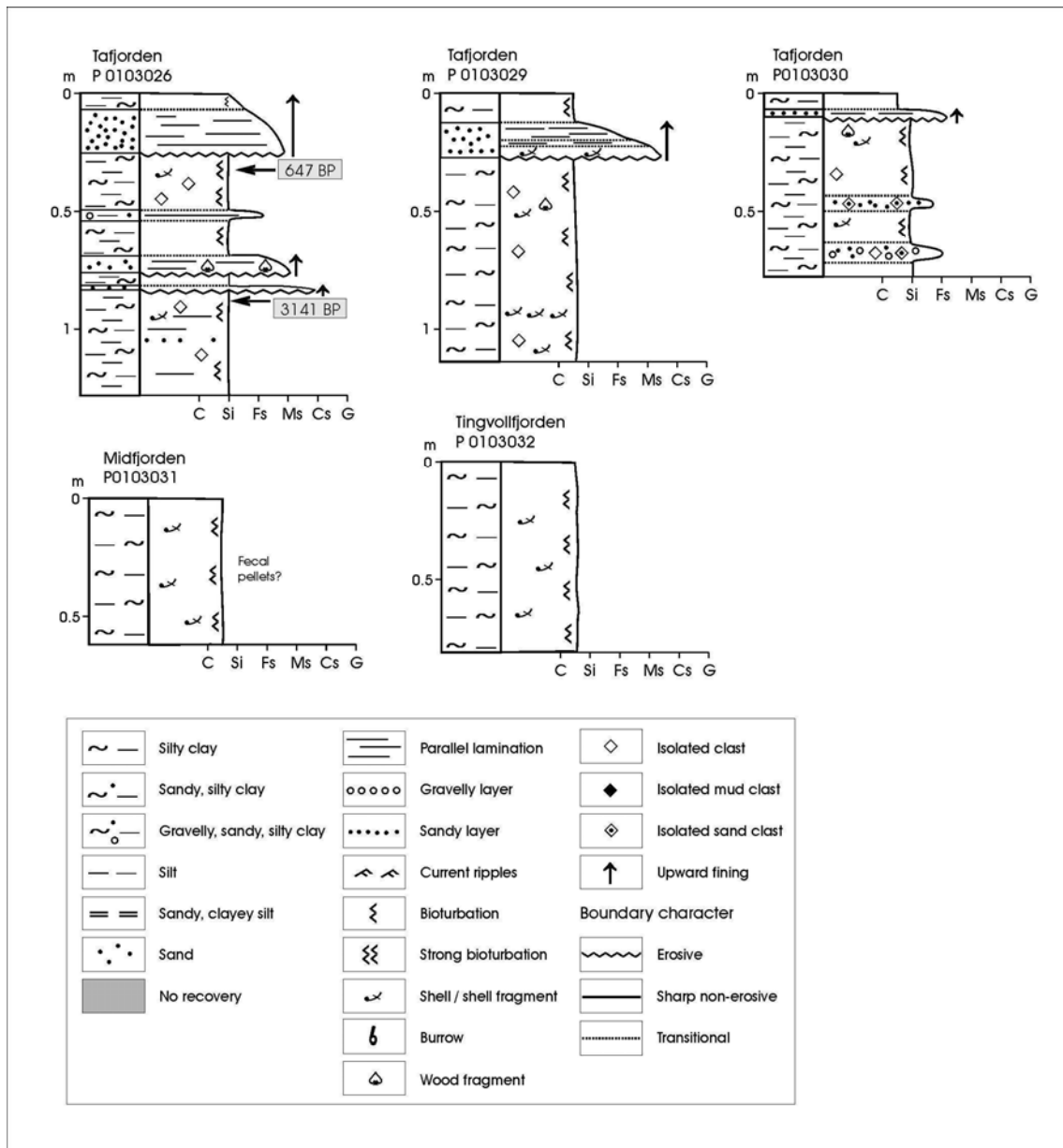


Figure 41. Cores from Tafjorden, Midfjorden and Tingvollfjorden.

5.4.2 Julsundet

During a Geoconsult cruise in November 2001 (Geoconsult 2002), one site was visited in Julsundet (Fig. 1) to obtain a long core (Table 1). NGU-6L/SC (6.47 m long, penetration

10.50 m) was aimed to penetrate the interpreted red, green and orange reflectors at approximately 1 m, 2 m and 3.5 m depths, respectively.

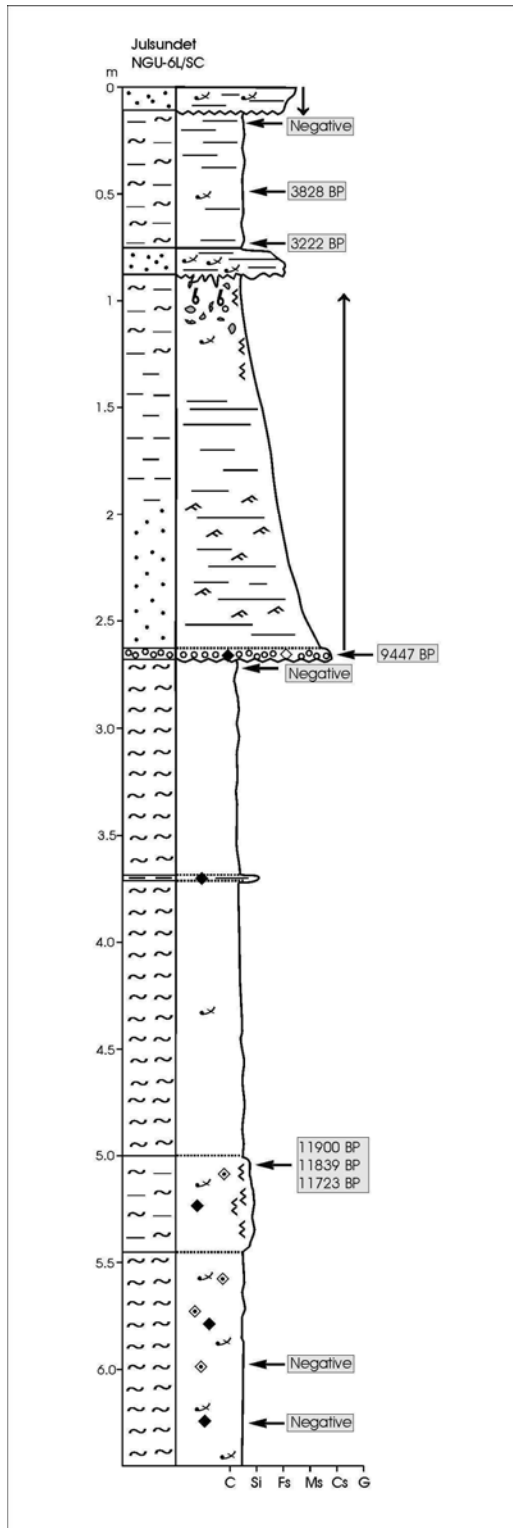


Figure 42. Core from Julsundet. Note that at 5.09-5.13 m depth, three possible ages around 11 800 BP are presented.

The uppermost 0.11 m of the core comprises very dark grey, poorly sorted, normally graded sand with many shells and shell fragments smaller than 1 cm (Fig. 42). Olive grey, homogeneous, normally graded silty clay/clayey silt occurs at 0.11-0.77 m. The uppermost part of this interval is laminated. A sample at 0.16-0.20 m depth did not contain enough foraminifers for ^{14}C -dating. Another sample at 0.45-0.50 m depth gave an age of 3828 BP (3475 ± 60 ^{14}C BP) (Table 3). At 0.77-0.88 m depth, a bed of clayey and silty fine sand with many shell fragments up to medium sand size occurs. The bed is laminated/layered, has a sharp, planar upper boundary and a sharp, undulating (load structures) lower boundary. We interpret this bed to be a turbidite. A sample from 0.71-0.75 m depth gave an age of 3222 BP (2965 ± 55 ^{14}C BP) (Table 3), which is a minimum age for the deposit. The dating results do not allow calculation of sedimentation rates for the normally graded silty clay/clayey silt at 0.11-0.77 m. The age of 3828 BP stratigraphically above a younger age suggest that this interval comprises resedimented material. It is thus not possible to date the uppermost, normally graded sand layer in the core. Possible interpretations are that this is ca. 2000 years old, while the fine sand layer at 0.77-0.88 m is ca. 3200 years old.

At 0.88-2.67 m depth, a upward fining unit with an erosive lower boundary occurs. The lowermost 5 cm of the unit is a gravel bed with clasts up to 1 cm in diameter and clay clasts (from the underlying unit) up to 2 cm in diameter. There is a well defined boundary towards planar laminated, upward fining, very coarse to fine sand at 2.62-2.50 m depth. At 2.50-1.90 m depth, cross-laminated and planar laminated, upward fining, fine to very fine sand occurs, while planar laminated, upward fining, very fine sand to silt occurs at 1.90-1.30 m depth. Bioturbated, upward fining clayey silt to silty clay occurs at 1.30-0.88 m depth, with large burrows in the uppermost part. A dating of shells from the lowermost gravel bed gave an age of 9447 BP (8485 ± 65 ^{14}C BP) (Table 3). The shells are most probably reworked from an older deposit (see below), and the dating result thus give a maximum age for the upward fining unit, which we interpret as a tsunami deposit related to the Storegga Slide.

At 2.67-5.02 m depth, light grey to grey, homogeneous clay occurs (Fig. 42). Black staining occurs at 2.67-2.82 m and 3.77-3.87 m depth. A sample at 2.69-2.77 m depth did not contain enough carbonate for ^{14}C dating. Laminated and partly cemented silt bands occur at 3.70-3.72 m and 5.02-5.09 m depth. Both of these cause spikes in the MSCL density data (Lepland et al. 2002). Bioturbated, homogeneous, olive grey silty clay/clayey silt occurs at 5.09-5.47 m depth. A dating at 5.09-5.13 m depth gave possible calendar ages of 11 900 BP, 11 839 BP and 11 723 BP ($10\,250 \pm 75$ ^{14}C BP) (Table 3), showing that this interval was deposited in the Younger Dryas. Homogeneous, olive grey silty clay with many small and large (up to 15 cm length) sand clasts occurs at 5.47-6.47 cm depth. The sand clasts are rich in shells and shell fragments, and are consolidated/partly cemented. Samples of sediment from between the sand clasts, at 5.92-5.97 and 6.23-6.27 m depth, did not contain enough foraminifers for dating, but the age of ca. 11 800 BP, above this interval, and the lithology suggest that these are glaciomarine sediments with sand clasts dropped from floating ice.

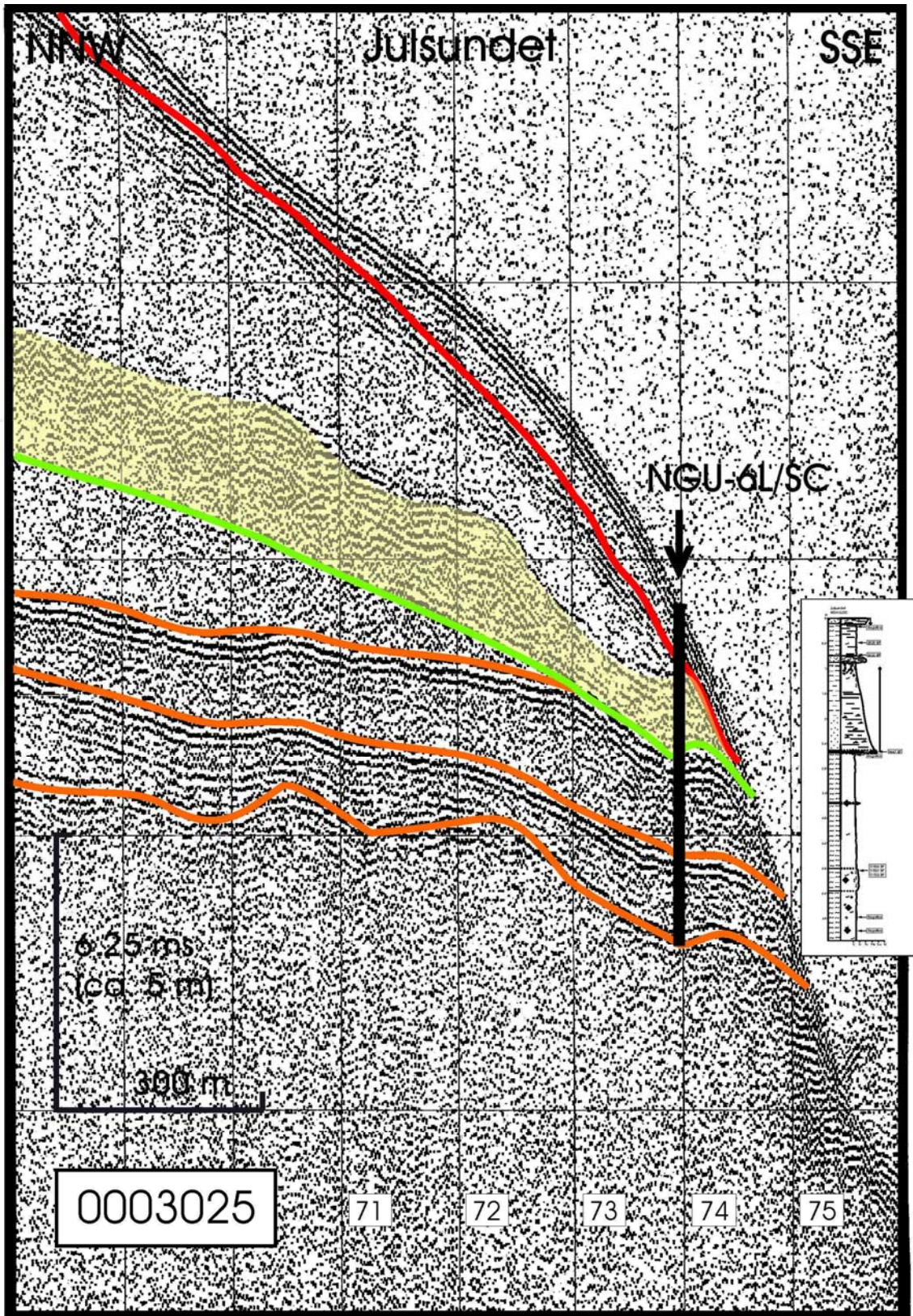


Figure 43. Seismic profile at the location of core NGU-6L/SC, Julsundet. Interpreted Storegga Slide deposits are in yellow. Colour coding of reflectors according to Longva et al. (2001). See Fig. 42 for lithology details.

The reasons for the relatively low core recovery (core length/penetration) may be several, e.g. sediment compaction, that the uppermost part of the seabed sediments did not enter the corer, that sediments in the lowermost part of the cored section did not enter the corer, or that the lowermost part of the cored section was lost during retrieval. We have assumed that the core is from the seabed downwards (Fig. 43), which fits well with our seismic interpretations. In this part of Julsundet, the interpreted red reflector of Longva et al. (2001a) (Fig. 43) occurs at the level of the fine sand bed at 0.77-0.88 m depth, which has a minimum age of 3222 BP and which rests on top of the Storegga Slide tsunami deposit. In Julsundet, we thus interpret the red reflector to be ca. 3200 years old. The interpreted green reflector can be correlated with the base of the upward fining unit at 2.67 m depth (the Storegga Slide tsunami deposit). Seismic data indicate that debrisflow deposits occur at this level further north in Julsundet. At the coring site, the seismic data indicate that the uppermost orange reflector of Longva et al. (2001a) has been eroded by the Storegga Slide tsunami. The age of ca. 11 800 BP ($10\,250 \pm 75$ ^{14}C BP) at 5.11 m depth is probably obtained close to the middle orange reflector, showing that in Julsundet, the orange reflectors are 10 000-13 000 years old (9000-11 000 ^{14}C years old), as suggested by Longva et al. (2001a).

5.5 Nordmøre

5.5.1 Tingvollfjorden

Core P0103032 (0.81 m long) was obtained from Tingvollfjorden (Table 1, Fig. 1). At this site, the aim was to penetrate into the interpreted green slide deposits, at ca. 2.3 m depth. The retrieved sediment comprises homogenous, bioturbated, olive grey silty clay with shells and shell fragments (Fig. 41). Due to the short core length and the homogenous nature of the sediment, it was decided not to date this core.

5.5.2 Halsafjorden

During a Geoconsult cruise in November 2001 (Geoconsult 2002), one site was visited in Halsafjorden (Fig. 1) to obtain a long core. Several large but relatively old slides occur along both fjord margins (Fig. 44). NGU-4L/SC (7.36 m long, penetration 12 m) (Table 1) was aimed to penetrate the total succession above the interpreted violet reflector (Fig. 45). The green, uppermost orange and violet reflectors were interpreted to occur at approximately 5.4 m, 8.5 m and 12.3 m, respectively (assuming a compressional wave velocity in the sea bed sediments of 1600 m/s). The reasons for the relatively low core recovery may be several, e.g. sediment compaction, that the uppermost part of the seabed sediments did not enter the corer, that sediments in the lowermost part of the cored section did not enter the corer, or that the

lowermost part of the cored section was lost during retrieval. In our interpretations, we have assumed that the core is from the seabed downwards (Fig. 45, see below).

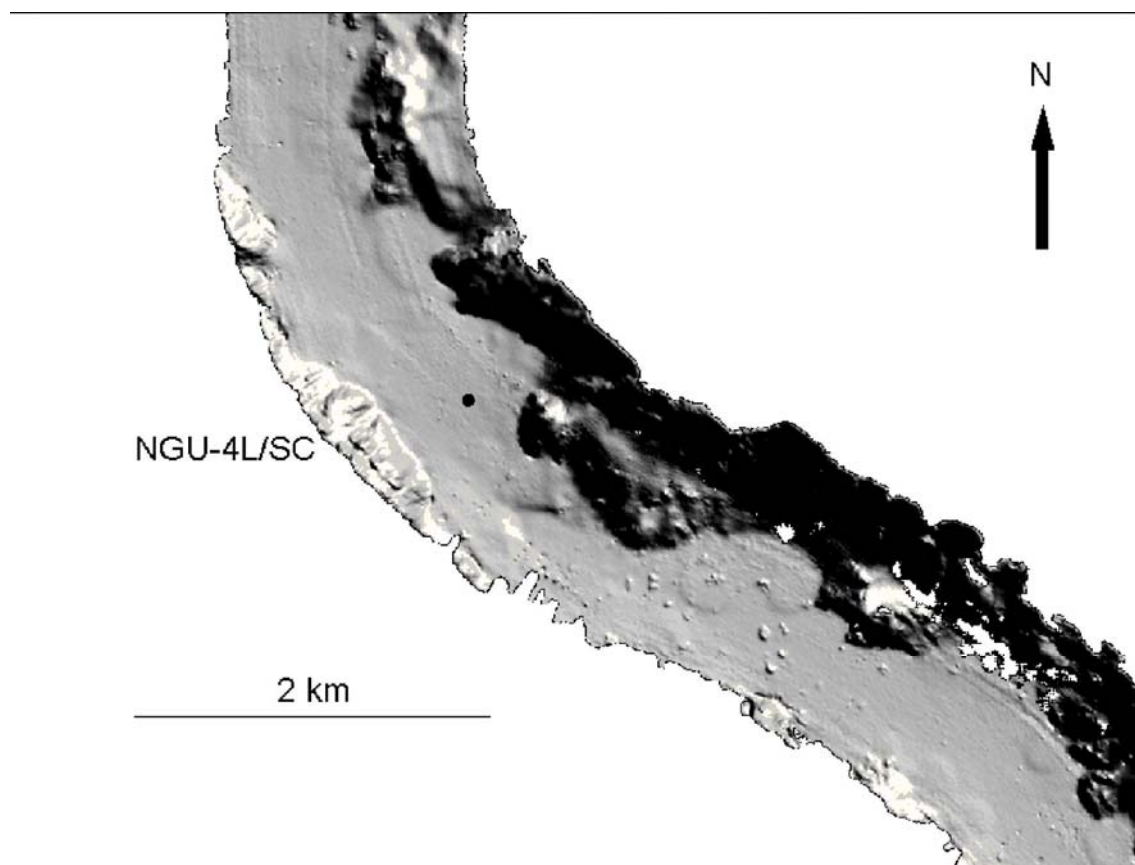


Figure 44. Shaded relief image from swath bathymetry and core location, Halsafjorden.

In the interval 0-6.91 m, the core comprises strongly bioturbated, olive grey, homogeneous silty clay/clayey silt with many shells and shell fragments less than 1 mm in diameter and five normally graded beds/turbidites (Fig. 46). A dating at 1.51-1.55 m depth gave an age of 3548 BP (3250 ± 50 ^{14}C BP) (Table 3).

The uppermost of the graded beds occurs at 3.61-3.70 m, and comprises dark grey, laminated medium sand with an erosive lower boundary. Upwards, the sand grades into silt. A dating at 3.71-3.75 m gave an age of 8374 BP (7530 ± 75 ^{14}C BP), which represents a maximum age for the deposit. We interpret this bed as a tsunami deposit related to the Storegga Slide.

The second graded bed occurs at 5.02-5.13 m depth, and comprises dark grey, laminated fine-very fine sand at 5.08-5.13 m depth, overlain by grey, laminated silt at 5.02-5.08 m depth. The bed is strongly influenced by loading/soft sediment deformation. A sample of deformed silty clay/clayey silt at 5.14-5.18 m depth contained a mixture of various faunas, indicating that the sediment is a debrisflow deposit. This sample was not dated. A sample at 4.98-5.02 m

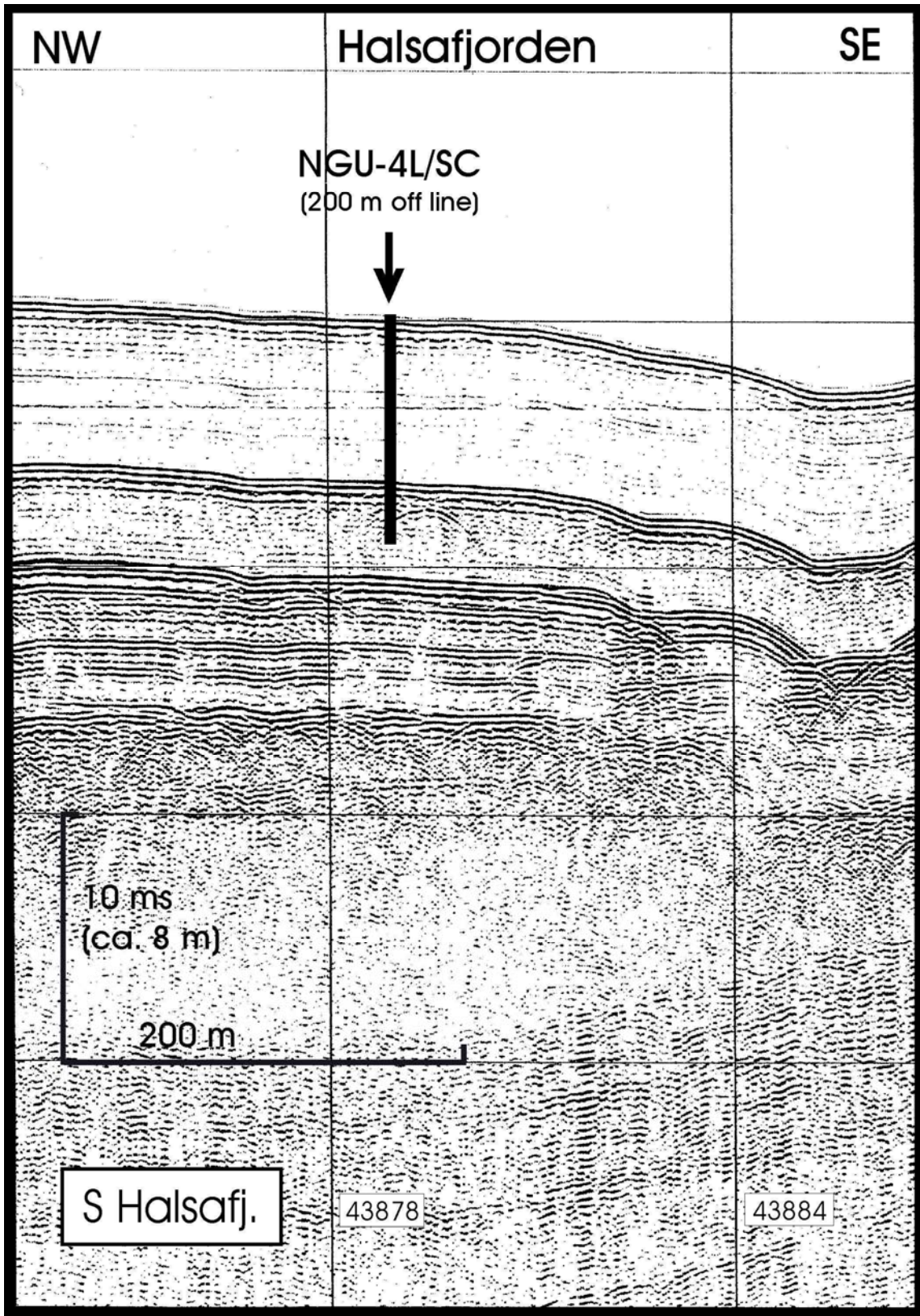


Figure 45. Seismic profile at the location of core NGU-4L/SC, Halsafjorden.

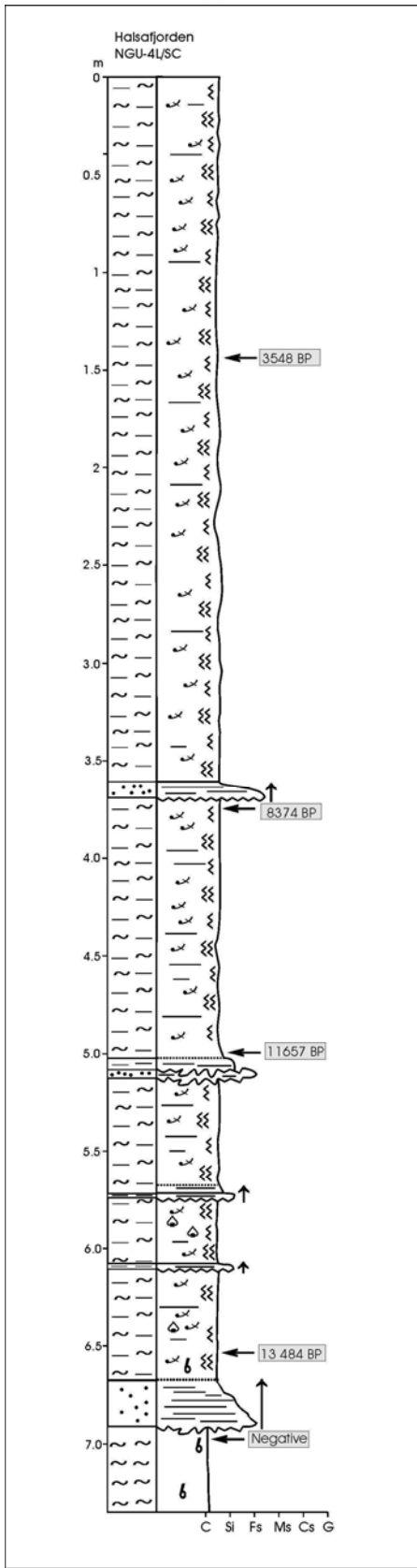


Figure 46. Core from Halsafjorden.

depth gave an age of 11 657 BP ($10\,160 \pm 75$ ^{14}C BP), which represents a minimum age for the debrisflow deposit. Two thin turbidites occur at 5.68-5.74 m (light grey silt at 5.74-5.73 m, clayey silt at 5.73-5.68 m) and 6.08-6.11 m (light grey silt fining up into clayey silt), while a thicker, grey, laminated fine sand to silt turbidite, strongly influenced by loading/soft sediment deformation, occurs at 6.68-6.91 m. Numerous black spots occur in the interval 6.11-6.36 m. A sample from 6.50-6.54 m depth gave an age of 13 484 BP ($11\,680 \pm 80$ ^{14}C BP) (Table 3), which is a minimum age for the underlying, thick turbidite. A sample from 6.91-6.93 m depth, below the turbidite, did not contain enough foraminifers for dating. Homogeneous, light grey clay occurs at 6.91-7.36 m depth.

At the coring site, the interpreted green reflector of Longva et al. (2001a) occurs at 6.75 ms (5-6 m) depth. We are uncertain which level in the core that can be correlated with this reflector. The most likely candidate (assuming that the core extends from the seabed downwards) is the turbidite at 5.02-5.13 m depth, with a minimum age of 11 657 BP. Another possible candidate is the turbidite at 6.68-6.91 m depth, which has a minimum age of 13 484 BP. The latter may in fact be correlated with the uppermost orange reflector interpreted by Longva et al. (2001a). It appears that in Halsafjorden, the reflectors are generally older than suggested by Longva et al. (2001a). This also implies that the uppermost extensive debrisflow deposits along the fjord margins are older than the Storegga Slide. If our assumption that the core extends from the seabed downwards is incorrect, our interpretations of major slides and debrisflow deposits at the 11 000-11 700 BP level, and not at the 8200 BP level, would probably have to be changed. It could also imply that a possible 2000-2200 BP event, in the upper part of the section, has not been preserved in the core. However, if the sedimentation rate has been relatively constant after the Storegga Slide event, as suggested by our dating results (ca. 0.45 mm/year), this suggests that the upper part of the stratigraphic section is preserved in the core.

6. LAKE INVESTIGATIONS IN SUNNMØRE AND NORDFJORD

Altogether 24 radiocarbon dates, including 3 AMS dates, were performed at Laboratoriet for radiologisk datering, NTNU, Trondheim (Table 4). All dates except two are on gyttja samples. The two exceptions are on shells from two late glacial diamictic zones in Nedstevatnet. One sample, from the lower part of core 10, in Storsætervatnet, was dated for timing the deglaciation, the others are related to sedimentary units that can be linked to mass movements. Such units are diamictic zones in glaciomarine silt (Medvatnet, Nedstevatnet), repeated stratigraphy (i.a. several Vedde Ash layers) in Storsætervatnet, distinct sedimentary hiati, and minerogenic laminae or beds in the Holocene gyttja. The ages of fine-grained laminae in gyttja were determined on samples that included equal amounts of material from above and below the laminae. Ideally these should give near precise age estimates. Thicker or more coarse grained beds were dated using samples either from above or beneath the layers.

Hence, these dates give minimum and maximum age estimates, respectively. Data from three of the lakes are presented in a recent thesis by Hovland and Sandnes (2002).

Table 4. ^{14}C radiocarbon dating results, lake cores.

Lake	Core ID	Depth (cm)	Sample ID	Lab. No.	Material	Sample weight (g)	Age ^{14}C (BP)	Calendar-year age (BP)	$\delta^{13}\text{C}$ (‰)	Remarks
Storsætervatnet	S1	72-77	S1-72	T-15551A	gyttja	5	4895±70	5607 (5661-5590)	-29,2	Above and beneath 9 mm silt lamina
Storsætervatnet	S4	181-183	S4-181	T-15552A	gyttja	7,1	8195±135	9181 (9416-9008)	-27,2	Above hiatus silt/gyttja
Storsætervatnet	S6	152-157	S6-154	T-15553A	gyttja	4,5	8055±150	9006 (9243-8649)	-26,8	Above hiatus silt/gyttja
Storsætervatnet	S9	129-133	S9-133	T-15554A	gyttja	5,6	2585±80	2744 (2765-2545)	-29	Above gravely sand layer
Storsætervatnet	S9	144-147	S9-144	T-15555A	gyttja	5,2	7895±115	8643 (8995-8544)	-29,8	Below gravely sand layer
Storsætervatnet	S9	181-179	S9-180	T-15556A	gyttja	1,9	8285±145	9366 (9473-9030)	-28,4	Above and beneath 1 cm sand layer
Storsætervatnet	S10	474	S10-474	TUa-3340A	gyttja	not determined	11345±75	13254 (13448-13159)	-26,8	Organic laminae below Vedde Ash
Medvatnet	M2	60-64	M2-62	T-15513A	gyttja	2,3	3090±95	3279 (3389-3167)	-29,9	Above and below 2 cm gravely silt layer
Medvatnet	M2	160-164	M2-160	T-15557A	gyttja	3,4	4855±120	5594 (5710-5472)	-29,3	Below pebbles and sand/silt clasts
Medvatnet	M4	90-93	M4-91	T-15514A	gyttja	3,3	3220±105	3449 (3567-3355)	-28,6	Above and below 2 thin silt lamina
Medvatnet	M6	0-4	M6-02	T-15515A	gyttja	1,6	2505±80	2619 (2745-2362)	-29,7	Above 9 cm thick sand layer
Nedstevatnet	N2	10-14	N2-12	T-15516A	gyttja	1,9	2880±105	2979 (3207-2865)	-29,7	Above thick layer containing sand clasts
Nedstevatnet	N2	40-45	N2-42	T-15517A	gyttja	4,9	5780±80	6600 (6718-6454)	-27,7	Below thick layer containing sand clasts
Nedstevatnet	N2	99-105	N2-103	T-15518A	gyttja	4,3	6430±65	7367 (7425-7270)	-26,4	Above and below silt/sand lamina
Nedstevatnet	N3	42-45	N3-40	T-15558A	gyttja	3,5	5950±95	6772 (6889-6667)	-27	Beneath 2 cm thick sand layer
Nedstevatnet	N3	300-306	N3-300	T-15520	shell	not determined	11030±70	13009 (13146-12907)	-1 (assumed)	diamicton containing Astarte and M. truncata
Nedstevatnet	N3	270	N3-270	T-15519	shell	not determined	10225±120	11793 (12325-11644)	-1 (assumed)	diamicton containing Mya truncata
Nedstevatnet	N5	14-18	N5-16	T-15521A	gyttja	2,8	2235±75	2208 (2343-2132)	-29,1	Above tsunami layer
Nedstevatnet	N5	90-91	N5-90	TUa-3322a	gyttja	not determined	8805±80	9845 (10147-9695)	-28	Above 2 thin sand lamina
Nedstevatnet	N5	96	N5-96	TUa-3341A	gyttja	not determined	9310±65	10434 (10636-10405)	-26,8	2 mm thick gyttja lamina
Nedstevatnet	N5	105-113	N5-109	T-15522A	brown silt	0,8	9985±190	11316 (11926-11198)	-24	Above and beneath 2 cm gravely sand layer
Rotevatnet	R1	171-178	R1-175	T-15525A	gyttja	6,4	5680±130	6700 (6854-6503)	-29,5	Above and beneath 3 mm silt lamina
Rotevatnet	R1	119-125	R1-121	T-15524A	gyttja	6,2	4605±115	5314 (5469-5053)	-29,4	Above and beneath 2 mm distinct silt lamina
Rotevatnet	R1	21-28	R1-24	T-15523A	gyttja	5,9	1865±100	1820 (1921-1633)	-29,5	Above and beneath silt lamina

6.1 Storsætervatnet

Storsætervatnet (277 m a.s.l., Eid commune) is located at the local watershed between Stigedalen and the lower part of Fladalen, which runs NNE-SSW (Fig. 4). The lake is located

at the bend where the two valleys join. It has an areal extent of 0.2 km² (A), a catchment area of 3.5 km² (B), and a greatest water depth of 11 m. The B:A ratio is 18.5. A thin, discontinuous till cover encompasses the lake. At the main river inlet there is a small delta, while a low-angled fan southeast of the lake has presumably a glaciofluvial origin. Storsætervatnet's catchment area (Fig. 4) is rather gentle compared to the two other investigated lakes in Stigedalen (Medvatnet and Nedstevatnet), and it is unlikely that large mass movements from the surrounding areas reach the lake. Litlesætervatnet, 250 m upstream in Fladalen, works as a sedimentation trap, and hence the allochthonous sediment transport into Storsætervatnet is sparse. Due to the large catchment area of Fladalselva, the water discharge may be rather great, although less than for Medvatnet and Nedstevatnet, further downstream.

One incentive for investigating Storsætervatnet is an observation of a repeated stratigraphy with two Vedde Ash layers in the northern part of the lake (Ekrene et al. 1992). The main trends of the postglacial vegetational development, based on pollen analysis from Storsætervatnet, have been expounded by Gjelsvik & Kui (1992).

Of the 10 cores from Storsætervatnet (sampled in water depths of 6-11 m, Table 2), S1 is from the southern part of the lake and S9 is from the central part. The remaining cores are from the narrow northern part, where the double Vedde Ash layer has been found. The core lengths vary from 0.5 m to 4.8 m (Fig. 47). All cores, except S7, penetrate into glaciolacustrine sediments (silt), which has a thickness of more than 1.7 m in S4. Laminated Vedde Ash layers (nearly black in their lower parts) up to 10-15 cm thick and with sharp, lower boundaries and gradual upper boundaries occur in 6 cores. S10 has 5 Vedde Ash layers, which are ascribed to repetition by postdepositional slumping and folding. In the lowermost half meter of S10, beneath the Vedde Ash layers, two laminated series occur, each containing 3-4 organic, fibrous bands, separated by 10 cm silt. Due to the similarity of the two laminated series, we are apt to suggest a repeated stratigraphy here, as for the Vedde Ash layers. A dating of the lowermost organic band gave an age of 13 254 BP ($11\,345 \pm 75$ ¹⁴C BP) (Table 4), which accordingly is a minimum age for the deglaciation of the lake.

The boundaries between Holocene gyttja and glaciolacustrine silt are transitional, except for S3, S4 and S6, where hiati were observed. In these cores, the Vedde Ash layers are missing. Dating results from gyttja immediately above the hiati in S4 and S6 gave ages of 9181 BP (8195 ± 135 ¹⁴C BP) and 9006 BP (8055 ± 150 ¹⁴C BP), respectively, indicating an erosional (slumping) event involving the removal of the top silt (including Vedde Ash) and the earliest Holocene gyttja in late Boreal chronozone, around 9200 BP. The Holocene gyttja is rather homogeneous in all the cores. The seismic data from Storsætervatnet frequently display vague, discontinuous and hummocky reflectors (Longva and Olsen 2001, Sønstegaard et al. 2001). It is thus difficult to establish the correlation between seismic reflectors and lithological boundaries in the cores.

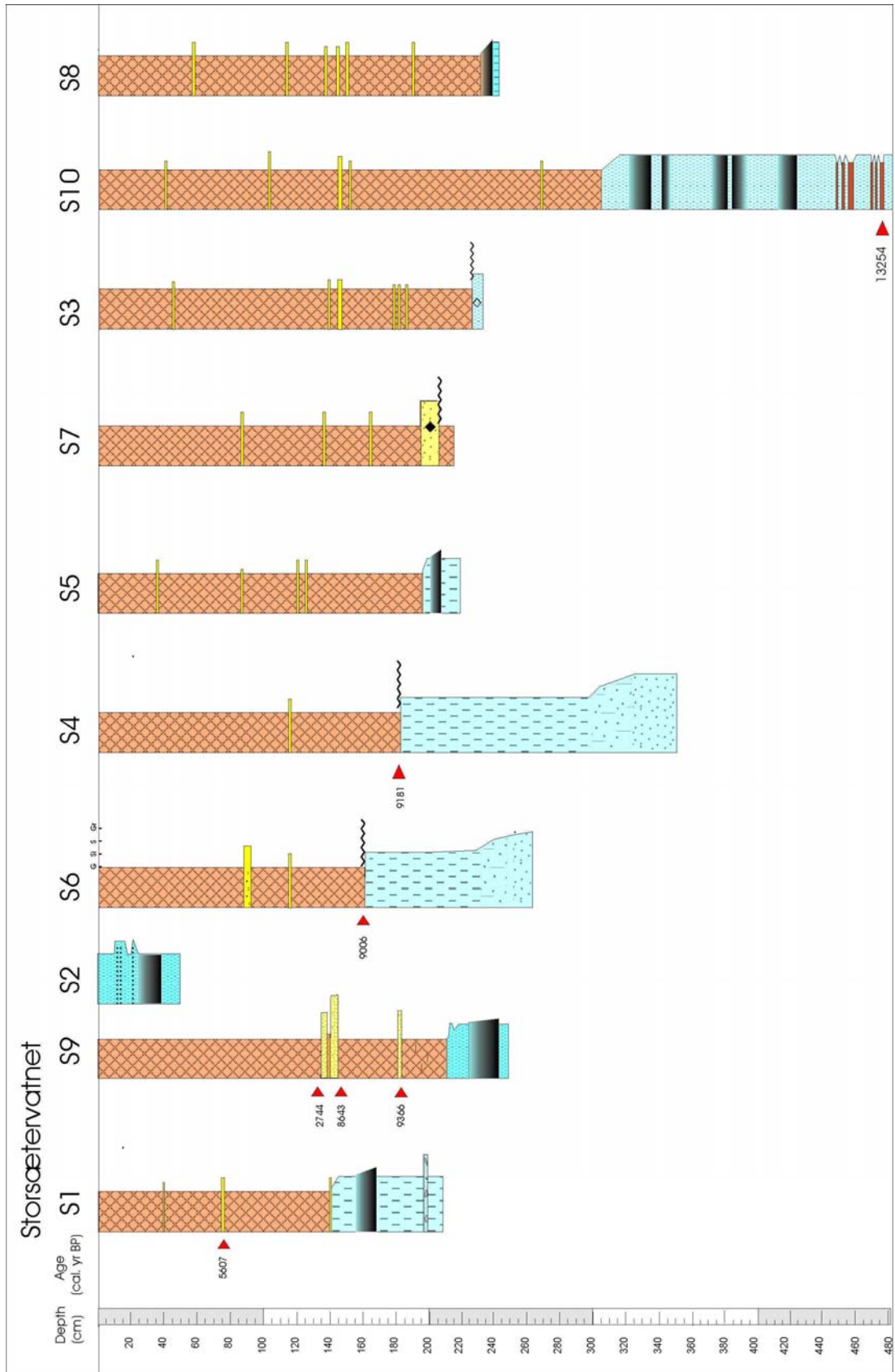


Figure 47. Cores from Storsætervatnet.

Three ages were obtained from core S9. A dating of a silt layer at 1.81-1.82 m depth gave an age of 9366 BP (8285 ± 145 ^{14}C BP). This lamina may possibly be related to the slumping that caused the hiatus in cores S3, S4 and S6. In contrast to the S4 and S6 dates, which are minimum ages, 9366 BP (8285 ± 145 ^{14}C BP) may reflect the actual age of the slumping, provided that the events can be correlated. The thick sand bed at 2 m depth in core S7 is also interpreted to be linked to the same event.

Two gravelly sand/silt layers, separated by 2 mm of gyttja, occur at 1.31-1.40 m depth in core S9. The lowermost layer exhibits upward fining, while the uppermost shows upward coarsening. A dating below the two layers gave an age of 8643 BP (7895 ± 115 ^{14}C BP), while a dating above gave an age of 2744 BP (2585 ± 80 ^{14}C BP). This is the thickest Holocene sand interval in Storsætervatnet, and since S9 is the core nearest to the river inlet, it is reasonable that the layers were deposited by debrisflows from the Fladalselva delta some time after 8643 BP, but before 2744 BP. The apparent long hiatus may be explained by a considerable erosion at the layers lower boundaries. The age of the uppermost debrisflow may be close to 2800 BP.

The lowermost layer is the most powerful Holocene event recorded in core S9, and one should expect to find traces of it all over the lake. In all cores, the faintly laminated gyttja contains one pronounced 5-90 mm thick sand/silt layer, nearly half way up the gyttja sequence (Fig. 47), whereas other laminae are only 1-2 mm thick. Our suggestion is that the pronounced sand/silt layers are synchronous and related to the same event. Dating of the layer at 0.72 m depth in core S1 gave an age of 5607 BP (4895 ± 70 ^{14}C BP). The spatial distribution of the layer supports the assumption that the main river (delta) was the source. In core S6, the layer is located deeper than in the other cores, which may explain the disproportionate great thickness of the layer there.

Assuming a constant sedimentation rate above the dated level in core S9, a silt lamina at 0.40 m can most probably be correlated with the 2800 BP level described above. The general setting, as described above, suggest that the silt laminae are either small turbidites or deposits related to heavy rainfall/river floods.

6.2 Medvatnet

Medvatnet (12.5 m a.s.l., Volda commune) is the third lowermost glacial basin of a series of 12 in the Stigedalen-Fladalen valley system (Fig. 4), that extends from the mountains at the Møre og Romsdal and Sogn og Fjordane border. It has an areal extent of 0.25 km² (A), a catchment area of 1.9 km² (B), and a greatest water depth of 23 m. The B:A ratio is 7.6. Medvatnet is located downstream of the much larger Bjørkedalsvatnet, and hence very little of the sediment input into lake Medvatnet derives from the main river. The drainage area of

Medvatnet is small, but the surrounding relief is large with steep valley sides reaching more than 1100 m a.s.l. to the west and nearly 1000 m to the east. Snow avalanches and small rock slides occur frequently, as seen from the barren stripes in the forest vegetation in the western valley side which constitutes most of the catchment area. There is a glaciofluvial delta deposit (gravel pit) southeast of the lake. Scree deposits cover the lower part of the valley sides.

Medvatnet lies well beneath the Younger Dryas sea level which, according to Fareth (1987), was 44 m a.s.l. Using late- and postglacial shoreline displacement curves from Sunnmøre (Svendsen and Mangerud 1987, 1990) it is reasonable to assume that Medvatnet isolated from the sea at ca. 10 200 BP (9200 ^{14}C BP) but was re-connected during a marine transgression (Tapes) at ca. 9200 BP (8300 ^{14}C BP) (Tapes). The last isolation might have taken place at ca. 5800 BP (5000 ^{14}C BP).

Of the 6 cores from Medvatnet (Table 2), M1 and M2 are from the northern part of the lake, whereas M3-M6 were cored along an ENE-WSW running seismic profile in the southern part of the lake. Water depths at the coring stations vary from 19 m to 22.5 m. The cores are 1.2-3.5 m long, and all of them penetrate the Holocene gyttja and into glaciomarine sediments (Fig. 48). The largest recognized thickness of the Holocene gyttja is 2.6 m. A gravelly sand unit, up to 30 cm thick, occurs in the lower part of the gyttja (0.2-0.7 m above its base) in all the cores. The unit consists of two to four gravelly sand layers (Fig. 49), which in three of the cores are separated by thin organic-rich horizons. The minerogenic beds may be massive, fining upwards or coarsening upwards. Wood fragments and crushed shells of bivalves and snails are common. The lower boundary, and often also the upper boundary of the unit, are sharp. The glaciomarine sediments consist mainly of silt (M4 also has a sand interval) and 15-20 cm thick diamictic beds (in cores M2 and M4). The seismic data from Medvatnet display many subparallel reflectors. Both the tsunami layer and the gyttja/silt boundary give reflections. According to these data, 0.5-1 m of the soft top gyttja has been lost during coring.

Four radiocarbon ages were obtained from the gyttja unit (Table 4). In core M2, a silty layer with gravel and coarse plant fragments, at 0.61-0.63 m depth, yielded an age of 3279 BP (3090 ± 95 ^{14}C BP). The poor sorting of this layer indicates that it is most likely a snow avalanche or a debrisflow deposit. Dating of another sample from below a distorted layer of poorly sorted sandy silt with pebbles up to 3 cm in diameter, at 1.58-1.60 m depth, gave an age of 5594 BP (4855 ± 120 ^{14}C BP). Also this layer probably represents a snow avalanche or debrisflow deposit, that was subsequently influenced by soft sediment deformation or possibly disturbed during sampling.

In core M4 (Fig. 48), two silt lamina at 0.91 and 0.92 m depth were dated and an age of 3449 (3220 ± 105 ^{14}C BP) was obtained. Under the conditions of a constant sedimentation rate above and below this level, a silt lamina at 0.70 m depth and a gravelly silt lamina at 1.15 m depth were deposited approximately 2600 BP and 4300 BP, respectively. Assuming a 8200 BP age of the Storegga tsunami deposit (see below), a constant sedimentation rate during the time interval 8200-3449 BP and no erosion associated with deposition of the thin coarse

grained laminae, a 4700 BP age of the gravelly silt lamina at 1.15 depth can be suggested. However, the lithology of this lamina indicates that it can possibly be correlated with the 5594 years old layer in core M2. We find the latter alternative most likely. The silt and gravelly silt lamina were probably deposited by snow avalanches or as turbidites/debrisflows during flood events.

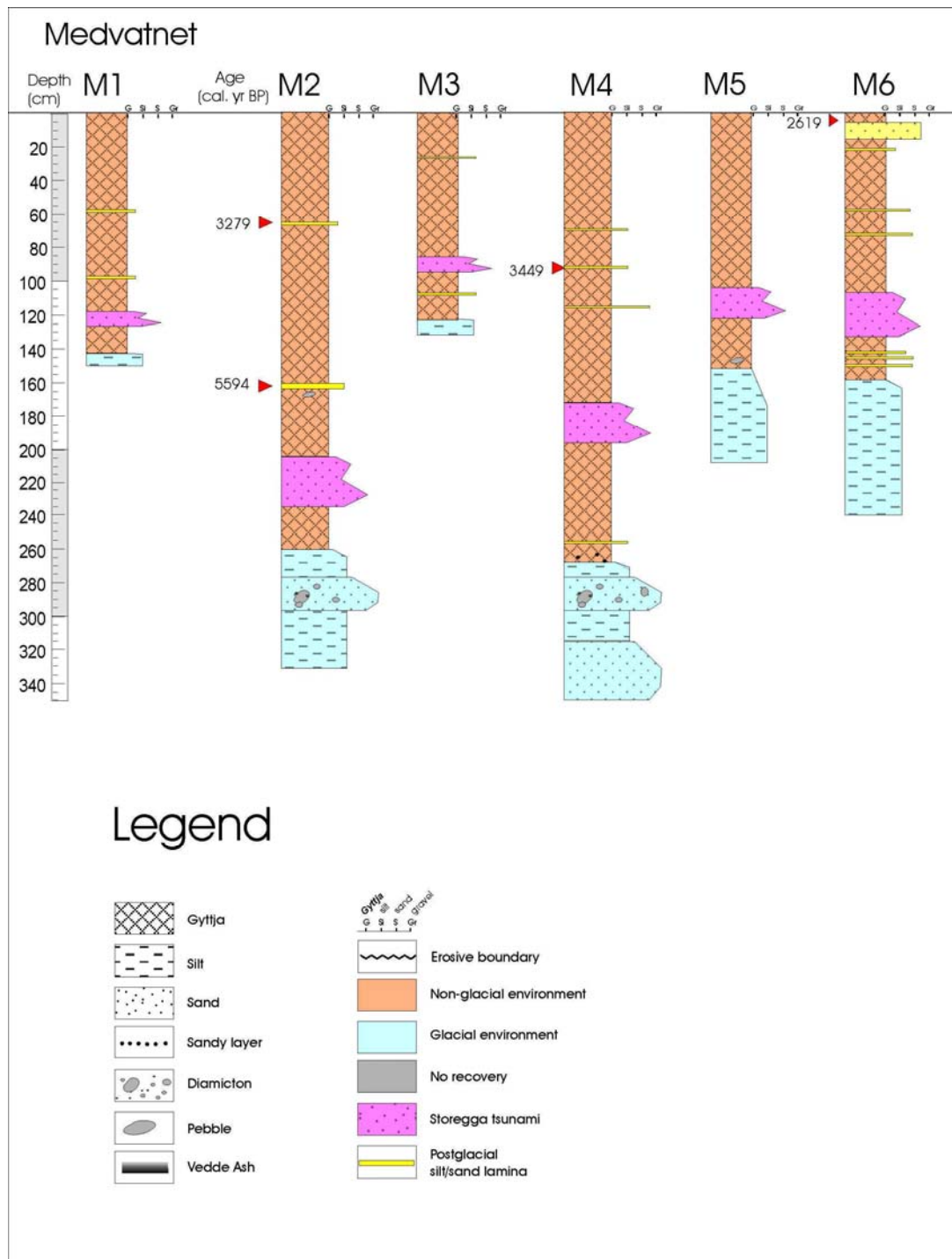


Figure 48. Cores from Medvatnet.

A dating from the uppermost part of core M6, above a sand layer at 0.09-0.18 m depth, gave an age of 2619 BP (2505 ± 80 ^{14}C BP) (indicating that the uppermost part of the lake sediments was probably lost during coring). The age represents a minimum age of the sand layer, which is most probably a turbidite derived from an area to the south or west of the lake. It can probably be correlated with the silt lamina interpreted to be ca. 2600 years old in core M4, 150 m further northeast within the same sub-basin. Such a correlation is also supported by seismic data. Obviously, the sedimentation rate has been low during accumulation of the uppermost part of M6. The turbidite that deposited this sand layer probably caused erosion of the underlying gyttja. It would thus be speculative to estimate the age of the two silt laminae between this layer and the interpreted Storegga tsunami deposit (see below)

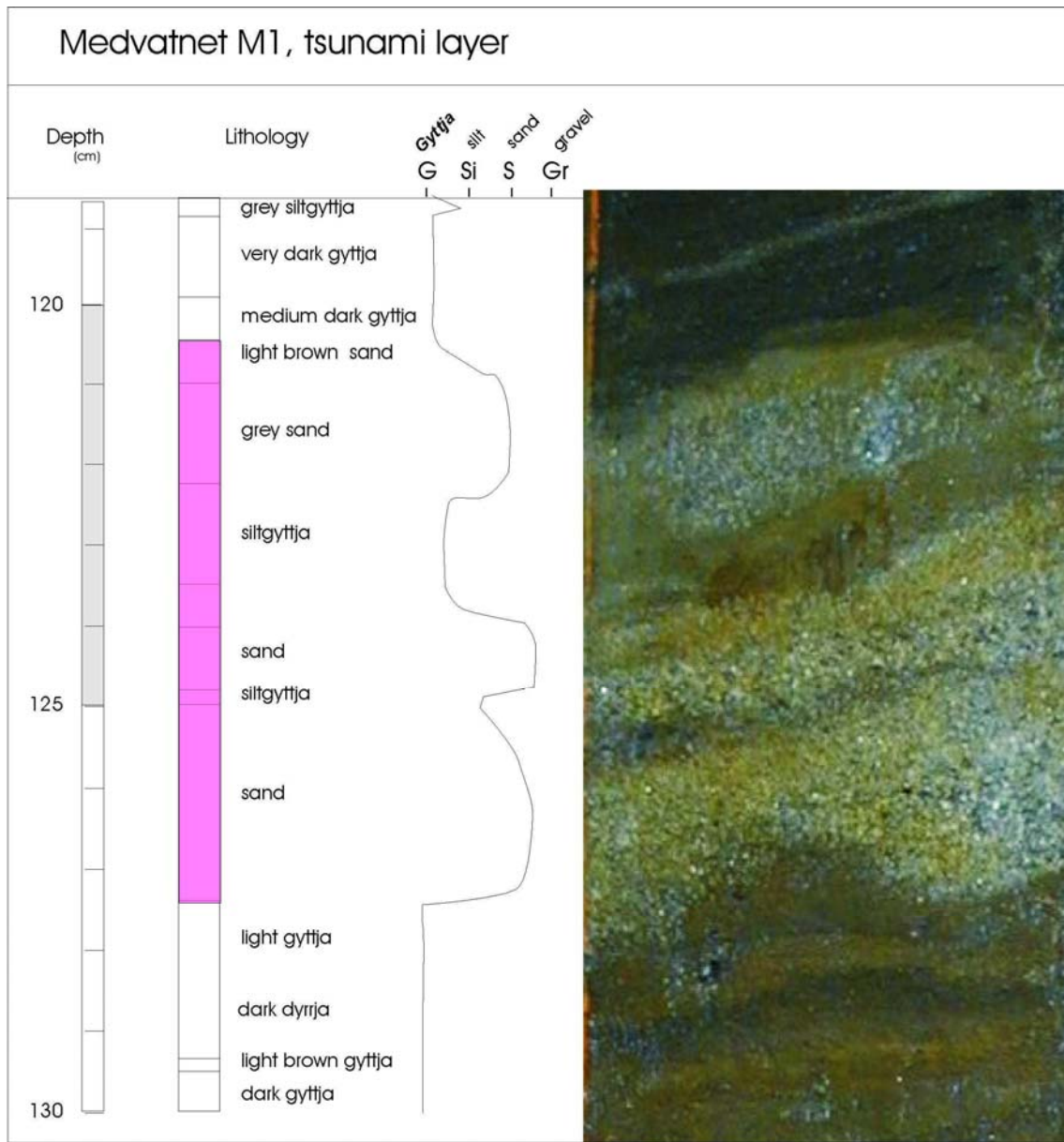


Figure 49. Interpreted Storegga Slide tsunami deposit, Medvatnet.

The gravelly sand unit in the lower part of the gyttja is most probably a tsunami deposit related to the Storegga Slide 8200 BP (7200 ¹⁴C BP) (Bondevik et al. 1997). This unit is therefore given its own (red) colour in the stratigraphic diagrams (Fig. 48). The unit has not been dated, however, its stratigraphic position e.g. in core M2, between the 5594 years old mass-movement deposit at 1.58-1.60 m depth and the base of the gyttja (ca. 11 000 BP) is consistent with this assumption. A very similar deposit occurs in Nedstevatnet (see below). Silt laminae in the lower part of the gyttja in cores M4 and M6 probably reflect small turbidity currents, snow avalanches or flood events in the first part of the Holocene, around 10-11 500 BP.

6.3 Nedstevatnet

Nedstevatnet (9 m a.s.l., Volda commune) lies 150 m downstream from Medvatnet (Fig. 4). It has an areal extent of 0.2 km² (A), a catchment area of 1.5 km² (B), and a greatest water depth of 20 m. The B:A ratio is 7.5. Both the lake and the drainage areas of Nedstevatnet are a little smaller than for Medvatnet. The eastern valley side (reaching up to 840 m a.s.l.) is steep with dense birch and spruce forest. The western valley side (reaching 1140 m a.s.l.) is scattered with scree deposits and snow avalanche trails.

Using sea-level curves from Sunnmøre (Svendsen and Mangerud 1987, 1990) it is reasonable to assume that Nedstevatnet was isolated from the sea ca. 4500 BP (4000 ¹⁴C BP). Correlation of seismic data with core stratigraphy (Figs. 50 and 51) suggests that up to 1 m of the most fluffy, near-surface gyttja was lost during coring, and most of the succession in the cores is thus interpreted to be marine. Both the interpreted Storegga Slide tsunami deposit and the base of the gyttja can be recognized in the seismic data, and probably also the young debrisflow deposit in the western part of the lake (see below).

Cores N1, N2, N3 and N5 (Table 2) are located in the deepest (water depths at coring sites are 15-18 m), south central part of the lake. The coring of N4 was not successful. The lengths of the cores vary from 3.1 m to 5.4 m. All cores penetrate into glaciomarine sediments (Fig. 50), which in N5 are more than 2 m thick. Ten samples were radiocarbon dated: 3 from N2, 3 from N3 and 5 from N5. Two dates are on shells from diamictic layers in the glaciomarine sediments in N3. Ages of 13 009 BP (11 030 ± 70 ¹⁴C BP) and 11 793 BP (10 225 ± 120 ¹⁴C BP) (Table 4) were obtained, showing that these were deposited during the Younger Dryas. Up to four silt and sand laminae occur at the boundary between glaciomarine sediments and gyttja. Dating of these in core N5 gave ages of 11 316 BP (9985 ± 190 ¹⁴C BP), 10 434 BP (9310 ± 65 ¹⁴C BP) and 9845 BP (8805 ± 80 ¹⁴C BP). These laminae may reflect small turbidity currents or flood events in the earliest Holocene.

An up to 0.35 m thick gravelly sand unit with shell fragments occurs within the gyttja, approximately 0.5 m above the glaciomarine sediments in all cores. A dating above the

deposit, in N5, gave an age of 2208 BP (2235 ± 75 ^{14}C BP). In this core the gyttja, above the gravelly sand unit, is only 0.2 m thick, compared to 1.5-2.95 m in the other 3 cores. The sedimentation rate is thus very low at site N5. We find it very likely that the gravelly sand unit is a tsunami deposit that can be related to the Storegga Slide. A strikingly similar gravelly sand layer occurs in all the cores in Medvatnet (see above).

Sand ca. 1 m above the interpreted Storegga tsunami deposit in N2 (sand lamina) and N3 (2 cm sand layer) gave ages of 7367 BP (6430 ± 65 ^{14}C BP) and <6772 BP (5950 ± 95 ^{14}C BP), respectively. These may represent two events, separated in time by 400-700 years, but could also be the same event. The sand lamina/layers probably represent turbidites.

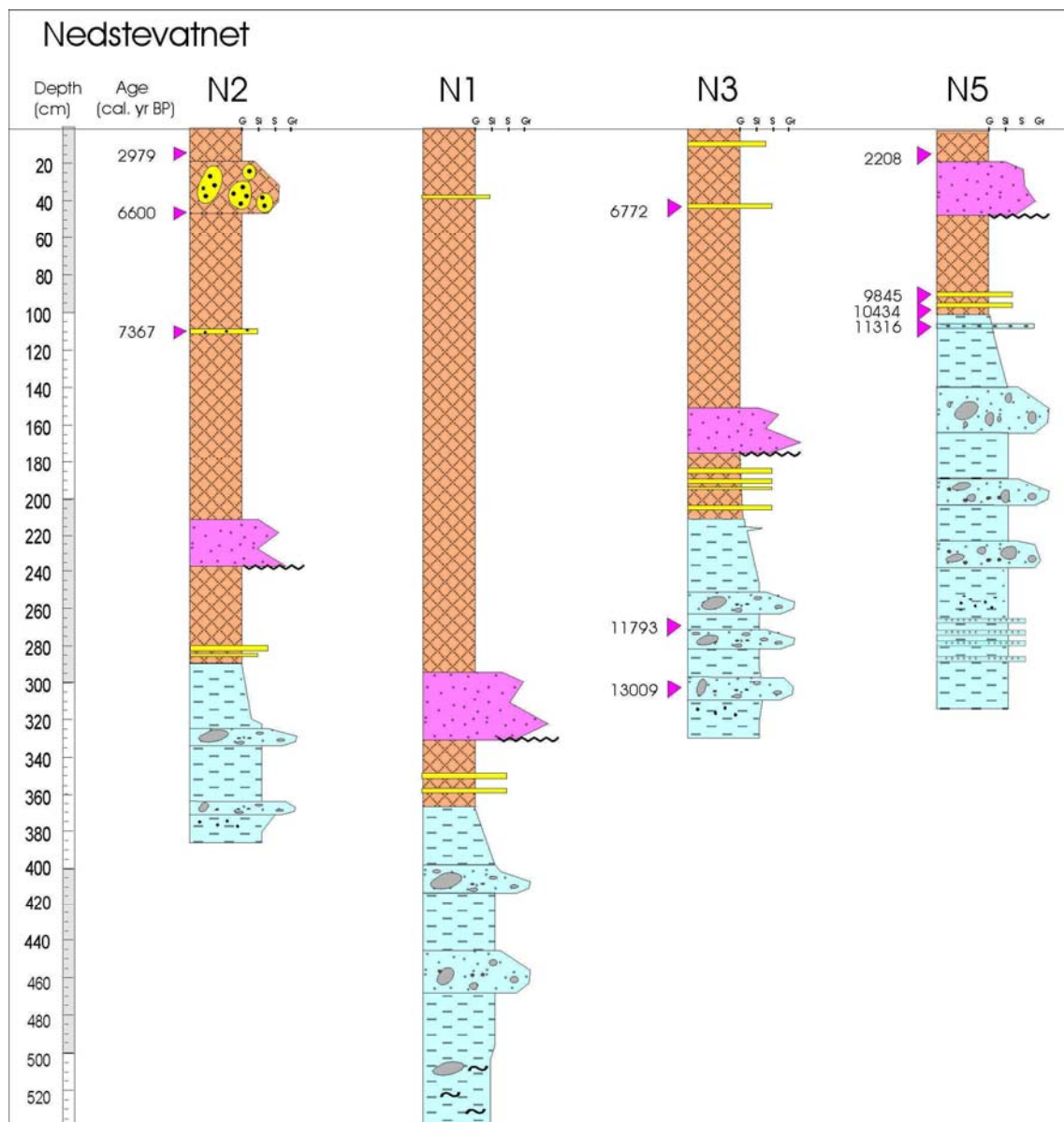


Figure 50. Cores from Nedstevatnet.

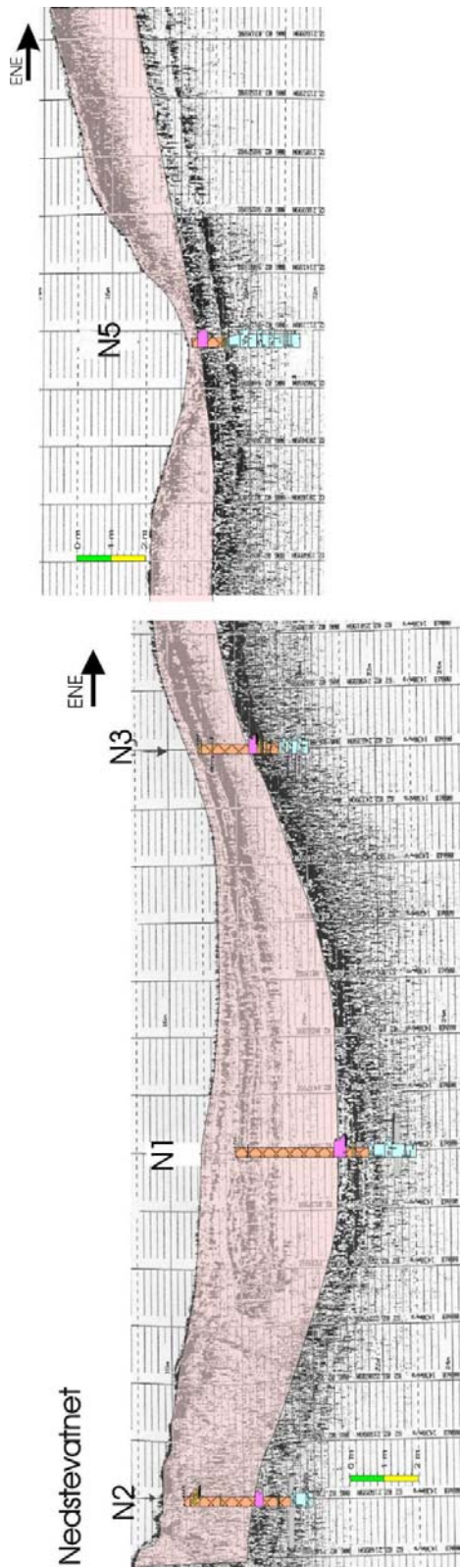


Figure 51. Correlation of seismic data (penetration echosounder) and cores, Nedstevatnet. Note that this correlation implies that the uppermost part of the soft gyttja has been lost during the coring process.

A 0.2 m thick sand layer/debrisflow deposit strongly influenced by soft sediment deformation (sand clasts in a gyttja matrix) occurs close to the top of core N2. At site N2 it can not be seen in the seismic data, probably due to a hummocky seabed disturbing the reflection pattern. In the central part of the lake, a reflector occurs approximately at the expected depth (Fig. 51). Silt laminae in the uppermost part of N1 and N3 can probably be correlated with the sand layer in the upper part of N2. Age determinations below and above the layer gave ages of 6600 BP (5780 ± 80 ^{14}C BP) and 2979 BP (2880 ± 105 ^{14}C BP), respectively. This debrisflow deposit is probably around 3200 years old. The old age beneath the deposit can probably be ascribed to erosion of younger sediments by the mass movement, while sedimentation rates after deposition of the layer have been low. If we assume the same sedimentation rate in the upper part of N3 as during the time interval 8200 BP (tsunami layer) to 6772 BP, the age of the silt lamina at 0.1 m depth becomes 6400 BP.

6.4 Rotevatnet

Rotevatnet (47 m a.s.l., Volda commune) is ca. 2 km long and 1 km wide (Fig. 4), and is the largest of the 5 lakes investigated. It has an areal extent of 2 km² (A), a catchment area of 29 km² (B), and a greatest water depth of 34 m. The B:A ratio is 14.5. Rotevatnet is located close to the lower end of an open, U-shaped glacial basin surrounded by mountains reaching 938 m a.s.l. (Kappefjellet, to the east). South of Rotevatnet there is a steep valley side up to Rotsethornet, which reaches 649 m a.s.l. The northern valley side up to Melshornet (807 m high) is relatively gentle. Six small rivers enter the lake, two of which derive from nicely eroded cirques in Litledalen and Høgedalen, to the southeast. The largest input of water is into the eastern part of the lake. The outlet is in the western end of the lake.

Most of the area around Rotevatnet is covered by till and glaciomarine silt and clay. Scree deposits occur south of the lake. Snow avalanches and landslides from Rotsethornet may enter directly into the lake. Shells are found in clay sediments around the lake, which implies that Rotevatnet lies beneath the late glacial marine limit. The seismic profiles display several very distinct and continuous reflectors in the lake sediments. There are no clear indications of disturbances (folds, distortions), in the seismic data.

Cores R1, R2 and R3 (Table 2) were obtained from the western part of the lake, in water depths between 6 m and 12.5 m. The core lengths vary from 2.3 to 2.9 m. The thickness of Holocene gyttja is in excess of 2 m in all the cores (Fig. 52). The lowermost 30-40 cm is a light brown, laminated gyttja or silty gyttja which gradually changes upwards to dark brown, homogeneous gyttja, but which is clearly laminated on the XRI photos (Lepland et al. 2002).

Cores R1 and R3 (Fig. 52) contain late glacial silt and poorly sorted, coarse sand beneath the Holocene gyttja. Shell fragments in the lowermost part of the silt/sand sequence in R3 indicate a marine depositional environment. A 2-3 cm thick Vedde Ash layer occurs higher up in the silt unit, close to the silt/gyttja boundary. Since distinct, visible Vedde Ash layers only

occur in freshwater sediments (Bard et al. 1994), it is assumed that Rotevatnet isolated from the sea before the Vedde Ash fall, i.e. before ca. 12 000 BP (10 300 ¹⁴C BP). Rotevatnet is situated 5-7 meters above the Younger Dryas sea level, which was at 40-42 m (Fareth 1987, Svendsen and Mangerud 1987). The well developed Younger Dryas marine terraces and shore lines in the area show that the lake in all probability was deglaciated in Allerød and/or Bølling chronozones, and that the isolation of the lake took place in (late) Allerød.

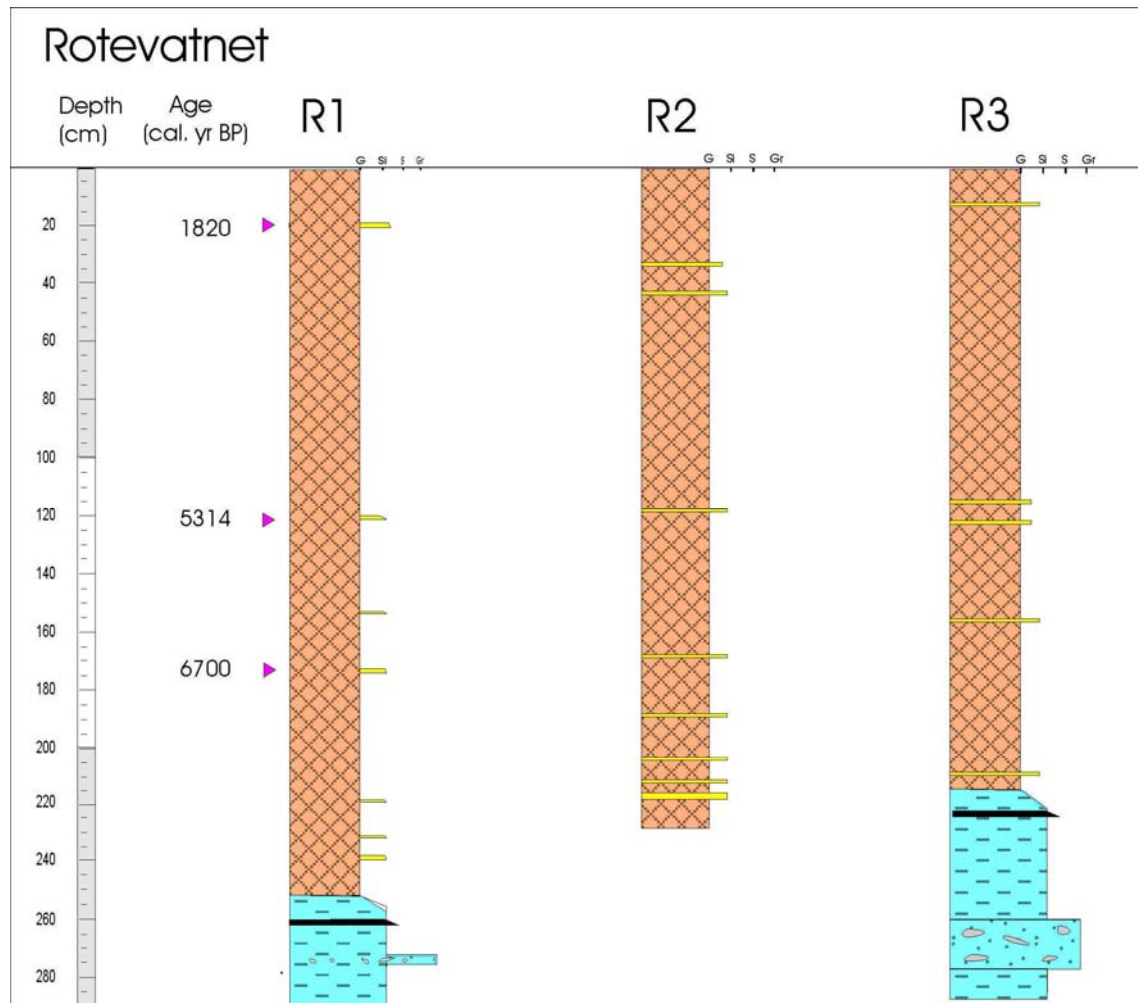


Figure 52. Cores from Rotevatnet.

Thin silt laminae in the gyttja may reflect postglacial mass movements. These laminae may be interpreted as distal turbidites, but can also be related to suspension fall out as a result of flood events or snow avalanches. Three thin (<3 mm) but distinct silt laminae from the middle and upper part of the dark gyttja, in core R1, yielded ages of 6700 BP (5880 ± 130 ¹⁴C BP), 5314 BP (4605 ± 115 ¹⁴C BP) and 1820 BP (1865 ± 100 ¹⁴C BP) (Table 4). Assuming a constant sedimentation rate of the gyttja between the two oldest of these, a silt lamina (Fig. 52) indicates another event around 6200 BP. Three silt laminae in the lower part of the gyttja are interpreted to be deposited in the earliest Holocene ca. 10-11 500 years ago.

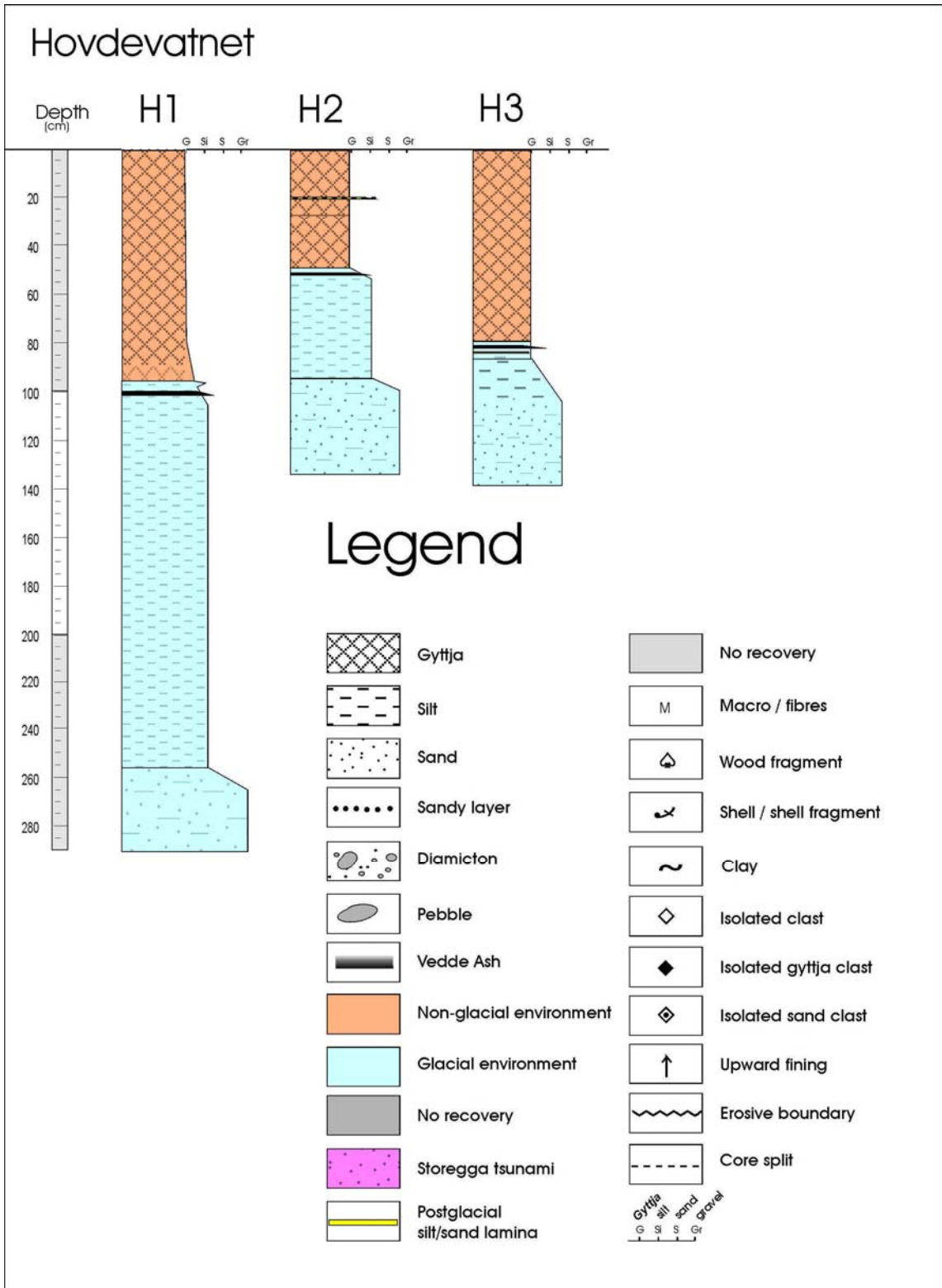


Figure 53. Cores from Hovdevatnet.

6.5 Hovdevatnet

Hovdevatnet (73 m a.s.l., Ørsta and Volda communes) is located close to the watershed between Voldafjorden and Ørstafjorden (Fig.4). It has an areal extent of 1 km² (A), a catchment area of 2.2 km² (B), and a greatest water depth of 16 m. The B:A ratio is 2.2, which means that the drainage area is only slightly larger than the lake itself. The surrounding slopes are gentle, and the highest point, to the west of the lake, is ca. 240 m.

Three cores were taken from the northwestern part of the lake, in water depths of 14-15 m (Table 2). Core lengths vary from 1.5 m to 2.9 m (Fig. 53). The succession comprises gyttja on top of glaciolacustrine silt, which in turn rests on sand. The boundaries between the individual units can relatively easily be recognized in the seismic data (see Sønstegaard et al. 2001). The greatest glaciolacustrine sediment thickness is nearly 2 m (H1). The Holocene gyttja recovered is ca. 1 m thick. The Vedde Ash appears as a <2 cm thick, black to grey layer close to the silt/gyttja transition zone (Fig. 53). The lowermost 30 cm of the gyttja is faintly laminated and has a light brown colour in contrast to the dark brown and nearly homogeneous upper part of the gyttja. Only one distinct sand lamina, 1 mm thick, was observed within the gyttja. Radiocarbon dating was not performed on cores from this lake.

7. TSUNAMI SEDIMENTARY FACIES

Tsunami sedimentary facies deposited by the Storegga Slide tsunami (8200 BP, 7200 ¹⁴C BP) in shallow marine basins and coastal lakes in western Norway have been studied by Bondevik et al. (1997). An erosional unconformity underlies the tsunami facies and is traced throughout the basins, with most erosion found at the seaward portion of the lakes. The lowermost tsunami facies is a graded or massive sand that locally contains marine fossils. The sand bed thins and decreases in grain size in a landward direction. Above follows coarse organic detritus with rip up clasts (organic conglomerate) and finer organic detritus. The tsunami unit generally fines upwards. The higher basins generally show one sand bed, whereas basins closer to the sea level 8200 years ago may show several sand beds separated by organic detritus. These alterations in the lower basins have been interpreted to reflect repeated waves of seawater entering the lakes. In basins that were some metres below sea level at 8200 BP, the tsunami deposits are relatively minerogenic and commonly present as graded sand beds. In some of these basins, organic-rich facies occur between the sand beds (Bondevik et al. 1997).

Two of the investigated lakes (Medvatnet and Nedstevatnet) exhibit a deposit that we ascribe to the Storegga Slide tsunami (see description above). Both of the lakes were a few metres below sea level at 8200 BP, while the other three investigated lakes were at too high elevation to be reached by the Storegga Slide tsunami wave. Those three lakes do not show any trace of the Storegga Slide tsunami. No obvious trace of younger or older deposits that can be related to a tsunami were found in any of the lakes. Thin silt and sand lamina and layers up to 2 cm,

probably formed by local snow avalanches, turbidity currents and debrisflows, were commonly found in the cores. There are a few thicker layers, but those can not be traced from core to core. Thicker sand beds in two cores from Nedstevatnet and Medvatnet only occur in the southernmost parts of the lakes, and are interpreted to represent debrisflows/turbidites. If the sand beds were tsunami deposits, they should be thickest and most pronounced in the parts of the lakes closest to where the tsunami wave would enter the basin, i.e. the north. Since this is not observed in Nedstevatnet and Medvatnet, the tsunami connection can be excluded.

Numerous examples of graded beds (gravel, sand, silt) have been observed in the investigated fjords. The majority of the graded beds in the fjords can be ascribed to turbidity currents, of which many have probably developed from subaerial and subaqueous slides and debrisflows. Also snow-avalanche deposits are common. In Sulafjorden, Julsundet and Halsafjorden, graded beds interpreted as tsunami deposits related to the Storegga Slide have been cored (see above).

No well-developed organic conglomerates were observed in the fjords, although some turbidites have a high content of organic detritus (e.g. in Ørstafjorden) and rip up-clasts (Breisunddypet). The absence of organic conglomerate in the fjord cores may reflect a lack of erodable organic detritus, in the deep fjords. Neither were multiple sand beds, which could indicate repeated tsunami waves, observed in the fjord cores. A possible tsunami deposit occurs in Breisunddypet (Fig. 39, see above).

No clear examples of gravity flow deposits overlain by tsunami deposits were observed. Such a relationship could indicate a local earthquake causing sediment failure and subsequent reworking by a tsunami. Closely spaced turbidites occur in two cores, one from Fjærlandsfjorden and one from Ørstafjorden (Figs. 21 and 34). In Fjærlandsfjorden, the turbidites could not be dated because of a low abundance of foraminifers in the sediments (probably related to a high sediment input from the glaciers). In Ørstafjorden, the turbidites are ca. 2200 years old (see above and below). The turbidites are separated by 3 cm of silty clay. It is possible that the first layer is a turbidite related to an earthquake, while the second is a tsunami deposit. Another possibility is that the first layer is a tsunami deposit, while the second is a turbidite caused by a tsunami. However, none of the layers need to be related to a tsunami.

8. TEMPORAL AND SPATIAL DISTRIBUTION OF EVENTS AND THEIR CAUSES

This chapter comprises a summary of the events that have been recorded in the various areas. Most of the data stem from the fjords and lakes that have been investigated in the present project, but we have also included data from Voldafjorden (Sejrup et al. 2001), Sognesjøen (Haflidason 2002) and some onland localities. Table 5 contains a summary of the recorded

events in the various areas. It should be noted that the ages of events are derived from our interpretation of dating results, sediment stratigraphy, swath bathymetry and seismic data. Most of the cores are too short to reach the oldest and deepest events, which are therefore underrepresented (e.g. the Storegga Slide tsunami). Negative evidences, i.e. absence of certain episodes in some areas, are also indicated. The data are shown graphically in Fig. 54.

Table 5. Temporal and spatial distribution of pre-historic, Holocene mass-movement events in investigated fjord and lake cores. Note that the ages of events are interpreted from dating results, sediment stratigraphy, swath bathymetry and seismic data. Negative evidences, i.e. absence of certain events in some areas, are indicated by an asterisk (*). Data from Sognesjøen and Voldafjorden are from Haflidason (2002) and Sejrup et al. (2001), respectively.

Area	Interpreted age (calendar age BP) of events observed in cores											
	<500	<1500	1700-1800	2000-2200	2800-3200	5300-5600	6000-6200	6700	7300	8000	9300	10-13000
Aurlandsfjorden	*	*	*	*	ca. 3000							10-11 500
Barsnesfjorden	500	*	1700									
Fjærlandsfjorden		<1500										
Sognesjøen	*	*	*	*	3000					8000		11-12 000
Dalsfjorden	*	*	*	2100								
Førdefjorden	*	*	*	2100								
Storsætervatnet					2800	5600	*	*	*	*	9300	
Medvatnet					2800, 3200	5500	*	*	*	8000		10-13 000
Nedstevatnet					3000	*	6400	6700	7300	8000		10-13 000
Rotevatnet			1800	*	*	5300	6200	6700	*	*		10-13 000
Vanylvsfjorden	*	*	*	*	2800							
Syvdsfjorden	*	ca. 1000	*	2100								
Voldafjorden	*	*	*	2100	*	*	*	*	*	8000	*	11-13 000
Ørstafjorden	*	*	*	2100								
Sulafjorden					*	*	*	*	*	8000		
Breisunddypet				?	?							
Tafjorden	<400		?	?	?							
Midfjorden												
Julsundet				?	?					8000		
Venje, Romsdalen		<1400										
Innfjorden					?							
Tingvollfjorden												
Halsafjorden				*	*	*	*	*	*	8000		11 700-13

8.1 Younger than 500 BP

Two young (<500 BP) turbidites are observed, one in Barsnesfjorden and one in Tafjorden (Table 5). These turbidites were most likely formed by local events during the climatic deterioration at the beginning of the Little Ice Age (550-80 BP). It is possible that the uppermost event in Tafjorden is related to the major rock avalanche in 1934. Numerous rock avalanches with or without associated tsunamis have been recorded in historical times (e.g. Fig. 7).

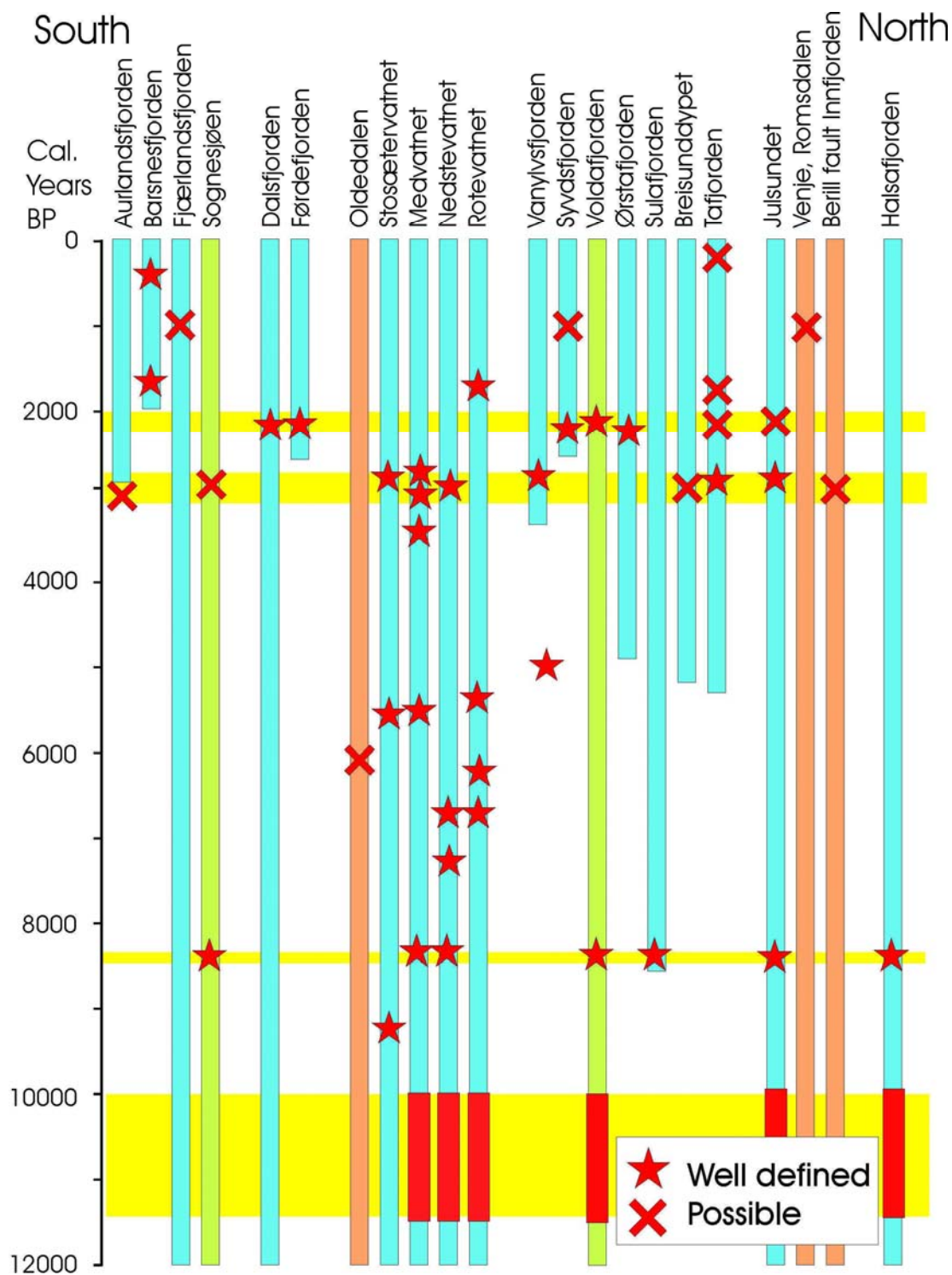


Figure 54. Temporal and spatial distribution of pre-historic mass-movement events. Note that the ages of events involve interpretation of dating results, sediment stratigraphy, swath bathymetry and seismic data. Blue: core recovery in this project; green: core recovery, cores from Sognesjøen (Haflidason 2002) and Voldafjorden (Sejrup et al. 2001); orange: land sites; yellow: time intervals of relatively high mass-movement activity. Red bars indicate several mass-movement episodes within the time interval 10 000-11 500 BP.

8.2 Younger than 1500 BP

Dating results show rock avalanches younger than 1500 BP on land at Venje in Romsdalen (Blikra et al. 2002) and probably younger than 1000 years in Fjærland (Lauritsen and Elvebakk 2001) (Table 5). The youngest prehistorical record of snow avalanches indicates a regional pulse around 1400 BP (Blikra and Nemec 1998, while Matthews et al. (1986) recognized an increase in solifluction rate from ca. 1000 BP, in Jotunheimen. Slide/debrisflow deposits approximately 1000 years old also occur in Trondheimsfjorden (Bøe et al. in prep.).

8.3 1700-1800 BP

The dating results show that a turbidite in Barsnesfjorden is ca. 1700 years old, while a mm-thick silt lamina from Rotevatnet is ca. 1800 years old (Table 5). A small turbidite in Tafjorden is estimated to be ca. 1700 years old. The observed deposits can probably be related to climatic variation, e.g. a flood event causing debrisflows evolving into turbidites and/or a severe winter with snow avalanches. A debrisflow deposit of similar age has been observed in Trondheimsfjorden (Bøe et al. in prep.).

8.4 2000-2200 BP

Our data show that mass movements did occur in fjords in Sunnmøre (Syvdsfjorden and Ørstafjorden) and in Sunnfjord (Førdefjorden and Dalsfjorden) in the period 2000-2200 years BP (Table 5, Figs. 54 and 55). Dating below and above turbidites gave ages of 2333 BP and 1780 BP in Syvdsfjorden, and 2454 BP and 1695 BP in Ørstafjorden. Dating below turbidites in Førdefjorden and Dalsfjorden gave ages of 2320 BP and 2297 BP, respectively (Table 5). Ages obtained below turbidites are maximum ages, due to erosion, and the real ages of the turbidites are probably 2000-2200 BP. In Voldafjorden, Sejrup et al. (2001) interpreted a turbidite to be 2100 years old. Longva et al. (2000) interpreted this turbidite to be related to extensive sliding, observed in seismic and swath bathymetric data, along the fjord margins. It is possible that mass-movement deposits 2000-2200 years old also occur in Tafjorden, Breisunddypet and Julsundet, but the dating has not provided conclusive evidence. Dating of a core from Breisunddypet gave a maximum age of 3352 BP for an erosion surface, while sediments above the erosion surface are clearly redeposited. It is possible that debrisflow deposits above the erosion surface are 2000-2200 years old, although other ages are just as likely (e.g. 2800-3200 BP).

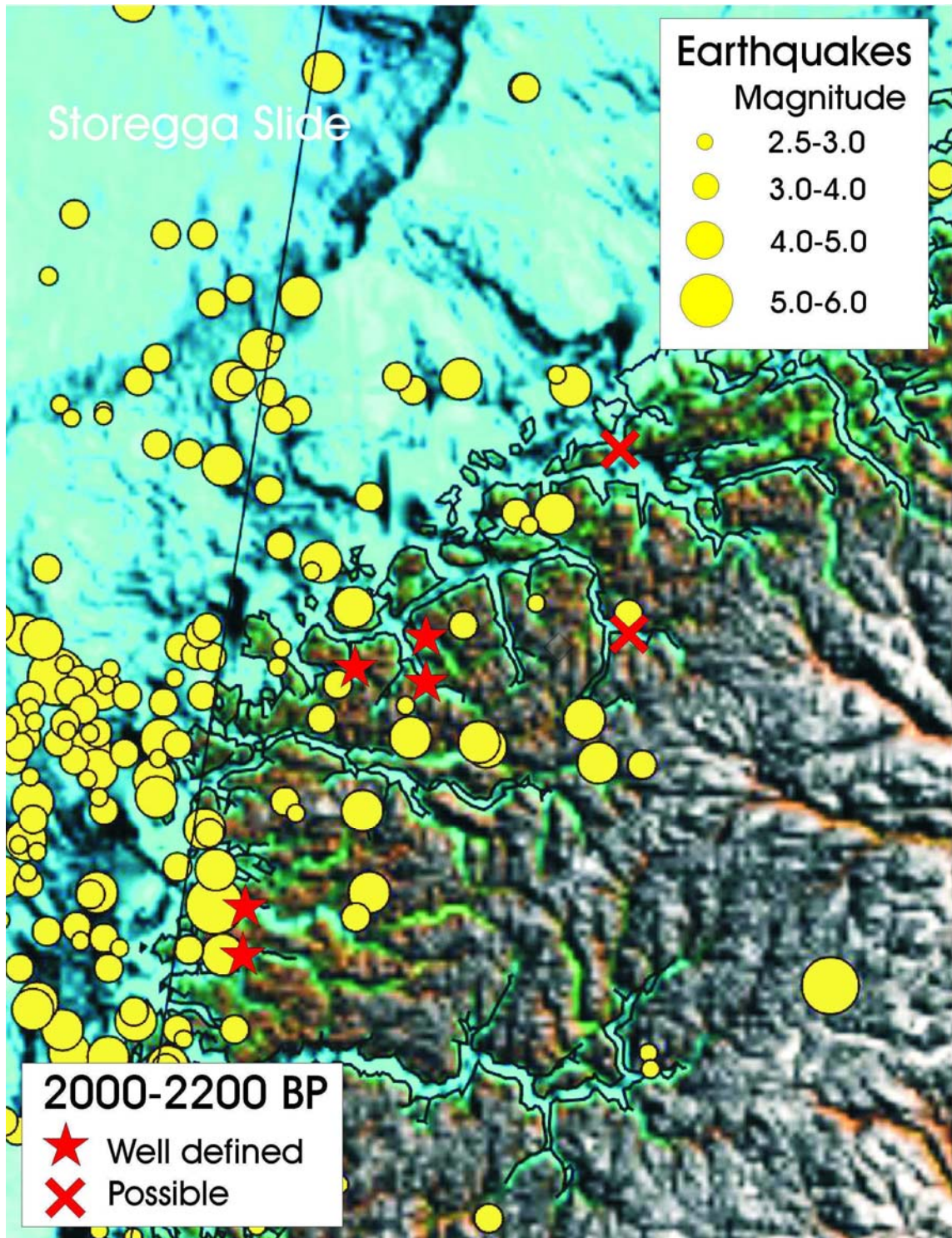


Figure 55. Geographical distribution of the 2000-2200 BP event(s). Basemap and earthquake data from Dehls et al. (2000).

The 2000-2200 BP event was not observed in any of the lake cores. This may possibly be ascribed to the fact that the uppermost up to 1 m of the gyttja sequence was lost during coring

(see above). However, there is no indication of any large slide in the Storegga area, that may have created a tsunami at that time, nor are any mass-movement deposits found on land. This suggests that the mass movements 2000-2200 BP were most likely related to one or more earthquakes on land or close to the coast, and not to a tsunami generated by an offshore megaslide. An increase in debrisflow activity, probably related to a climatic change around 2200 BP, has been indicated from other studies (see Chapter 3).

Seismic and core data show that major slide and debrisflow deposits at the 2000-2200 BP stratigraphic level are thick and very extensive along fjord margins only in Sunnfjord and Sunnmøre. Our conclusion is that the mass movements 2000-2200 years ago were related to one or more earthquakes causing failures in locally unstable sedimentary successions in turn causing local (regionally less significant) tsunamis. The geographical distribution of deposits suggests that the epicenter(s) of the triggering earthquake(s) were located in the Sunnfjord-Sunnmøre region. This area is neotectonically active (Dehls et al. 2000), and earthquakes up to magnitude 5 (Richter scale) occur regularly today. The present models for the decrease in seismic activity between the great burst of seismicity about 8000 years ago and the present level include a reasonable likelihood for magnitudes up to 7 as late as 2000 years ago (NORSAR 2001). For stable regions like the Norwegian margin one can also at times expect several relatively strong earthquakes over a short period of time, e.g. 200-400 years, within a geographically restricted area, such as New Madrid in USA and Kutch in India (NORSAR 2001).

The 2000-2200 BP turbidite in Syvdsfjorden contains wood fragments and rip-up clasts of the underlying sediment. This could possibly be interpreted as an organic conglomerate, which is typical for tsunami deposits (see above). Similarly, the turbidite in Ørstafjorden, and the one in Tafjorden that is possibly be related to the same event, contain wood fragments. However, the only tsunami sedimentary facies observed with certainty in the cores from the investigated lakes and fjords is related to the Storegga Slide.

8.5 2800-3200 BP

Mass-movements are observed to have occurred in several fjords and lakes during this time interval (Table 5, Figs. 54 and 56). In Vanylvsfjorden, dating beneath a turbidite gave an age of 2962 BP, suggesting that the turbidite is ca. 2800 years old. Dating beneath a turbidite in Tafjorden gave an age of 3141 BP, suggesting that this turbidite is ca. 2900 years old. An age of 2778 BP above mass-movement deposits in Aurlandsfjorden suggests an event around 3000 BP there. In Julsundet, an age of 3222 BP was obtained above a turbidite, suggesting that it is around 3000 years old. We are uncertain how to interpret the age of 3352 BP beneath an erosion surface in Breisunddypet. One interpretation could be that the sediments above the erosion surface, comprising rip-up clasts of the underlying beds as well as layers of bioclastic sand, represent debrisflow and slide deposits 2800-3200 years old (see discussion above).

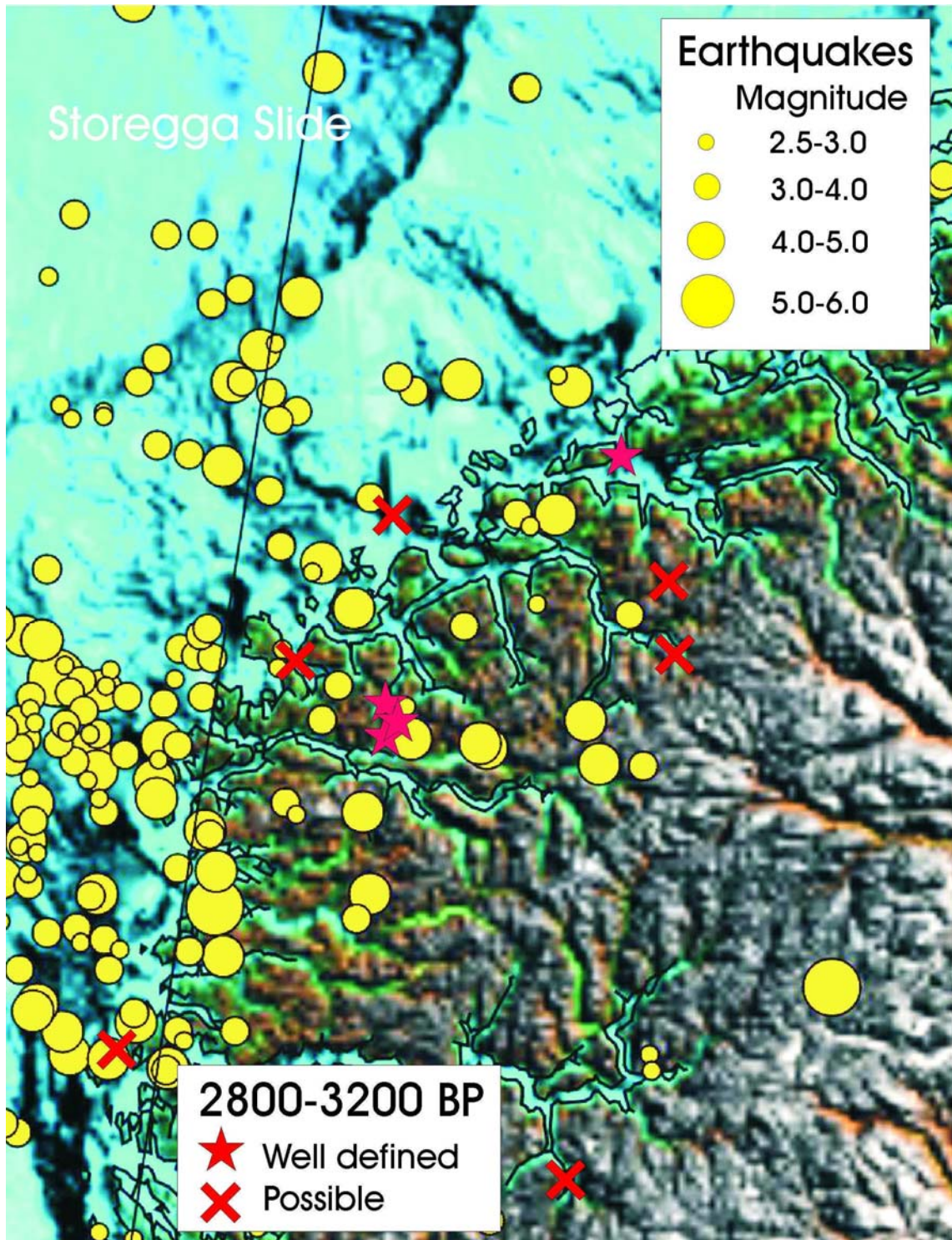


Figure 56. Geographical distribution of events in the time period 2800-3200 BP. Basemap and earthquake data from Dehls et al. (2000).

In Storsætervatnet, an age of 2744 BP was obtained immediately above an inversely graded sand layer, interpreted to be a debrisflow deposit. It is probable that this was deposited

approximately 2800 years ago. In Nedstevatnet, an age of 2979 BP was obtained on a sample a few centimetres above a sand layer, probably a debrisflow deposit, influenced by soft sediment deformation. We interpret this deposit to be ca. 3200 years old. In Medvatnet, a gravely silt layer with plant fragments, possibly a snow avalanche deposit was dated, and an age of 3279 BP was obtained. A dating above a turbidite in Medvatnet gave an age of 2619 BP. A low sedimentation rate at this site suggests that the turbidite was deposited some time during the interval 2600-3000 BP. It is therefore included among the deposits of the time interval 2800-3200 BP (Table 5).

Haflidason (2002) observed a turbidite in cores from Sognesjøen. Dating immediately below this turbidite gave two ages of ca. 2900-3200 BP. The spread of ages within the 2800-3200 BP interval is probably too great to consider simultaneous occurrence of all these events. The rather frequent mass-movements during this time interval may reflect a climatic influence. An increase in debrisflow processes, probably related to a climatic change around 3200 BP, has also been shown from other studies (see Chapter 3).

A series of dates in the inner fjord areas of Møre og Romsdal suggests high rock-avalanche activity during the second half of the Holocene. Some dates of rock avalanches around 3000 BP in Innfjorden and Tafjorden may suggest that these are related to movement on the Berill fault.

Two closely occurring silt lamina in Medvatnet are ca. 3400 years old. These isolated events were probably related to snow avalanches or floods. As they are only recorded in Medvatnet, they have not been given a separate event column in Table 5. Because of the inaccuracy in the radiometric dating method, it is possible that they can be included among the events during the time period 2800-3200 BP.

8.6 5300-5600 BP

A 2 cm thick, gravely silt layer in Medvatnet is 5594 years old, a 9 mm thick silt lamina in Storsætervatnet is 5607 years old, while a mm-thick silt lamina in Rotevatnet is 5314 years old (Table 5). The interpretation of these deposits is that they are related to snow avalanches or flood events. This fits well with previous studies in Western Norway, which have shown increased snow avalanche activity from 5400 BP and a higher number of large spring floods between 5800 BP and 5000 BP (see Chapter 3).

8.7 6000-6200 BP

One mm-thick silt lamina, in a core from Rotevatnet, has been estimated to be ca. 6200 years old (Table 5). The lamina represents an isolated event, possibly a snow avalanche or a flood

event. This may correlate with mass-movement deposits in Oldedalen (Nordfjord) that are ca. 6000 years old Nesje (2002).

8.8 6700 BP

Dating of a mm-thick silt lamina in Rotevatnet gave an age of 6700 BP, while a 2 cm thick sand turbidite from Nedstevatnet gave an age of 6772 BP (Table 5). There is no description in the literature of other events or climatic changes at this time. We therefore interpret them as local events related to floods or snow avalanches.

8.9 7300 BP

Dating of a sand lamina in Nedstevatnet gave an age of 7367 BP (Table 5). We interpret this lamina to represent an isolated turbidite, probably related to a flood event. There is no description in the literature of other events or climatic changes at this time.

8.10 8200 BP

Storegga Slide tsunami deposits have been cored in five fjords: Sognesjøen (Haflidason 2002), Voldafjorden (Sejrup et al. 2001), Sulafjorden, Julsundet and Halsafjorden. These deposits are thickest and most voluminous in Sunnmøre. In the central part of Halsafjorden, the cored tsunami deposit is only ca. 10 cm thick, while it is almost 2 m thick in Sulafjorden (Hagen 1981) and Julsundet.

A gravelly sand bed is observed in the lower part of all the cores from Medvatnet and Nedstevatnet. This sand bed strongly resembles tsunami deposits related to the Storegga Slide in lakes along the coast of Mid- and Western Norway (Bondevik et al. 1997a, b, 1998). Dating of a sand lamina in gyttja ca. 1 m above the sand bed, in core N2, gave an age of 7367 BP, while dating of a silt/sand lamina in gyttja ca. 0.5 m below it, in core N5, gave an age of 9845 BP. The sand bed is thus interpreted to be deposited by the Storegga Slide tsunami, 8200 years ago (Table 5). At that time, both Medvatnet and Nedstevatnet were beneath the contemporary sea level, while the other investigated lakes were too highly elevated to be reached by the tsunami.

8.11 9300 BP

Dating of a 1-cm silt layer in Storsætervatnet gave an age of 9366 BP (Table 5). This layer may be a turbidite deposited during the erosion of the glaciomarine sequences in cores S3, S4 and S6, or it could also be a turbidite derived from the delta of Fladalselva. This appears to be an isolated event only occurring in Storsætervatnet.

8.12 10 000-11 700 BP

Seismic data show that there is a striking similarity in areal distribution and volume of major mass-movement deposits at the 2000-2200 BP and ca. 11 000-11 700 BP (see discussion on the age of this event earlier in the report and in Chapter 9) stratigraphic levels in some fjords in Sunnmøre, e.g. in Voldafjorden and Syvdsfjorden. This may suggest a common triggering mechanism. If our interpretation of the 2000-2200 BP event above is correct, i.e. that debrisflows and turbidites were released by an earthquake on land or close to the coast (see Chapter 8.4), this would indicate that the older regional event was triggered in the same way.

Major slide and debrisflow deposits at the 2000-2200 BP and 11 000-11 700 BP stratigraphic levels are thick and very extensive along fjord margins in Sunnfjord and Sunnmøre. Similar deposits occur at the 11 000-11 700 BP level also in Nordmøre, but they are fewer and not that extensive there. This suggests that the epicenters of the triggering earthquakes were located in the Sunnfjord-Sunnmøre region (see Chapter 8.4).

Several thin silt and sand lamina/layers occur in the lowermost part of the Holocene gyttja or in the uppermost part of the glaciomarine succession, in several of the lake cores (Table 5). Three closely spaced lamina in core N5 were dated, and ages of 11 316 BP, 10 434 BP and 9845 BP were obtained. In addition, dating of shells in diamictic layers (debrisflow deposits) in the uppermost part of the glaciomarine succession in core N3 gave ages of 11793 BP and 13 009 BP. It is possible that the uppermost diamictic layer in core N3 can be correlated with the 11 000-11 700 years old major debrisflow deposits in the fjords. This suggest that the earliest Holocene was a time of frequent mass movements. We ascribe this mainly to rapid land uplift (with or without associated earthquakes) and highly erodable river banks due to lack of a stabilising vegetation (see Chapter 3). Also the data from Aurland, Sjørdalen, Voldafjorden and Halsafjorden show that this was a time of frequent mass movement. In Aurland, rock avalanches may be related to gravitational faulting.

9. CORRELATION OF SEISMIC DATA AND FJORD CORE DATA

In the previous chapter, it has been shown that slides, debrisflows and turbidity currents occurred in five fjords around 2000-2200 BP. This is in accordance with the postulated ca. 2000 BP event of Longva et al. (2001a), following observations of turbidites in Voldafjorden (Sejrup et al. 2001). Longva et al. (2001a) recognized a very prominent reflector (the red reflector) in the southern part of Sunnmøre and possibly in Nordfjord and Sunnfjord. The reflector occurs within a succession of acoustically transparent sediments, but slides and debrisflow deposits were observed to be associated with it along the fjord margins. A major task in the present project has been to investigate the interpreted red reflector to establish its nature and age in various fjords, and to decide if it was caused by climatic variations, a tsunami (possibly caused by an earthquake affecting the offshore area), an earthquake only affecting parts of northwest Western Norway, or a combination of the latter two.

In Dalsfjorden, seismic data suggest that the turbidite in the upper part of P0103012 can be correlated with the turbidite in core P0103013 (which is 2000-2200 years old, accounting for an erosion at its base). This correlation implies that the coarse-grained deposits in the lower part of P0103012, i.e. the wedge of chaotic deposits seen in the seismic data and interpreted to be related to the 2000 event (red reflector) by Longva et al. (2001a) (Fig. 27), is older than the turbidite. The age of 9458 BP probably reflects old sediments redeposited by a later event, but we do not know the age of that.

We have no conclusive evidence from Vanylvsfjorden, but our data indicate that the interpreted red reflector is older than 2000 BP. A turbidite at a shallower level than the interpreted red reflector is thought to have a maximum age of ca. 2800 BP. In Syvdsfjorden, a 2000-2200 years old turbidite was found at the level of the interpreted red reflector. In Ørstafjorden, our data show that the interpreted red reflector occurs at a deeper level than a turbidite that is 2000-2200 years old.

In Sulafjorden, the interpreted red reflector can be traced towards the site of core NGU-2L/SC, but there is no change of sediment type or physical parameters (and no seismic reflector) at the expected depth (2 m) of the reflector in the core. A radiocarbon dating at 1.82-1.86 m depth gave an age of 4851 BP (4265 ± 55 ^{14}C BP), showing that the reflector is significantly older than postulated by Longva et al. (2001a). There is no trace of a ca. 2000 BP event in this part of Sulafjorden (assuming that the core actually represents the stratigraphic interval from the seabed downwards, see Chapter 5.3.5).

At the coring site in Julsundet, the red reflector of Longva et al. (2001a) is interpreted to occur at the level of the coarse-grained bed at 0.77-0.88 m depth, which has a minimum age of 3222 BP and which rests on top of the Storegga Slide tsunami deposit. In Julsundet, we interpret the red reflector to be around 3000 years old.

Our data indicate that the interpreted red reflector is **not** ca. 2000 years old in all the fjords in Sunnmøre and Sunnfjord. In some fjords, e.g. in Dalsfjorden, Ørstafjorden, Vanylvsfjorden and Julsundet, it appears to be older. Also in these fjords it reflects mass-movement events. Our interpretation is that there was no large event ca. 2000 years BP that caused (large) simultaneous slides in **all** fjords in this region. However, since turbidites of this age can be recognized in five fjords (Dalsfjorden, Førdefjorden, Voldafjorden, Ørstafjorden and Syvdsfjorden) and these turbidites generally seem to be related to large slides along the fjord margins, we tend to believe that an earthquake, or a series of local earthquakes, at this time may have triggered the mass movements. Where the interpreted red reflector appears to be older than 2200 BP, it can possibly be related to slides, debrisflows and turbidites in the period 2800-3200 BP.

At a deeper level, Longva et al. (2001a) observed another reflector/slide level, which they termed the green reflector (Fig. 3) and tentatively interpreted to reflect the Storegga Slide event. This reflector was observed to represent the upper boundary of acoustically transparent (locally stratified) sediments. In most of the investigated fjords, there are thick and extensive slide and debrisflow deposits at this level, particularly along the margins of the fjords. This can clearly be seen in swath bathymetric data. The frequency of slides at the green reflector was interpreted to be lower in Nordmøre than further south.

In Voldafjorden, Longva et al. (2000) had problems correlating core data and seismic reflectors. In the core, the stratigraphic thickness between the 2100 BP and the 8200 BP events is ca. 2 m, while in the seismic data it is ca. 3.5 m. The green reflector associated with the middle fjord margin debrisflow deposits was apparently situated deeper than the 8200 BP event, possibly at the level of the ca. 11 000 BP turbidite in the core described by Sejrup et al. (2001). One cause for this could be sediment compaction. The alternative interpretation suggested here is that the middle (green) fjord margin debrisflow deposit in Voldafjorden can in fact be correlated with the ca. 11 000 years old turbidite, and that the Storegga Slide tsunami is not generally associated with extensive fjord margin debrisflow deposits, as previously thought. One problem with the alternative interpretation is that Storegga Slide tsunami deposits are not recognized with certainty in the seismic data from Voldafjorden, Sulafjorden and Halsfjorden.

The reasons for the relatively low core recovery (core length/penetration) may be several, e.g. sediment compaction, that the uppermost part of the seabed sediments did not enter the corer, that sediments in the lowermost part of the cored section did not enter the corer, or that the lowermost part of the cored section was lost during retrieval. In our interpretations, we have assumed that the cores are from the seabed downwards (see discussions in previous chapters). If this assumption is incorrect, our interpretations of major slides and debrisflow deposits at the 11 000-11 700 BP level, and not at the 8200 BP level, would probably have to be changed. The correlation of core data and seismic data in Voldafjorden, Sulafjorden and Halsafjorden is still uncertain, and we are therefore not able to conclude what may have triggered the Storegga Slide.

At the coring site in Halsafjorden, the interpreted green reflector of Longva et al. (2001a) occurs at 6.75 m (5-6 m) depth. We are uncertain which level in the core that can be correlated with this reflector. The most likely candidate (assuming that the core extends from the seabed downwards) is the turbidite at 5.02-5.13 m depth, with a minimum age of 11 657 BP. Another possible candidate is the turbidite at 6.68-6.91 m depth, which has a minimum age of 13 484 BP. The latter may in fact be correlated with the uppermost orange reflector interpreted by Longva et al. (2001a). It appears that in Halsafjorden, the reflectors are generally older than suggested by Longva et al. (2001a). This also implies that the uppermost extensive debrisflow deposits along the fjord margins are older than the Storegga Slide (if our assumption about core depth is correct).

We do not know how thick the tsunami deposit is at the coring stations in Sulafjorden, but find it unlikely that its base is at the green reflector interpreted by Longva et al. (2001a) (ca. 6.8 m depth), which would give a thickness of tsunami sediments of more than 3.5 m over a wide area and an enormous volume of tsunami sediments in Sulafjorden (assuming that the core extends from the seabed downwards). We find this unlikely, especially as a tsunami deposit should be expected to decrease in thickness away from the fjord entrance (see Chapter 7). It is more likely that the tsunami deposit is underlain by silty clays and further by slide deposits (seen along the fjord margins) at a deeper level.

Storegga Slide tsunami deposits are also seen as a reflector in the penetration echosounder data from Medvatnet and Nedstevatnet (e.g. Fig. 51).

In Julsundet, the interpreted green reflector can be correlated with the base of the upward fining unit at 2.67 m depth, which dating has shown is a Storegga Slide tsunami deposit. The seismic data indicate that the uppermost orange reflector of Longva et al. (2001a) was eroded by the Storegga Slide tsunami. The age of ca. 11 800 BP ($10\,250 \pm 75$ ^{14}C BP) at 5.11 m depth is probably obtained close to the middle orange reflector, showing that in Julsundet, the interpreted orange reflectors are probably 10-13 000 (9000-11 000 ^{14}C) years old as suggested by Longva et al. (2001a). One of them can possibly be correlated with the 11-11 700 years old debrisflows in other fjords.

The interpreted violet reflector has not been dated due to short core lengths at critical locations.

10. MASS-MOVEMENT TRIGGERING MECHANISMS

Most vertical ground movements onland during the Holocene have been directly expressing the isostatic rebound following the deglaciation, with only a small amount of the associated movement release being expressed in terms of active faulting. The relation between rebound

and tectonics is not well understood, however, even though it is reasonable to assume that reactivation of old faults in seismically active zones may be either enhanced or localized by this rebound. Triggering mechanisms for large rock avalanches in the region are also poorly understood, but extreme rainfall, building up high water pressure in fractures, and large magnitude earthquakes are probably the most important factors. Increased movements, seen as widening of clefts, have been observed for quite long periods before rock-avalanche events (e.g. Tjelle, Tafjord and Loen slides). This suggests that gravitational creep can be active for long periods, in which case the failure itself does not necessarily need to be controlled by earthquake or rainfall events. Creep is a relatively slow process that in many cases seems to occur prior to rock-avalanches (Blikra et al. 2002b).

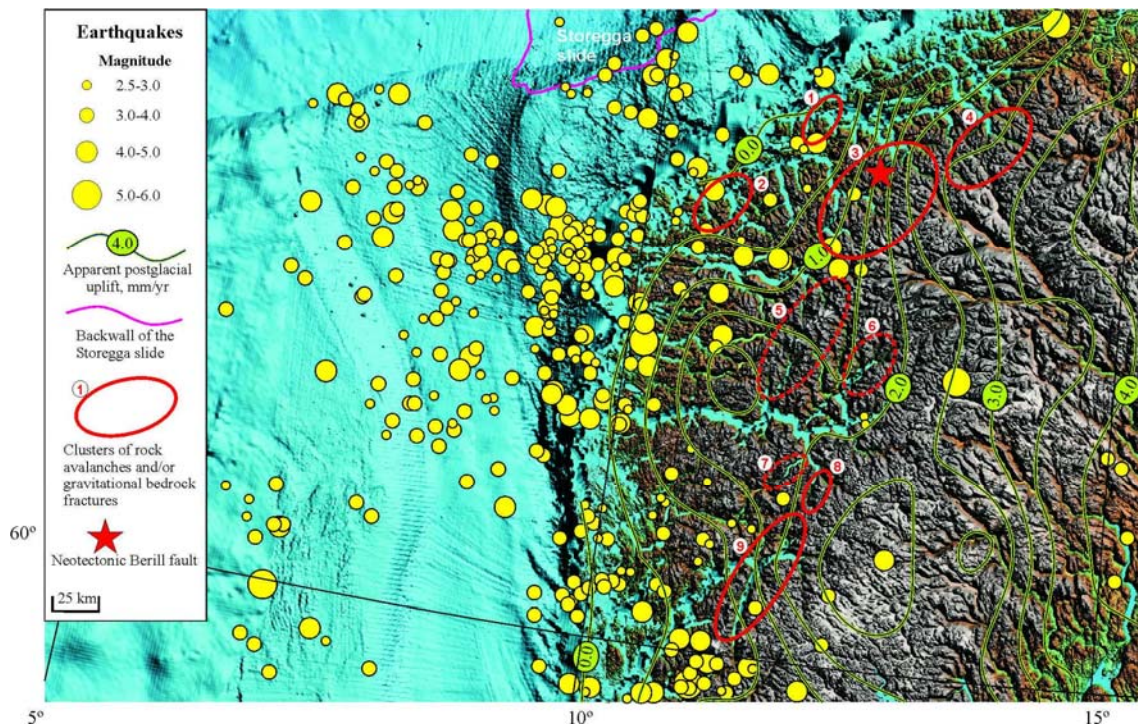


Figure 57. Earthquake data (NORSAR) and apparent land uplift plotted on a Landsat 7 satellite image base. Modified from Dehls et al. (2000). Clusters of rock avalanches and gravitational bedrock fractures as well as the neotectonic Berill fault are shown.

The reviews by Keefer (1984) and Jibson (1994) indicate that triggering of large rock avalanches require a minimum earthquake magnitude of about 6.0. Deep, coherent slides in bedrock (rock slumps and rock-block slides), seem to require even stronger earthquakes (M 6.5). The contemporary earthquake distribution in southern Norway shows that the area with the highest earthquake activity is found off and along the western coast of Norway (Byrkjeland et al. 2000, Dehls et al. 2000) (Fig. 57). Even though earthquakes of magnitude 6 or higher have not been recorded in Norway in historical times, the potential of large earthquakes (M 6.5-7) in the future is far from negligible. For the time period between 8000

BP (when the activity was very high) and the present (with low activity) there must have been some gradual decline, providing even higher likelihood for magnitudes in the range 6.5-7 (NORSAR 2001). The support for this is not only from the gradual decrease from a higher level but also from the fact that geologically similar (stable continental) regions elsewhere have been shown to exhibit more than a dozen earthquakes above magnitude 7. Moreover, return times for the largest earthquakes in such regions (few which have been glaciated) are typically several thousand years (e.g. Johnston and Kanter 1990).

Review of historical and recent data on seismically induced landslides shows that the full range of landslide types can be initiated by seismic activity, and 81% of all slope failures occurred in the region with mean horizontal peak ground acceleration (PGA) greater than 1.5 m/s^2 (Sitar & Kahazai 2001). PGA of 1.5 m/s^2 may result from an earthquake with magnitude somewhat above M 6 within a distance of 20-30 km. Seismic hazard analysis for Norwegian onshore and offshore areas shows that large areas of northwestern Norway can at present expect PGA values of more than 1.5 m/s^2 for an annual probability of 10^{-3} (NORSAR and NGI 1998). This shows that earthquake-triggered landslides should be expected in western Norway.

Fig. 57 shows earthquake data and apparent land uplift (Dehls et al. 2000). Most earthquakes occur offshore northwestern Norway, where a few earthquakes of magnitude 5-6 have been recorded in historical times. Although there is no evidence of a connection, it is worth mentioning that the long-lived, NNE-WSW striking Møre-Trøndelag Fault Complex intersects the N-S trending Øygarden Fault Zone in this area. Only a few earthquakes are, however, recorded along the Møre-Trøndelag Fault Complex. This major fault zone may be dominated by creep (Pascal and Gabrielsen 2001), hence, it is an open question whether or not sufficient build-up of stress may occur on the zone. However, if the fault complex periodically locks, significant earthquake swarms can be expected.

The relationship between earthquake magnitude, area affected by landslides and distance from epicentres and ruptures has been analysed by Keefer (1984) (e.g. Fig. 58). If an area of 500 km^2 was influenced by mass movements during an earthquake, this would imply a magnitude of 5.7-6.2. The area affected by slides is often an ellipse (Adams 1981).

The clusters of rock avalanches and gravitational bedrock fractures at Oterøya and Øtrefjellet are about 25 km long and 15 km wide (Fig. 57), which give areal extents of $300\text{-}350 \text{ km}^2$. This would imply earthquakes of magnitude 5.5-6.2 (Fig. 58). According to Keefer (1984), deep bedrock failures probably require even stronger earthquakes, possibly of M 6.5. The area affected by other types of mass failures would then become much larger, at least 800 km^2 (e.g. 40 km long and 25 km wide).

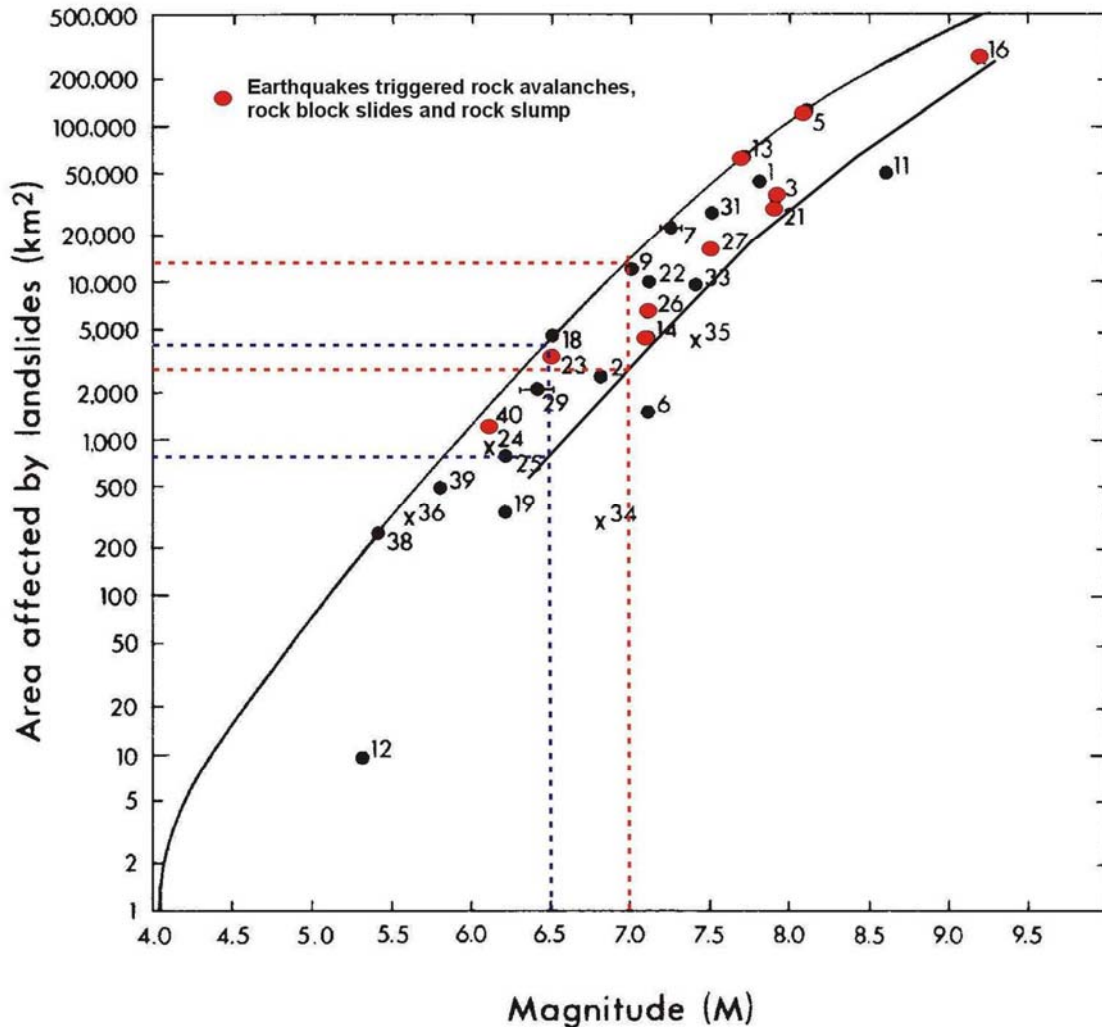


Figure 58. Area affected by landslides versus earthquake magnitude (after Keefer 1984). Events triggering rock avalanches, rock-block slides and rock slumps are shown in red. An earthquake of M 6.5 may cause landslides in an area of 800-4000 km^2 , while an earthquake of M 7.0 may cause landslides in an area of 3000-15 000 km^2 . The areas of rock avalanches and bed rock fractures at the coast (areas 1 and 2 in Fig. 57) are about 600-800 km^2 , while area 3 in Innfjorden is 2000-2500 km^2 .

The Berill fault may help to explain some rock avalanches in the region southeast of Molde (Fig. 57) although no earthquakes have been recorded to be associated with it. The fault is situated in the area of the highest gradient of land uplift in western Norway (Fig. 57). The Berill fault, which has an offset of 2-4 m, would need an earthquake of about M 6.5 to create the fault rupture (even if the fault has been created through a sequence of events there must have been, as inferred from simple scaling relations, a large one of about that size). This implies that an area of 800 to 4000 km^2 was affected by slides (40-90 km long and 25-50 km wide) (Fig. 58). Such an area is indicated in Fig. 59, and this seems to correlate well with the

distribution of slides (Fig. 57). According to the relationship between magnitude and rupture, an earthquake of M 6.5 should be expected to trigger slides up to 60 km away, while the relationship between magnitude and epicentre suggests landslides up to 80 km away (Keefer 1984). An earthquake of magnitude 7.0 would cause slides in an area of 3000-12 000 km² (e.g. 75-150 km long and 45-90 km wide) (Fig. 58). Areas that could be affected by slides during an earthquake of M 6.5 and 7.0, with a centre in the Oterøya-Øtrefjellet cluster, are shown in Fig. 59.

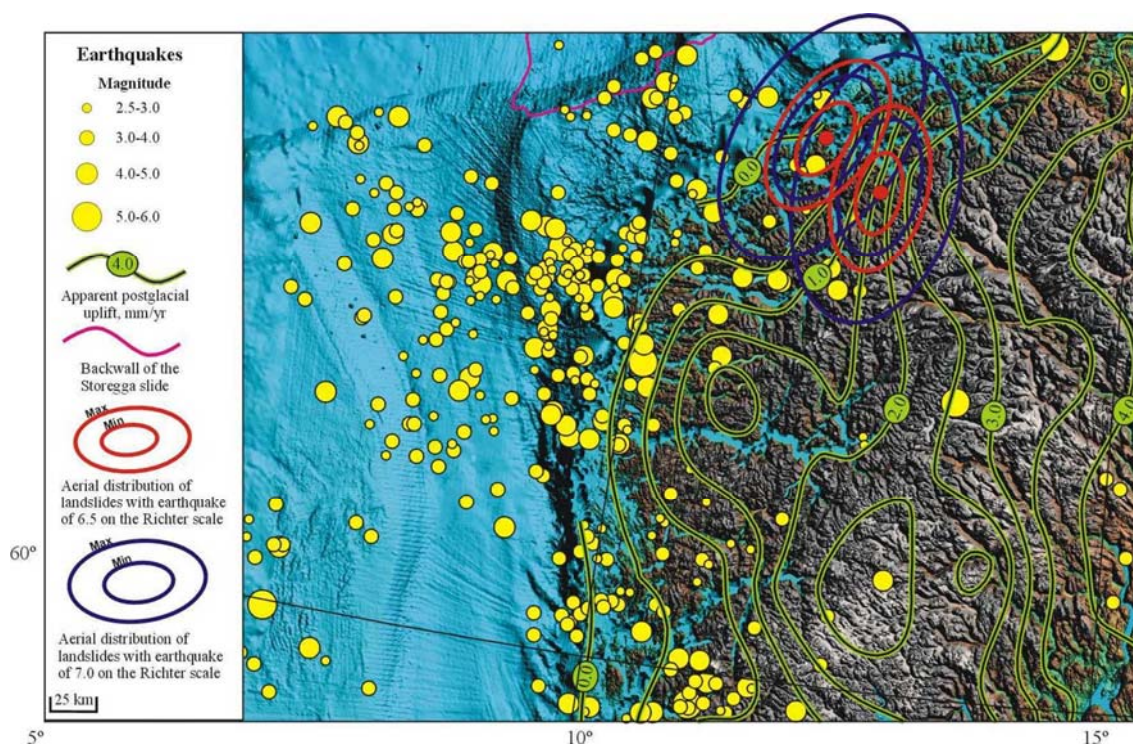


Figure 59. Earthquake data (NORSAR) and apparent land uplift plotted on a Landsat 7 satellite image base (modified from Dehls et al. 2000). Aerial distribution of potential landslides during earthquake events of magnitude 6.5 and 7.0 in area 1 and 3 shown in Fig. 57. Potential areas affected by landslides are derived from the relationship found by Keefer (1984), see Fig. 58.

It has been shown from other areas, e.g. in Canada (Benjuemea et al. 2002), that relatively small earthquakes may cause sliding of soft sediments in narrow and deep fjords. The acoustic impedance at the overburden/bedrock discontinuity leads to a high value for the resonance amplification effect. Substantial variations in amplification effects occur due to large variations in stratigraphy and bedrock topography. This effect may explain why small earthquakes cause sliding of unstable sediments in one fjord, but not in the neighbouring fjord.

11. CONCLUSIONS

In this project, seismic data, swath bathymetry and cores from 16 fjords and 5 lakes in Sogn og Fjordane and Møre og Romsdal have been investigated with the aim to collect and compile data on slides, avalanches and gravitational faults that may have resulted from large earthquakes or tsunamis in northwestern Norway.

A major task in the project has been to investigate the spatial extent and interpret the origin of a postulated mass-movement event ca. 2000 years ago and to evaluate its causes: climatic variations, a tsunami (possibly caused by an earthquake affecting the offshore area), an earthquake only affecting parts of western Norway, or a combination of an earthquake and a tsunami. Several other mass movements, including Storegga Slide tsunami deposits and pre-Storegga Slide slide and debrisflow deposits have been studied, both in fjord and lake sediments.

Five of the investigated fjords (Dalsfjorden, Førdefjorden, Syvdsfjorden, Voldafjorden, Ørtafjorden) provide evidence for an event 2000-2200 years ago. There is no indication of a large slide in the Storegga area, that may have created a tsunami at that time, nor are any mass-movement deposits found on land. This suggests that the 2000-2200 BP slides, debrisflows and turbidity currents in the fjords were most likely related to one or more earthquakes on land or close to the coast, and not to a tsunami generated by an offshore megaslide. An increase in debrisflow activity, probably related to a climatic change around 2200 BP, has been indicated from other studies. Our data show that the red reflector of Longva et al. (2001) is not 2000-2200 years old in all the investigated fjords, but that it generally reflects major mass-movement events.

Storegga Slide (8200 BP) tsunami deposits are observed in lake cores from Sunnmøre as well as in fjord cores from Sogn (Sognesjøen), Sunnmøre (Voldafjorden and Sulafjorden), Romsdal (Julsundet) and Nordmøre (Halsafjorden). The correlation of cores and seismic data is still uncertain. The main causes for this are sediment compaction during coring, and poor core recovery. In some cases, the corer has probably not sampled the uppermost part of the seabed sediments. In other cases, the sediments in the lowermost part of the cored units have not entered the corer, or they were lost during core retrieval. In general, we have assumed that the retrieved cores are from the seabed downwards. A consequence of this interpretation is that the green fjord margin slide/debrisflow deposits of Longva et al. (2001) are older (11 000-11 700 BP) than the Storegga Slide tsunami deposits. As the correlation of core data and seismic data in Voldafjorden, Sulafjorden and Halsafjorden is still uncertain, we are not able to conclude what may have triggered the Storegga Slide.

Seismic data show that there is a striking similarity in areal distribution and volume of major mass-movement deposits at the 2000-2200 BP and the interpreted 11 000-11 700 BP stratigraphic levels in some fjords in Sunnmøre. This suggests a common triggering mechanism, i.e. one or several earthquakes. The major slide and debrisflow deposits at the

2000-2200 BP and 11 000-11 700 BP stratigraphic levels are thick and very extensive along fjord margins in Sunnfjord and Sunnmøre. In Nordmøre, similar deposits occur at the 11 000-11 700 BP level, but they are fewer and not that extensive. This suggests that the epicenters of the triggering earthquakes were located in the Sunnfjord-Sunnmøre region, which is a neotectonically active region with earthquakes up to magnitude 5 occurring regularly today.

Turbidites, debrisflow and snow avalanche deposits from the time interval 2800-3200 BP were found in several fjords and lakes. The spread of ages within the 2800-3200 BP interval is probably too great to consider simultaneous occurrence of all these events, and a climatic cause is suggested. An increase in debrisflow processes, probably related to a climatic change around 3200 BP, has also been shown from other studies. A series of dates in the inner fjord areas of Møre og Romsdal suggests high rock-avalanche activity during the second half of the Holocene. Some rock avalanches in Innfjorden and Tafjorden may be related to movement on the newly discovered Berill fault, possibly around 3000 BP.

Several other periods of mass-movement activity (debrisflows, turbidity currents, floods, snow avalanches) have been recorded, e.g. 1700-1800 BP and 5300-5600 BP. These are only observed in a few basins, and are thus interpreted to be related to local climatic variations. Clusters of rock avalanche deposits in the coastal area probably reflect old events, possibly just after the deglaciation. Many small debrisflow deposits and turbidites in the early Holocene can probably be related to rapid land uplift and high rates of erosion, at that time.

12. REFERENCES

- Aarseth, I., Lønne, Ø. and Giskeødegaard, O. 1989: Submarine slides in glaciomarine sediments in some western Norwegian fjords. *Marine Geology* 88, 1-21.
- Adams, J. 1981: Earthquake-dammed lakes in New Zealand. *Geology* 9, 215-219.
- Anda, E., Blikra, L.H. and Braathen, A. 2002: The Berill fault - first evidence of neotectonic faulting in southern Norway. *Norsk Geologisk Tidsskrift* (in press).
- Barnett, C., Dumayne-Peaty, L. and Matthews, J. A. 2001: Holocene climatic change and tree-line response in Leirdalen, central Jotunheimen, south central Norway. *Review of Palaeobotany and Palynology* 117, 119-137.
- Bard, E., Arnold, M., Mangerud, J., Paterne, M., Labeyrie, L., Duprat, J., Melieres, M.-A., Sønstegaard, E. and Duplessy, J.-C. 1994: The North Atlantic atmosphere-sea surface ^{14}C gradient during the Younger Dryas climatic event. *Earth and Planetary Science Letters* 126, 275-287.
- Benjuema, B., Hunter, J.A., Pulland, S.E., Burns, R.A. and Good, R.L. 2002: Near-surface seismic studies to estimate potential earthquake ground motion amplification at a thick soil site in the Ottawa river valley, Canada (unpublished manuscript).
- Bennett, K.D. 1984: The post-glacial history of *Pinus sylvestris* in the British Isles. *Quaternary Science Reviews* 3, 133-150.
- Birks, H.J.B. 1988: Long-term ecological changes in the British uplands. In Usher, M.B. and Thompson, D.B.A. (eds): *Ecological Change in the Uplands*. Oxford: Blackwell Scientific Publications, 37-56.
- Birks, H.J.B. 1990: Changes in vegetation and climate during the Holocene of Europe. In Boer, M.M. and De Groot, R.S. (eds), *Landscape-Ecological Impact of Climatic Change*. Amsterdam: IOS Press, 133-158.
- Blikra, L. H. and Nemeč, W. 1993a: Postglacial avalanche activity in western Norway: depositional facies sequences, chronostratigraphy and palaeoclimatic implications. In Frenzel, B., Matthews, J. A. and Gläser, B. (editors), *Solifluctation and climate variation in the Holocene*. Paläoklimaforschung 11, Stuttgart: Gustav Fischer Verlag, 143-162.
- Blikra, L. H. and Nemeč, W. 1993b: Postglacial fan deltas in western Norway: a case study of snow avalanche-dominated, colluvial fans prograding into deep fjords. In *Abstracts 3rd International workshop on fan deltas*, University of Seoul, 1-4.

- Blikra, L.H. and Nemeč, W. 1998: Postglacial colluvium in western Norway: depositional processes, facies and palaeoclimatic record. *Sedimentology* 45, 909-959.
- Blikra, L.H. and Selvik, S.F. 1998: Climatic signals recorded in snow avalanche-dominated colluvium in western Norway: depositional facies successions and pollen records. *The Holocene* 8, 631-658.
- Blikra, L.H., Dehls, J. and Olesen, O. 2000a: Gravitational-slope features from Odda in Hardanger to Aurland in Sogn, western Norway. 26-30 In: Dehls, J & Olesen, O. (Red): Neotectonics in Norway, Annual Technical Report. *NGU Report 2000.01*.
- Blikra, L.H., Longva, O. and Anda, E. 2000b: Large rock avalanches in western Norway. Poster report: Interpraevent, Villach, Österreich, June 2000.
- Blikra, L.H., Braathen, A. and Skurtveit, E. 2001: Hazard evaluation of rock avalanches; the Baraldsnes area. *NGU Report 2001.108*.
- Blikra, L.H., Tønnesen, J.F. and Longva, O. 2002a: Fjellskred og stabilitet i fyllittområder – Geologiske og geofysiske studier. *NGU Report 2002.005*.
- Blikra, L.H., Braathen, A., Anda, E., Stalsberg, K. and Longva, O. 2002b: Rock avalanches, gravitational bedrock fractures and neotectonic faults onshore northern West Norway: Examples, regional distribution and triggering mechanisms. *NGU Report 2002.016*, 48 pp.
- Bondevik, S., Svendsen, J.I., Johnsen, G., Mangerud, J. and Kaland, P.E. 1997a: The Storegga tsunami along the Norwegian coast, its age and runup. *Boreas* 26, 29-53.
- Bondevik, S., Svendsen, J.I. and Mangerud, J. 1997b: Tsunami sedimentary facies deposited by the Storegga tsunami in shallow marine basins and coastal lakes, western Norway. *Sedimentology* 44, 1115-1131.
- Bondevik, S., Svendsen, J. I. and Mangerud, J. 1998: Distinction between the Storegga Tsunami and the Holocene marine transgression in coastal basin deposits of western Norway. *Journal of Quaternary Science* 13, 529-537.
- Byrkjeland, U., Bungum, H. and Eldholm, O. 2000: Seismotectonics of the Norwegian continental margin. *Journal of Geophysical Research* 105, 6221-6236.
- Bøe, R., Rise, L., Blikra, L.H., Longva, O. and Eide, A. (in prep): Holocene slides and turbidites in Trondheimsfjorden, central Norway: investigated from high resolution seismic data, swath bathymetry and deep boreholes.

Dahl, S. O. and Nesje, A. 1996: A new approach to calculating Holocene winter precipitation by combining glacier equilibrium-line altitude and pine-tree limits: a case study from Hardangerjøkulen, central southern Norway. *The Holocene* 6, 381-398.

Dehls, J., Olesen, O., Bungum, H., Hicks, E.C., Lindholm, C.D. and Riis, F. 2000a: Neotectonic map: Norway and adjacent areas. *Geological Survey of Norway*.

Ekrene, A., Espedal, T. and Stue, K. 1992: Yngre Dryas - Lokalglasiasjon og stratigrafi i Nordfjord. Kandidatoppgåve, Høgskulen i Sogn og Fjordane.

Fareth, O.W. 1987: Glacial geology of Middle and Inner Nordfjord, western Norway. *Norges geologiske undersøkelse* 408, 1-55.

Geoconsult 2002: Ormen Lange nearshore survey 2001. Survey results - Syvdsfjord, NGU 1L to 6L, Kjerringsundet, Stavenes, Skår/Baraldsnes and Bjørnsundet (NH0185). Final report.

Gjelsvik, J.L. and Kui, T.W. 1992: Hovedtrekkene i den postglacial vegetasjonsutviklingen i midtre Nordfjord basert på pollenundersøkelser i Storsætervatnet, Eid kommune. Unpubl. thesis, Sogn og Fjordane College.

Gunnarsdóttir, H. 1996: Holocene vegetation history in the northern parts of the Gudbrandsdalen valley, south central Norway. Unpubl. Dr. Scient. Thesis No. 8, University of Oslo, Oslo.

Grøsfjeld, K., Larsen, E., Sejrup, H. P., de-Vernal, A., Flatebø, T., Vestbø, M., Haflidason, H. and Aarseth, I. 1999: Dinoflagellate cysts reflecting surface-water conditions in Voldafjorden, western Norway during the last 11 300 years. *Boreas* 28, 403-415.

Haflidasson, H. 2002: Chronological investigation of the Storegga Slide Events: Summary Report to Norsk Hydro. University of Bergen, Department of Geology, Report No. 100-01/02, 42 pp.

Hafsten, U. 1987: Vegetation, climate and evolution of the cultural landscape in Trøndelag, Central Norway, after the last ice age. *Norsk Geografisk Tidsskrift* 41, 101-120.

Hagen, J. 1981: Maringeologiske undersøkelser i Sulafjorden, Breisunddjupet og tilgrensende områder av kontinentalhylla utenfor Møre. Unpublished master thesis, University of Bergen, 373 pp.

Hovland, C. and Sandnes, R. 2002: Sein- og postglacial stratigrafi i tre vatn på Sunnmøre og i Nordfjord. Kandidatoppgåve ved Høgskulen i Sogn og Fjordane 2002.

- Jibson, R.W. 1994: Using landslides for Palaeoseismic analysis. In McCalpin (ed.): *Paleoseismology*. International geophysics series 62. Academic Press. 397-438.
- Johnston, A.C. and Kanter, L.R. 1990: Earthquakes in stable continental crust. *Scientific American* 262 (3), 42-49.
- Jonasson, C. 1991: *Holocene Slope Processes of Periglacial Mountain Areas in Scandinavia and Poland*. Doctoral Thesis, Uppsala University. UNGI Rapport 79.
- Jonasson, C. 1993: Holocene debris-flow activity in northern Sweden. In Frenzel, B., Matthews, J. A. and Gläser, B. (editors) *Solifluction and climate variation in the Holocene*. Paläoklimaforschung 11, Stuttgart: Gustav Fischer Verlag, 179-195.
- Karlén, W. and Matthews, J. A. 1992: Reconstructing Holocene glacier variations from glacier lake sediments: studies from Nordvestlandet and Jostedalsbreen-Jotunheimen, southern Norway. *Geografiska Annaler* 74A, 327-348.
- Keefer, D.K. 1984: Landslides caused by earthquakes. *Geological Society of America Bulletin* 95, 406-421.
- Kullman, L. 1988: Holocene history of the forest-alpine tundra ecotone in the Scandes Mountains (central Sweden). *New Phytologist* 108, 101-110.
- Kullman, L. 1989: Tree-limit history during the Holocene in the Scandes Mountains, Sweden, inferred from subfossil wood. *Review of Palaeobotany and Palynology* 58, 163-171.
- Kullman, L. 1993: Dynamism of the altitudinal margin of the boreal forest in Sweden. In Frenzel, B., editor, *Oscillations of the alpine and polar tree limits in the Holocene*. *Paläoklimaforschung* 9, 41-55.
- Lauritsen, T. and Elvebakk, H. 2001: Georadarundersøkelser av fjellskred ved Fjærland, Sogn og Fjordane. *Geological Survey of Norway Report 2001.004*.
- Lepland, A., Bøe, R., Sønstegaard, E. Haflidason, H., Hovland, C., Olsen, H. and Sandnes, R. 2002: Sedimentological descriptions and results of analytical tests of sediment cores from fjords and lakes in northwest Western Norway - final report. *NGU Report 2002.14*, 198 pp.
- Longva, O., Blikra, L.H. and Olsen, H.A. 2000: Voldafjorden; detaljert djupnemåling og undersjøiske ras. *NGU Report 2000.116*.
- Longva, O. and Olsen, H.A. 2001: Regional landslide occurrences and possible post-glacial earthquake activity in northwest Western Norway: Phase A2; Penetration echosounding in 5 lakes in Sunnmøre and Nordfjord. *NGU Report 2001.049*, 23 pp.

Longva, O., Blikra, L.H., Olsen, H.A. and Stalsberg, K. 2001a: Regional landslide occurrences and possible post-glacial earthquake activity in northwest Western Norway: Phase A1: interpretation of seismic data and proposal of core-locations in fjords and along the coast. *NGU Report 2001.048*, 46 pp.

Longva, O., Bøe, R. and Howe, J. 2001b: Cruise 0103 with R/V Seisma to fjords in Sogn og Fjordane and Møre og Romsdal - cruise report (Phase B1). *NGU Report 2001.100*, 22 pp.

Matthews, J. A., Harris, C. and Ballantyne, C. K. 1986: Studies on a gelifluction lobe, Jotunheimen, Norway: ^{14}C chronology, stratigraphy, sedimentology and palaeoenvironment. *Geografiska Annaler 68A*, 345-360.

Matthews, J. A., Dahl, S. O., Berrisford, M. S., Nesje, A., Dresser, P. Q. and Dumayne - Peaty, L. 1997: A preliminary history of Holocene colluvial (debris-flow) activity, Leirdalen, Jotunheimen, Norway. *Journal of Quaternary Science 12*, 117-129.

Matthews, J. A., Dahl, S. O., Nesje, A., Berrisford, M. S. and Andersson, C. 2000: Holocene glacier variations in central Jotunheimen, southern Norway based on distal glaciolacustrine sediment cores. *Quaternary Science Reviews 19*, 1625-1647.

Mikalsen, G., Sejrup, H.P. and Aarseth, I. 1999: Late Holocene changes in ocean circulation and climate: Foraminiferal and isotopic evidence from Sulafjord, western Norway. In: Michalsen, G. *Western Norwegian Fjords; recent bentic foraminifera, stable isotopic composition of fjord and river water, and Late Holocene variability in basin water characteristics*. Dr. Scientarium Thesis, University of Bergen.

Nesje, A. 2002: A rockfall avalanche in Oldedalen, inner Nordfjord, western Norway, dated by means of a sub-avalanche *Salix* sp. Tree trunk. *Norsk Geologisk Tidsskrift* (in press).

Nesje, A. and Dahl, S.O. 2001: The Greenland 8200 cal. yr. BP event in loss-on-ignition profiles in Norwegian lacustrine sediment sequences. *Journal of Quaternary Science 16*, 155-166.

Nesje, A., Dahl, S. O., Andersson, C. and Matthews, J. A. 2000: The lacustrine sedimentary sequence in Sygneskardvatnet, western Norway: a continuous, high-resolution record of the Jostedalsbreen ice cap during the Holocene. *Quaternary Science Reviews 19*, 1047-1065.

Nesje, A., Dahl, S. O. and Løvlie, R. 1995a: Late Holocene glaciers and avalanche activity in the Ålfotbreen area, western Norway: evidence from a lacustrine sedimentary record. *Norsk Geologisk Tidsskrift 75*, 120-126.


- Nesje, A., Dahl, S.O., Matthews, J.A. and Berrisford, M.S. 2001: A ~4500-year record of river floods obtained from a sediment core in lake Atnsjøen, eastern Norway. *Journal of Paleolimnology* 25, 329-342.
- Nesje, A., Johannessen, T. and Birks, H. J. B. 1995b: Briksdalsbreen, western Norway: climatic effects on the terminal response of a temperate glacier between AD 1901 and 1994. *The Holocene* 5, 343-347.
- Nesje, A., Kvamme, M., Rye, N. and Løvlie, R. 1991: Holocene glacial and climatic history of the Jostedalbreen region, western Norway; evidence from lake sediments and terrestrial deposits. *Quaternary Science Reviews* 10, 87-114.
- NORSAR 2001: Ormen Lange Geohazards Study, Task 9; Earthquake Hazard Considerations. Report for Norwegian Geotechnical Institute (NGI) and Norsk Hydro a.s., September 2001, 95 pp.
- NORSAR and NGI 1998: Development of a seismic zonation for Norway. Final report for Norwegian Council for Building Standardization (NBR), march 15, 162pp.
- Pascal, C. and Gabrielsen, R. 2001: Numerical modelling of cenozoic stress pattern in the mid-Norwegian margin and the northern North Sea. *Tectonics* 20, 585-599.
- Robinson, P., Tveten, E. and Blikra, L.H. 1997: A post-glacial bedrock failure at Oppstadhornet, Oterøya, Møre og Romsdal: a potential major rock avalanche. *NGU Bulletin* 433, 46-47.
- Sejrup, H.P., Haflidason, H., Flatebø, T., Klitgaards Kristensen, D., Grøsfjeld, K. and Larsen, E. 2001: Late-glacial to Holocene environmental changes and climate variability: evidence from Voldafjorden, western Norway. *Journal of Quaternary Science* 16, 181-198.
- Selsing, L. and Wishman, F. 1984: Mean summer temperatures and circulation in a Southwest Norwegian mountain area during the Atlantic period, based upon changes of the alpine pine-forest limit. *Annual Glaciology* 5, 127-132.
- Sitar, N. and Khazai, B. 2001: Characteristics of seismically induced landslides in recent earthquakes. In M. Kühne, H.H. Einstein, E. Krauter, H. Klapperich, and R. Pöttler (eds.) *Int. Conf. On Landslides, Causes, Impacts and Countermeasures, EdsVGE*. Davos, Switzerland.
- Sletten, K., Blikra, L.H., Ballantyne, C.K., Nesje, A and Dahl, S.O. 2002: The occurrence of Holocene debris flows, based on a lacustrine sedimentary record from Ulvådalen, western Norway: chronostratigraphy, sediment characteristics and palaeoclimatic implications. *The Holocene* (in press).

Svendsen, J.I. and Mangerud, J. 1987: Late Weichselian and Holocene sea-level history for a cross-section of western Norway. *Journal of Quaternary Science* 2, 113-132.

Svendsen, J.I. and Mangerud, J. 1990: Sea-level changes and pollen stratigraphy on the outer coast of Sunnmøre, western Norway. *Norsk Geologisk Tidsskrift* 70, 111-134.

Sønstegeard, E., Sandnes, R., Hovland, C. and Bøe, R. 2001: Regional landslide occurrences and possible post-glacial earthquake activity in northwest Western Norway: sediment cores from five lakes in Nordfjord and Sunnmøre (Phase B2). *NGU Report 2001.101*, 42 pp.

APPENDIX 1

		REVIEW REPORT					
		REVIEW CONCERNS ORMEN LANGE PHASE 2					
SINTEF Civil and Environmental Engineering Rock and Soil Mechanics Address: NO-7465 Trondheim, NORWAY Location: Alfred Getz vei 2 Telephone: +47 73 59 31 76 Fax: +47 73 59 47 78 Location: Høgskoleringen 7a Telephone: +47 73 59 46 00 Fax: +47 73 59 53 40 Enterprise No: NO 948 007 029 MVA		REVIEWED REPORT Postglacial mass movements in western Norway with special emphasis on the 2000-2200 BP and 2800-3200 BP periods – Status report Doc.: 37-00-NN-G15-00126		FOR YOUR ATTENTION	COMMENTS ARE INVITED	FOR YOUR INFORMATION	AS AGREED
		DISTRIBUTION Svein Elvanes, Norsk Hydro Tor Inge Tjelta, Statoil		X			
FILE CODE	CLASSIFICATION						
611	Project-internal						
ELECTRONIC FILE CODE		REVIEW REPORT NO.					
Review report Postglacial mass movements in western Norway No.13-02.doc		STF-NH-OL-13/1					
PROJECT NO.	DATE	PERSON RESPONSIBLE / AUTHOR	CHECKED BY	NUMBER OF PAGES			
222009	2002-06-24	Geir Svanfoss Kåre Rokoengen	Gudmund Eiksund	2			

ABSTRACT:

SINTEF is performing a verification study on Norsk Hydro's activities related to seabed stability at Ormen Lange.

Contract No.: NHT-B44-5110651-00
 Contract Name: Verification Seabed Stability Ormen Lange Phase 2

The present report contains comments from the verification group to the report:

Postglacial mass movements in western Norway with special emphasis on the 2000-2200 BP and 2800-3200 BP periods – Status report.
Doc.: 37-00-NN-G15-00126
NGU-Report 2002.020.

The review has been performed by:

- Kåre Rokoengen, NTNU

FINDINGS

General

The report is quite extensive with some 109 pages and 57 figures. As **some laboratory results with interpretation are still missing**, the report is called a status report.

Traces of the Storegga Tsunami have, after first having been recognised in Scotland, been found regionally along the coast of western Norway (Bondevik et al. 1997a, b). The question addressed in the NGU report is if other such events but younger could be identified. For this purpose a very extensive project in several phases have been conducted (p. 11 –14) with bathymetry, seismic profiling, sampling and laboratory investigations.

We feel that the report in its present stage in some respects is a bit preliminary as important results are still to come.

The project represents probably the most extensive survey for slides on land and in fjords in Norway so far. It will also no doubt add significantly to our knowledge about the geological development of the Norwegian fjords.

Specific comments

The connection between profiling and sampling should be strengthened. It has been defined several reflectors with tentative ages before sampling (p. 8-9): violet (12.000 C-14 years), orange (11.000-9.000), green (ca. 7000 – Storegga ?) and red (2000). This is very interesting and it is therefore disappointing that the proposed most important **reflectors are not shown in any illustration** with seismic profile or on cores. We think that if this is done it would improve the quality of the final report.

Some question marks were made during reading: Dating on p. 38. Core P0103005 did not contain enough forams for dating, but shells up to 1 cm. Why have not shells been dated where possible to avoid contamination?

Fig. 55: The Berill fault very difficult to find.

P. 74 Ekrene et al. 1992 not in the reference list.

Fig. 45 legend not given before Fig 51 and figures difficult to read.

Could have wanted some more about how the Storegga Tsunami shows up of in the fjord cores in deep water.

Recommendations:

For the Ormen Lange project the results should be good news (?). No really regional event has been identified after the ca. 7000 year. Still it seems rather uncertain if the “red reflector” really is of the same age in several fjords. It was also found in just 4 of the 16 fjords investigated. The NGU report seems thus **not to indicate any really large synchronous event that could have been triggered from megaslides offshore**. This will, however, hopefully become more clearly when the rest of the datings become available.

The report also clearly demonstrates how difficult it is to really prove or disprove with dating whether layers are of the exact same age or not.

APPENDIX 2

COMMENTS TO THE REVIEW REPORT BY SINTEF

The connection between profiling and sampling has been strengthened. The most important reflectors, as interpreted by Longva et al. (2001a) from Voldafjorden, are shown in Fig. 3. In addition, the colour coding is shown on the seismic profile from Julsundet. The connection between interpreted seismic profiles and core data is shown for Julsundet and Syvdsfjorden. We have not shown the colour coding and interpretations of Longva et al. (2001a) in all seismic figure examples, as the present report documents that the interpreted red reflector is not of the same age in all fjords, and that the interpreted green reflector is in most cases probably older than the Storegga Slide.

Dating on p. 38: Samples from below the two turbidites and from below the debrisflow deposit in core P0103005 did not contain enough foraminifers for dating. Shells up to 1 cm were found in the debrisflow deposit, but this represents redeposited sediments (probably glaciomarine sediments), and would thus not give an age of great interest for this project. We did not date shells at stratigraphic levels away from the turbidites and the debrisflow deposit, as this would not give the age of mass-movement events.

Fig. 55 (now Fig. 57): The asterisk showing the location of the Berill fault has been expanded.

P. 74: Ekrene et al. (1992) has been added to the reference list.

Fig. 45 (now Fig. 47): Figure text now refers to Fig. 51 for legend.

Concerning Storegga Slide deposits in the deep fjords, the text has been expanded and the interpretations changed since the status report was released. This is mainly due to several new dating results.

It has been shown that the interpreted red reflector is not of the same age in all the fjords. 2000-2200 years old deposits are only found in 5 fjords in Sunnfjord and Sunnmøre. The new data show that there has been no really large, synchronous event triggered by a megaslide offshore, after the Storegga Slide 8200 years ago.